expecting the unexpected

indicators of resilience as early-warning signals for critical transitions

Vasilis Dakos

expecting the unexpected:
indicators of resilience as early-warning signals for critical transitions

Thesis committee

Thesis supervisor
Prof. Dr. Marten Scheffer
Professor, Department of Aquatic Ecology and Water Quality Management
Wageningen University, The Netherlands

Thesis co-supervisor
Dr. Ir. Egbert H. van Nes
Associate Professor, Department of Aquatic Ecology and Water Quality Management
Wageningen University, The Netherlands

Other members
Prof. Dr. Jordi Bascompte, Estación Biológica de Doñana, CSIC, Sevilla, Spain
Prof. Dr. Jef Huisman, University of Amsterdam, The Netherlands
Prof. Dr. Rik B. J. Leemans, Wageningen University, The Netherlands
Prof. Dr. Peter C. de Ruiter, Wageningen University, The Netherlands

This research was conducted under the auspices of the Graduate School of Socio-Economic and Natural Sciences of the Environment (SENSE).

expecting the unexpected:
indicators of resilience as early-warning signals for critical transitions

Vasilis Dakos

Thesis

Submitted in partial fulfillment of the requirements for the degree of doctor

at Wageningen University

by the authority of the Rector Magnificus

Prof. Dr. M. J. Kropff,

in the presence of the

Thesis committee appointed by the Academic Board

to be defended in public

on Wednesday 1th of June 2011

at 4 p.m. in the Aula.

Vasilis Dakos

Expecting the Unexpected:
Indicators of Resilience as Early-Warning Signals for Critical Transitions

160 pages.

Thesis, Wageningen University, Wageningen, NL (2011)
With references, with summaries in Dutch, English, and Greek.

ISBN 978-90-8585-870-6

στους γονείς μου
[to my parents]

cover: Vasilis Dakos (inspired by PARS Foundation Findings on Elasticity)

Propositions

1. Early-warning signals are not predictive tools [this thesis].
2. Post-perturbation recovery time is the most rigorous indicator of critical slowing down prior to critical transitions [this thesis].
3. Detecting an upcoming crisis is a necessary but not sufficient condition for avoiding it.
4. The probability that a finding that is published as new has been shown before is high.
5. Conducting research following a business model will inevitably lead to a scientific "bubble".
6. The environmentalist paradox lies not in the fact that human well-being increases in the face of declining ecosystem services, but rather in the fact that humans do not seem to realize that such trend is unsustainable.
7. The Unexpected is more common than expected.

Propositions belonging to the Thesis entitled:

'Expecting the Unexpected:
Indicators of Resilience as Early-Warning Signals for Critical Transitions'

Vasilis Dakos
Wageningen, 1st June 2011

contents

Chapter 1

Introduction

"To expect the unexpected shows a thoroughly modern intellect."
Oscar Wilde

What do ecosystems, financial markets, and the climate have in common?
They can all change in abrupt, irreversible, and unexpected ways.

During the 1960s and 1970s, Caribbean coral reefs had been exposed to increasing stress from overfishing and eutrophication (Hughes 1994). Nonetheless reefs were thought to be resilient ecosystems, and indeed when a hurricane damaged the reefs in 1981, corals appeared to recover, as they had after countless hurricanes in their history. After a couple of years, however, the real surprise kicked-in. Sea urchins - an efficient grazer of fleshy algae - suffered almost complete eradication due to a pathogen-induced disease (Lessios et al. 1984). Released from the urchins' grazing control, fleshy algae started to dominate the reef, and corals crashed (Hughes 1994). It was an abrupt, unexpected shift that until today remains irreversed (Bellwood et al. 2004).

In 2007, the financial sector snowballed into a crisis that still keeps the global economy largely in recession (The Economist, 2007). A multiple set of causes (Krugman, 2009), such as the credit boom, the mortgage bubble and the unregulated shadow banking system are now held responsible for this collapse reminiscent of the past Great Depression. However, the fact that the resulting systemic risk was so widely underestimated, confirms that even for the most well studied human institutions, our understanding of the underlying complexity is rather limited. It proved that the highly interlinked financial markets are not immune to abrupt shifts (May et al. 2008). Whether the 2007 shift will be reversible is still unclear.

Around 12,800 years ago, one of the most dramatic climate changes in recent Earth's history happened: the Younger Dryas (Rahmstorf 2002). During this period, the climate collapsed from a warm state to very cold conditions (Clark et al. 2002). Probably an influx of meltwater from Greenland's icesheets triggered an abrupt collapse of the North Atlantic thermohaline circulation (Rahmstorf 1996; Stommel 1961). Centuries later, the collapse to the Younger Dryas was reversed, the North Atlantic circulation suddenly switched on, and the temperature jumped back. Since then the climate remained relatively stable facilitating the rise of human civilizations. However, given that the sensitivity of the North Atlantic circulation and other elements of the Earth system to anthropogenic forces is poorly known, the possibility of similar tipping events in the future cannot be excluded (Lenton et al. 2008).

While abrupt, irreversible, and unexpected changes appear to be the exception rather than the rule in most systems, they can clearly have great implications for society. It has been argued that such events may be the result of simple underlying mechanisms (Scheffer 2009) rather than pure chance. The fact that such mechanisms are identifiable in disparate systems - like ecosystems, financial markets, or the climate - suggests that, under certain conditions, many systems could behave in such radical and unpredictable ways. In the following, I will explain the essence of how this works and present an outline of how, in this thesis, ideas about estimating the risk of abrupt, irreversible, and unexpected transitions are developed and tested.

Big Surprises Triggered by Small Forces

Everyday examples illustrate that small changes in external conditions - like increasing pull to an elastic band - usually result in smooth responses to the state of a system - the elastic band expands (Figure 1.1a). Such a response is gradual, unsurprising, and reversible: once we relax the stretch, the elastic band regains its previous shape.

In other cases, small changes in conditions may cause disproportionally strong changes in the state of the system (Figure 1.1b). Such marked responses around a threshold in conditions can still be continuous and reversible, in the sense that when conditions are restored to previous levels, the system returns to its former state.

There are situations, however, where minute changes in conditions may trigger extreme discontinuous responses that are not easily reversible (Figure 1.1c). This happens when at a threshold, the system abruptly shifts towards a contrasting state ($threshold_1$ in Figure 1.1c).

Such abrupt shifts triggered by small forces correspond to so-called *catastrophic bifurcations* (Gilmore 1981; Strogatz 1994; Thom 1994). Catastrophic bifurcations are abrupt changes in the qualitative behavior of a system that occur at specific thresholds in external conditions (see Glossary). Catastrophic bifurcations arise in systems with *alternative stable states* (or, in general, *alternative attractors*, see Glossary): systems that may be in more than one different configurations under the same external conditions (May 1977; Scheffer et al. 2001; Sutherland 1974). For instance, the two branches in Figure 1.1c represent two alternative stable states for the same range of conditions.

How do alternative stable states arise? The tale of Shallow lakes

Among the various systems that are considered to exhibit alternative stable states (Scheffer and Carpenter 2003; Beisner et al. 2003), but see (Schroder et al. 2005), shallow lakes are perhaps the best-documented example. Under the same conditions, a shallow lake may be in a clear-water state dominated by submerged aquatic vegetation or in a turbid-water state (Scheffer et al. 1993). The mechanism that allows the existence of alternative stable states in this, as well as in other systems, is the presence of a *positive feedback* (see Glossary).

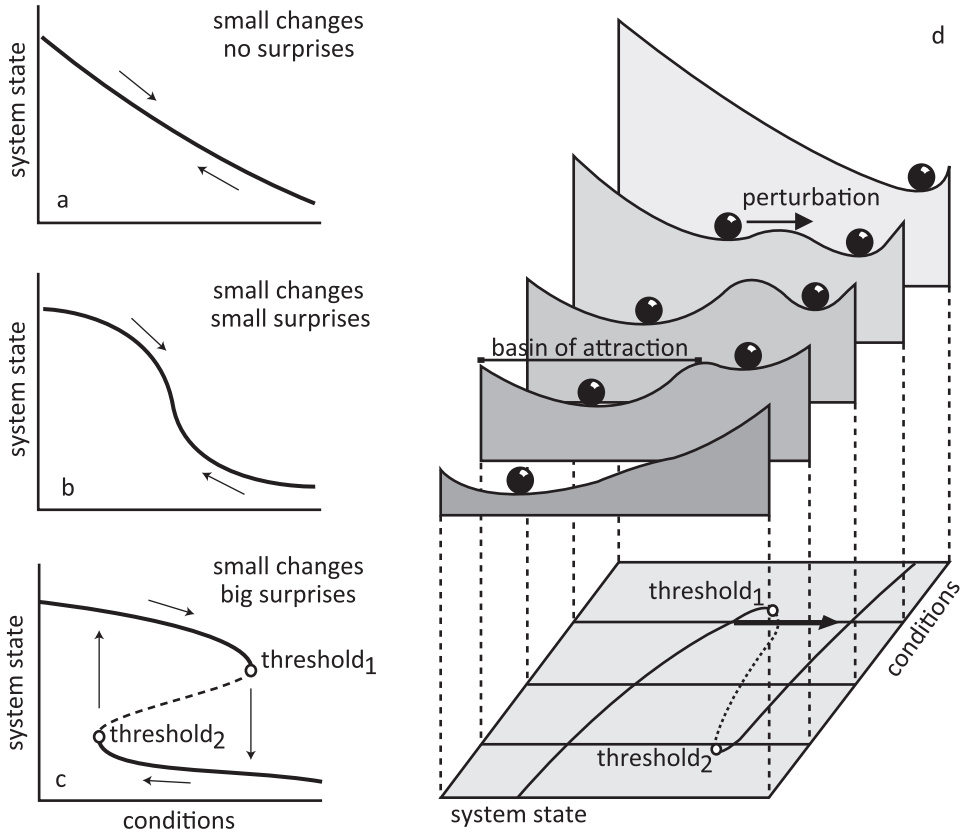

Figure 1.1 System responses to smooth changes in conditions: (**a**) *Gradual and reversible response*: Changes in the system state occur in an expected way. (**b**) *Abrupt and reversible response*: The system state reacts in a continuous expected manner. (**c**) *Abrupt and irreversible response*: A discontinuous unexpected change of the system state takes place. (**d**) Stability landscape illustrating the transition of a system state between two alternative stable states. The valleys in the landscape represent the basins of attraction that correspond to the alternative stable states of the system. As conditions approach the critical *threshold*$_1$, the basin of attraction shrinks till the point that only a tiny perturbation may tip it to the alternative state. [Thin arrows show the trajectory of the system state as conditions increase or decrease. Black balls represent the two alternative stable states of the system at the bottoms of the valleys in the stability landscape. Open circles *threshold*$_1$ and *threshold*$_2$ mark the unexpected shifts that occur at critical threshold conditions (*catastrophic bifurcations*). Dotted line in panels (**c**) and (**d**) represents the border between the basins of attraction of the two alternative stable states: the line corresponds to the hilltops separating the two valleys in the stability landscape.][modified from Scheffer (2009)]

In shallow lakes, positive feedbacks that can sustain the clear-water state include effects of submerged aquatic vegetation on nutrient cycling, sediment stabilization, and predator-prey interactions (Scheffer 1998), leading to clear water which in turn promotes the development of submerged vegetation. As a result, a shallow lake can remain in a clear-water state even under high nutrient loading conditions. In the absence of submerged vegetation, however, high nutrient loading conditions promote a turbid-water state. This contrasting turbid-water state is also sustained by a set of positive feedbacks. For instance, sediment resuspension that hinders vegetation settlement and high nutrient availability that triggers phytoplankton blooms, both promote the stability of the turbid state.

How do transitions between alternative stable states occur?

Although positive feedbacks promote the existence of alternative stable states, there is often a critical threshold in conditions at which the feedbacks are not strong enough to sustain a particular state. In the example of shallow lakes, submerged vegetation cannot keep favorable conditions for its growth when nutrient loading levels become too high. In that case, the system collapses to the alternative state (Figure 1.1c, $threshold_1$). A major implication of the collapse is the fact that restoring conditions below the critical threshold at which the shift occurred, does not lead to the recovery of the system to its former state. This is a direct consequence of the feedbacks that now keep the system in the alternative state unless another critical threshold is reached at which the new state cannot be sustained anymore (Figure 1.1c, $threshold_2$). The difference between the two critical thresholds marks the *hysteresis* in the system: the disparity in the paths of shifting between alternative states.

A simple way to illustrate the transitions between alternative stable states caused by smooth changes in external conditions is to think of the behavior of a system as the motion of a ball in a landscape of valleys and hilltops (Figure 1.1d). The position of the ball in the landscape represents the state of the system. The bottoms of the valleys correspond to the alternative states. In Figure 1.1d, two valleys exist for the same range of conditions. These valleys represent the *basins of attraction* of the two alternative stable states of the system, and are separated by hilltops. In which valley the ball will end up depends on the side of the hilltop where its path started. Obviously, the wider the basin of attraction is, the higher the chance will be that the ball is going to end up in it. Importantly, the width and the steepness of the basin of attraction also determine how easily a perturbation may tip the ball over the hilltop to the alternative valley. The capacity of the system to absorb such perturbations without shifting to an alternative state reflects the *resilience* of the state of the system (Holling 1973). In Figure 1.1d, as conditions bring the system close to the *critical* $threshold_1$, the basin of attraction of the current state of the system shrinks and so does its resilience: even a tiny perturbation is enough to shift the sphere to the alternative valley.

In this thesis, I focus on transitions between alternative stable states that occur when changes in external conditions undermine the resilience of a system. I will refer to these transitions as *critical transitions*.

Foreseeing the Unexpected

It would be helpful if we could identify which systems under which circumstances would be most likely to go through a critical transition. Unfortunately, good predictive models are mostly lacking. In fact, as illustrated by the examples of coral reef collapse and financial crisis, even in relatively well-studied systems a loss of resilience preparing the system for a critical transition is very difficult to detect.

In this thesis I explore the idea that generic rules may allow us to estimate the risk of dramatic events such as the outbreak of global pandemics, collapses of marine fisheries, or the threat of desertification even if we do not mechanistically understand the functioning of such complex systems.

Thesis Outline

Chapter 2 is an all-you-need-to-know review of the generic early-warning signals for critical transitions. It describes the notion of critical slowing down as the fingerprint of catastrophic bifurcations, and explains how critical slowing down causes certain statistical system properties to deviate prior to critical transitions. It reviews how recovery time (van Nes and Scheffer 2007), autocorrelation (Held and Kleinen 2004; Ives 1995), variance (Carpenter and Brock 2006), and low frequency spectral frequencies (Kleinen et al. 2003), all increase in the vicinity of a critical transition, as well as how skewness peaks due to the asymmetry of the system's basin of attraction (Guttal and Jayaprakash 2008). Additionally, it describes potential early-warning signals estimated using spatial information rather than time-series. Various examples of these leading indicators are presented in cases derived from different fields, ranging from ecosystems and the climate to the human physiology.

In **Chapter 3**, we propose a new leading indicator for critical transitions in spatially-organized systems. We demonstrate that the state of neighboring patches becomes increasingly similar prior to a systemic shift. We show that this warning signal can be quantified as a rise in spatial correlation between neighboring patches, and we prove that it is direct consequence of critical slowing down close to bifurcation points.

In **Chapter 4,** we crashtest autocorrelation and variance; the flagships of early-warning signals. Using analytical and simulation results, we investigate whether there can be cases where autocorrelation and variance cannot capture an approaching transition. We address three different cases where the performance of indicators may fail, and we demonstrate that autocorrelation is a more robust indicator than variance.

In **Chapter 5**, we test at the same time whether all proposed generic leading indicators do signal an approaching shift in three spatially-explicit models that describe desertification

in semi-arid ecosystems. We measure recovery time, correlation, variance, and skewness prior to transition, and compare these results to specific spatial signatures before a shift, such as patch size distributions and pattern formation. We show that there is no silver bullet indicator except for rising recovery time upon perturbations.

In **Chapter 6,** we provide the first evidence of a generic leading indicator occurring prior to critical transitions in a real system. We show how autocorrelation increases in the vicinity of eight large-scale climate shifts in the Earth's history, and we compare our results to simulated time-series from models that describe the same climatic events. Our analysis offers a methodological framework for measuring leading indicators in time-series.

The findings of the thesis are brought together in the **Afterthoughts**. Therein, I question the generality of the early-warning signals, I address their potential applicability, and I ponder their further development and their value for avoiding critical transitions in the world around us.

Chapter 2

Early-warning signals for critical transitions: A review

Complex dynamical systems, ranging from ecosystems to financial markets and the climate, can have tipping points at which a sudden shift to a contrasting dynamical regime may occur. Although predicting such critical points before they are reached is extremely difficult, work in different scientific fields is now suggesting the existence of generic early-warning signals that may indicate for a wide class of systems if a critical threshold is approaching.

This chapter is based on the paper: M. Scheffer , J. Bascompte, W. A. Brock, V. Brovkin, S. R. Carpenter, V. Dakos, H. Held, E. H. van Nes, M. Rietkerk and G. Sugihara (2009). Early-warning signals for critical transitions. *Nature* 461: 53-59. We are grateful to the support of Institute Para Limes and the South American Institute for Resilience and Sustainability Studies.

Introduction

It is becoming increasingly clear that many complex systems have critical thresholds—so-called tipping points—at which the system shifts abruptly from one state to another. In medicine, we have spontaneous systemic failures such as asthma attacks (Venegas et al. 2005) or epileptic seizures (Litt et al. 2001; McSharry et al. 2003); in global finance, there is concern about systemic market crashes (Kambhu et al. 2007; May et al. 2008); in the Earth system, abrupt shifts in ocean circulation or climate may occur (Lenton et al. 2008); and catastrophic shifts in rangelands, fish or wildlife populations may threaten ecosystem services (MA 2005; Scheffer et al. 2001).

It is notably hard to predict such critical transitions, because the state of the system may show little change before the tipping point is reached. Also, models of complex systems are usually not accurate enough to predict reliably where critical thresholds may occur. Interestingly, though, it now appears that certain generic symptoms may occur in a wide class of systems as they approach a critical point. At first sight, it may seem surprising that disparate phenomena such as the collapse of an overharvested population and ancient climatic transitions could be indicated by similar signals. However, as we will explain here, the dynamics of systems near a critical point have generic properties, regardless of differences in the details of each system (Schroeder 1991). Therefore, sharp transitions in a range of complex systems are in fact related. In models, critical thresholds for such transitions correspond to bifurcations (Kuznetsov 1995). Particularly relevant are 'catastrophic bifurcations' (see Box 2.1 for an example), where, once a threshold is exceeded, a positive feedback propels the system through a phase of directional change towards a contrasting state. Another important class of bifurcations are those that mark the transition from a stable equilibrium to a cyclic or chaotic attractor. Fundamental shifts that occur in systems when they pass bifurcations are collectively referred to as critical transitions (Scheffer 2009; Wissel 1984).

We will first highlight the theoretical background of leading indicators that may occur in non-equilibrium dynamics before critical transitions, and illustrate how such indicators can perform in model generated time-series. Subsequently, we will review emerging empirical work on different systems and discuss prospects and challenges.

Theory

Critical slowing down and its symptoms

The most important clues that have been suggested as indicators of whether a system is getting close to a critical threshold are related to a phenomenon known in dynamical systems theory as 'critical slowing down' (Wissel 1984). Although critical slowing down occurs for a range of bifurcations, we will focus on the fold catastrophe (Box 2.1) as a starting point. Inappropriate use of this classical model caused some controversy in the past (Zahler and Sussmann 1977), but it is now considered to capture the essence of shifts at tipping points in a wide range of natural systems ranging from cell signalling pathways (Bagowski and Ferrell 2001) to ecosystems (May 1977; Scheffer et al. 2001) and the

climate (Lenton et al. 2008). At fold bifurcation points (F_1 and F_2, Box 2.1), the dominant eigenvalue characterizing the rates of change around the equilibrium becomes zero. This implies that as the system approaches such critical points, it becomes increasingly slow in recovering from small perturbations (Figure 2.1). It can be proven that this phenomenon will occur in any continuous model approaching a fold bifurcation (Wissel 1984). Moreover, analysis of various models shows that such slowing down typically starts far from the bifurcation point, and that recovery rates decrease smoothly to zero as the critical point is approached (van Nes and Scheffer 2007). Box 2.2 describes a simple example illustrating this.

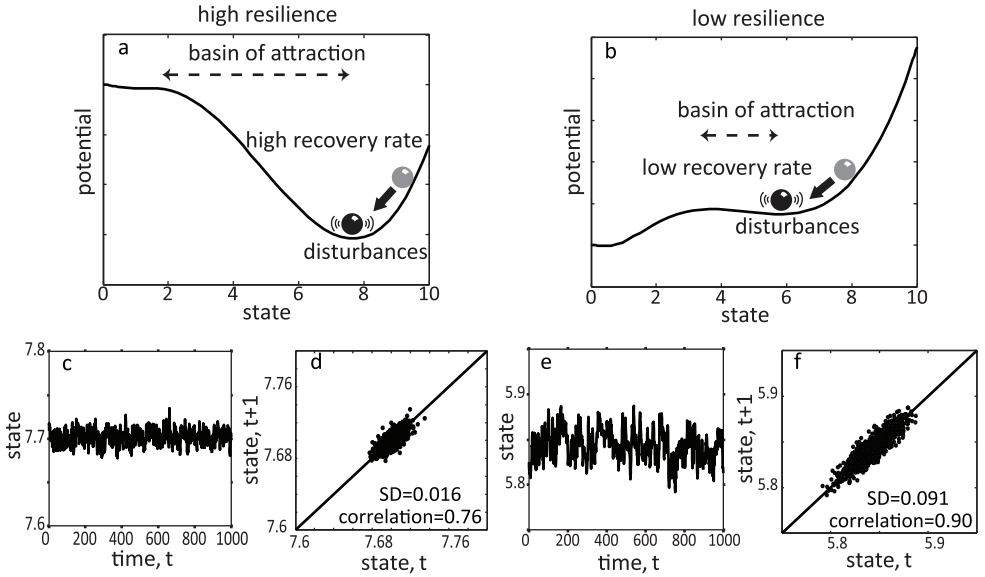

Figure 2.1 Some characteristic changes in non-equilibrium dynamics as a system approaches a catastrophic bifurcation (such as F_1 or F_2, Box 2.1). (**a**, **b**, **c**) Far from the bifurcation point (**a**), resilience is large in two respects: the basin of attraction is large and the rate of recovery from perturbations is relatively high. If such a system is stochastically forced, the resulting dynamics are characterized by low correlation between the states at subsequent time intervals (**b**, **c**). (**d**, **e**, **f**) When the system is closer to the transition point (**d**), resilience decreases in two senses: the basin of attraction shrinks and the rate of recovery from small perturbations is lower. As a consequence of this slowing down, the system has a longer memory for perturbations, and its dynamics in a stochastic environment are characterized by a stronger correlation between subsequent states and a larger variance (**e**, **f**). Plots produced from a stochastically forced differential equation (May 1977) representing a harvested population: $dX/dt=X(1-X/K)-c(X^2/(X^2+1))$, where X is population density, K is the carrying capacity (set to 10) and c is the maximum harvest rate (set to 1 for high resilience and 2.6 for low resilience).

BOX 2.1 | Critical transitions in the fold catastrophe model

The equilibrium state of a system can respond in different ways to changes in conditions such as exploitation pressure or temperature rise (Box 2.1 Figure a, b, c). If the equilibrium curve is folded backwards (Box 2.1 Figure c, d), three equilibria can exist for a given condition. The grey dotted arrows in the plots indicate the direction in which the system moves if it is not in equilibrium (that is, not on the curve). It can be seen from these arrows that all curves represent stable equilibria, except for the dashed middle section in Box 2.1 Figure c, d. If the system is driven slightly away from this part of the curve, it will move further away instead of returning. Hence, equilibria on this part of the curve are unstable and represent the border between the basins of attraction of the two alternative stable states on the upper and lower branches. If the system is very close to a fold bifurcation point (for example point F_1 or point F_2), a tiny change in the condition may cause a large shift in the lower branch (Box 2.1 Figure d). Also, close to such a bifurcation a small perturbation can drive the system across the boundary between the attraction basins (Box 2.1 Figure c). Thus, those bifurcation points are tipping points at which a tiny perturbation can produce a large transition. Small perturbations can also cause large changes in the absence of true bifurcations, provided that the system is very sensitive in a certain range of conditions (Box 2.1 Figure b). Finally, a shift in system state may simply be caused by a sudden large external force (Box 2.1 Figure a). Early-warning signals tend to arise as systems approach a bifurcation point such as in Box 2.1 Figure c, d, and also if systems approacha non-catastrophic threshold such as the one shown in Box 2.1 Figure b.

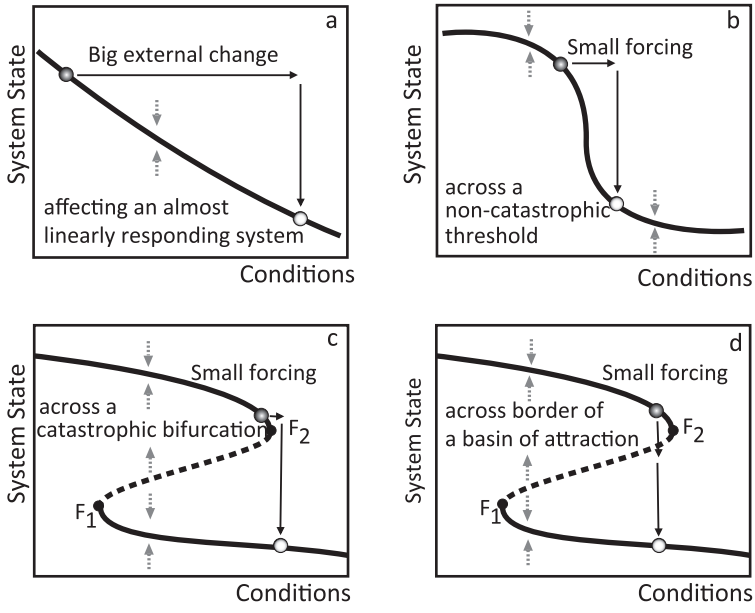

The most straightforward implication of critical slowing down is that the recovery rate after small experimental perturbation can be used as an indicator of how close a system is to a bifurcation point (van Nes and Scheffer 2007). Because it is the rate of change close to the equilibrium that matters, such perturbations may be very small, posing no risk of driving the system over the threshold. Also, models indicate that in spatially extensive systems at risk of systemic collapse, small-scale experimental probing may suffice to test the vicinity of the threshold for such a large-scale transition. For instance, it has been shown that recovery times after local perturbation increase in models of fragmented populations approaching a threshold for global extinction (Ovaskainen and Hanski 2002).

For most natural systems, it would be impractical or impossible to monitor them by systematically testing recovery rates. However, almost all real systems are permanently subject to natural perturbations. It can be shown that as a bifurcation is approached in such a system, certain characteristic changes in the pattern of fluctuations are expected to occur. One important prediction is that the slowing down should lead to an increase in autocorrelation in the resulting pattern of fluctuations (Ives 1995) (Figure 2.1). This can be shown mathematically (Box 2.3), but it is also intuitively simple to understand. Because slowing down causes the intrinsic rates of change in the system to decrease, the state of the system at any given moment becomes more and more like its past state. The resulting increase in 'memory' of the system can be measured in a variety of ways from the frequency spectrum of the system (Kleinen et al. 2003; Livina and Lenton 2007). The simplest approach is to look at lag-1 autocorrelation (Dakos et al. 2008; Held and Kleinen 2004), which can be directly interpreted as slowness of recovery in such natural perturbation regimes (van Nes and Scheffer 2007). Analyses of simulation models exposed to stochastic forcing confirm that if the system is driven gradually closer to a catastrophic bifurcation, there is a marked increase in autocorrelation that builds up long before the critical transition occurs (Figure 2.2d). This is true not only for simple models (Dakos et al. 2008), but also for highly elaborate and relatively realistic models of spatially complex systems (Lenton et al. 2009).

Increased variance in the pattern of fluctuations is another possible consequence of critical slowing down as a critical transition is approached (Carpenter and Brock 2006) (Figure 2.1). Again, this can be formally shown (Biggs et al. 2009b) (Box 2.3), as well as intuitively understood: as the eigenvalue approaches zero, the impacts of shocks do not decay, and their accumulating effect increases the variance of the state variable. In principle, critical slowing down could reduce the ability of the system to track the fluctuations, and thereby produce an opposite effect on the variance (Berglund and Gentz 2006). However, analyses of models show that an increase in the variance usually arises and may be detected well before a critical transition occurs (Carpenter and Brock 2006) (Figure 2.2).

In summary, the phenomenon of critical slowing down leads to three possible early-warning signals in the dynamics of a system approaching a bifurcation: slower recovery from perturbations, increased autocorrelation and increased variance.

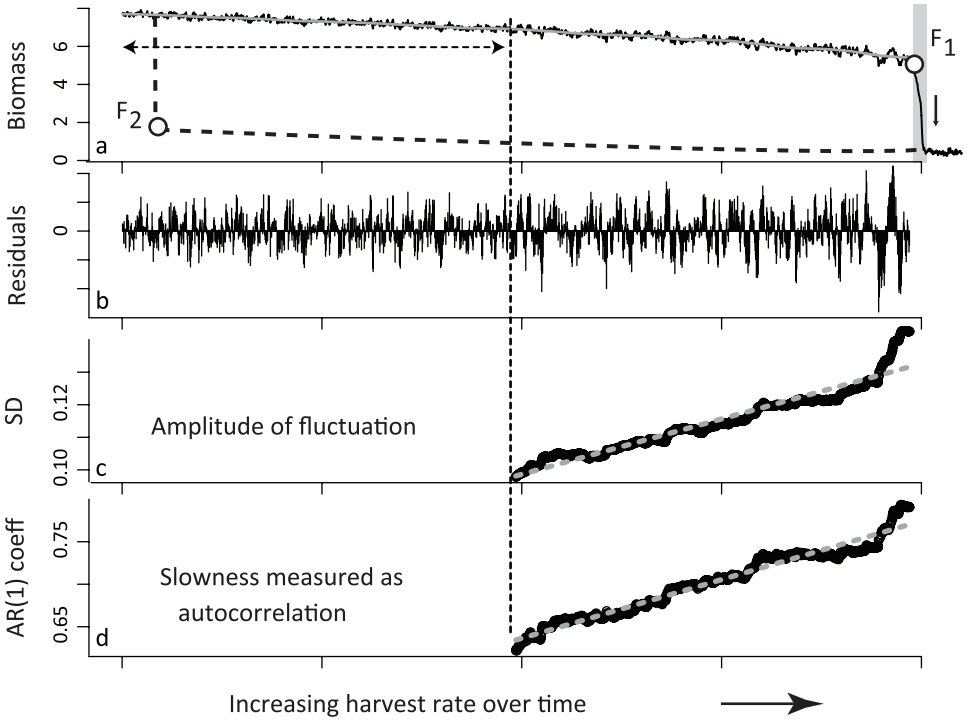

Figure 2.2 Two examples of early-warning signals for a critical transition in a time-series generated by a model of a harvested population (May 1977) driven slowly across a bifurcation. Analysis of the filtered time-series (**b**) shows that the catastrophic transition is preceded by an increase both in the amplitude of fluctuation, expressed as s.d. (**c**), and in slowness, estimated as the lag-1 autoregression (AR(1)) coefficient (**d**), as predicted from theory. In panel (**a**) the gray band identifies the transition phase. The horizontal dashed arrow marks the width of the moving window used to compute the indicators shown in (**c**) and (**d**), and the gray line is the trend used for filtering (see Dakos et al. (2008) for the methods used). The dashed curve and the points F_1 and F_2 represent the equilibrium curve and bifurcation points as in Box 2.1 panels (**c**) and (**d**).

Skewness and flickering before transitions

In addition to autocorrelation and variance, the asymmetry of fluctuations may increase before a catastrophic bifurcation (Guttal and Jayaprakash 2008). This does not result from critical slowing down. Instead, the explanation is that in catastrophic bifurcations such as fold bifurcations (Box 2.1), an unstable equilibrium that marks the border of the basin of attraction approaches the attractor from one side (Box 2.1). In the vicinity of this unstable point, rates of change are lower (reflected in a less steep slope in the stability landscapes). As a result, the system will tend to stay in the vicinity of the unstable point relatively longer than it would on the opposite side of the stable equilibrium. The skewness of the distribution of states is expected to increase not only if the system approaches a

catastrophic bifurcation, but also if the system is driven closer to the basin boundary by an increasing amplitude of perturbation (Guttal and Jayaprakash 2008).

BOX 2.2 | Critical slowing down: an example

To see why the rate of recovery rate after a small perturbation will be reduced, and will approach zero when a system moves towards a catastrophic bifurcation point consider the following simple dynamical system, where γ is a positive scaling and *a* and *b* are parameters:

$$\frac{dx}{dt} = \gamma(x - a)(x - b) \qquad (1)$$

It can easily be seen that this model has two equilibria, $\overline{x}_1 = a$ and $\overline{x}_2 = b$, of which one is stable and the other is unstable. If the value of parameter *a* equals that of *b*, the equilibria collide and exchange stability (in a transcritical bifurcation). Assuming that equilibrium x_1 is the stable equilibrium, we can now study what happens if the state of the equilibrium is perturbed slightly ($x = \overline{x}_1 + \varepsilon$):

$$\frac{d(\overline{x}_1 + \varepsilon)}{dt} = f(\overline{x}_1 + \varepsilon)$$

Here f(x) is the right hand side of equation (1). Linearizing this equation using first-order Taylor expansion yields

$$\frac{d(\overline{x}_1 + \varepsilon)}{dt} = f(\overline{x}_1 + \varepsilon) \approx f(\overline{x}_1) + \left.\frac{\partial f}{\partial x}\right|_{\overline{x}_1} \varepsilon$$

which simplifies to

$$f(\overline{x}_1) + \frac{d\varepsilon}{dt} = f(\overline{x}_1) + \left.\frac{\partial f}{\partial x}\right|_{\overline{x}_1} \varepsilon \Rightarrow \frac{d\varepsilon}{dt} = \lambda_1 \varepsilon \qquad (2)$$

With eigenvalues λ_1 and λ_2 in this case, we have

$$\lambda_1 = \left.\frac{\partial f}{\partial x}\right|_{a} = -\gamma(b - a) \qquad (3)$$

and, for the other equilibrium

$$\lambda_2 = \left.\frac{\partial f}{\partial x}\right|_{b} = \gamma(b - a) \qquad (4)$$

If $b>a$ then the first equilibrium has a negative eigenvalue, λ_1, and is thus stable (as the perturbation goes exponentially to zero; see equation (2)). It is easy to see from equations (3) and (4) that at the bifurcation ($b=a$) the recovery rates λ_1 and λ_2 are both zero and perturbations will not recover. Farther away from the bifurcation, the recovery rate in this model is linearly dependent on the size of the basin of attraction ($b-a$). For more realistic models, this is not necessarily true but the relation is still monotonic and is often nearly linear.

Another phenomenon that can be seen in the vicinity of a catastrophic bifurcation point is flickering. This happens if stochastic forcing is strong enough to move the system back and forth between the basins of attraction of two alternative attractors as the system enters the bistable region before the bifurcation (Horsthemke 2006). Such behavior is also considered an early-warning, because the system may shift permanently to the alternative state if the underlying slow change in conditions persists, moving it eventually to a situation with only one stable state. Flickering has been shown in models of lake eutrophication (Carpenter and Brock 2006) and trophic cascades (Carpenter et al. 2008), for instance. Also, as discussed below, data suggest that certain climatic shifts and epileptic seizures may be presaged by flickering. Statistically, flickering can be observed in the frequency distribution of states as increased variance and skewness as well as bimodality (reflecting the two alternative regimes) (Carpenter and Brock 2006).

Indicators in cyclic and chaotic systems

The principles discussed so far apply to systems that may be stochastically forced but have an underlying attractor that corresponds to a stable point (for example the classic fold catastrophe illustrated in Box 2.1). Critical transitions in cyclic and chaotic systems are less well studied from the point of view of early-warning signals. Such transitions are associated with different classes of bifurcations (Kuznetsov 1995). First, there are the bifurcations that mark the transitions between stable, cyclic and chaotic regimes. An example is the Hopf bifurcation, which marks the transition from a stable system to an oscillatory system (Strogatz 1994). Like the fold bifurcation, this bifurcation is signalled by critical slowing down (Chisholm and Filotas 2009): close to the bifurcation, perturbations lead to long transient oscillations before the system settles to the stable state.

Another class of bifurcations are the non-local bifurcations (Kuznetsov 1995) that occur if intrinsic oscillations bring the system to the border of the basin of attraction of an alternative attractor. Such basin-boundary collisions (Vandermeer and Yodzis 1999) are not associated with particular properties of stable or unstable points that can be analytically defined. We know of no explicit work on early-warning signals for such transitions. Nonetheless, the dynamics may be expected to change in a characteristic way before basin-boundary collisions occur. For instance, oscillations may become ‘stretched’, as the system dwells longer in the vicinity of the basin boundary, where rates of change are slower (Rinaldi and Scheffer 2000), implying increased autocorrelation. Finally, there is the phenomenon of phase locking between coupled oscillators. Again, alternative attractors are often involved (Vandermeer et al. 2001) and the corresponding bifurcations are associated with critical slowing down (Leung 2000), suggesting the existence of early-warning signals. Indeed, rising variance and flickering occur before an epileptic seizure, a phenomenon associated to the phase locking of firing in neural cells (see below).

Spatial patterns as early-warning signals

In addition to early-warning signals in time-series, there are particular spatial patterns that can arise before a critical transition. Many systems can be seen as consisting of numerous

coupled units each of which tends to take a state similar to that of the units to which it is connected. For instance, it is well known that financial markets affect each other. Also, the attitudes of individuals towards certain issues is affected by the attitudes of their peers (Holyst et al. 2002; Scheffer et al. 2003), and the persistence of species in habitat patches in a fragmented landscape depends on the presence of the same species in neighboring patches from which recolonization can happen (Bascompte and Sole 1996; Hanski 1998). In such systems, phase transitions may occur (Schroeder 1991; Solé et al. 1996) much as in ferromagnetic materials, where individual particles affect each others' spin. As gradual change in an external forcing factor (for example a magnetic field) drives the system closer to a transition, the distribution of the states of the units in such systems may change in characteristic ways. For instance, scale-invariant distributions of patch sizes occur close to a systemic transition, and there is a general tendency towards increased spatial coherence, measured as increased cross-correlation (or in oscillating units, resonance) among units before a critical event (Schroeder 1991; Solé et al. 1996).

Certain classes of spatial system deviate from this general pattern and can have other, more specific, indicators of imminent transitions. For instance, in systems governed by local disturbance (for example grazers foraging locally on vegetation patches), scale-invariant power-law structures that are found for a large parameter range vanish as a critical transition is approached (Kéfi et al. 2007a). In systems that have self-organized regular patterns (Turing 1952), critical transitions may be signalled by particular spatial configurations. For instance, models of desert vegetation show that as a critical transition to a barren state is neared, the vegetation becomes characterized by regular patterns because of a symmetry-breaking instability. These patterns change in a predictable way as the critical transition to the barren state is approached (Figure 2.3), implying that this may be interpreted as early-warning signal for a catastrophic bifurcation (Rietkerk et al. 2004).

In conclusion, when it comes to interpreting spatial patterns it is important to know which class of system is involved. Although broad classes have similar early-warning signals, there is no 'one-size-fits-all' spatial pattern announcing critical transitions.

Precursors of transitions in real systems

Most of the work on early-warning signals for critical transitions has so far been done using simple models, and empirical proof that critical slowing down occurs at bifurcations has been provided by controlled experiments with lasers (Tredicce et al. 2004) and neurons (Matsumoto and Kunisawa 1978). The question therefore remains of whether highly complex real systems such as the climate or ecosystems will show the theoretically expected early-warning signals. Results from elaborate and relatively realistic climate models including spatial dynamics and chaotic elements (Lenton et al. 2009) suggest that some signals might be robust in the sense that they arise despite high complexity and noisiness. Nonetheless, it is clearly more challenging to pick up early-warning signals in complex natural systems than in models. We now review some emerging results on the climate and ecosystems. Also, we highlight empirical successes in finding early-warning

signals of transitions in systems for which we have a relatively poor understanding of the mechanisms that drive the dynamics, such as the human brain and financial markets.

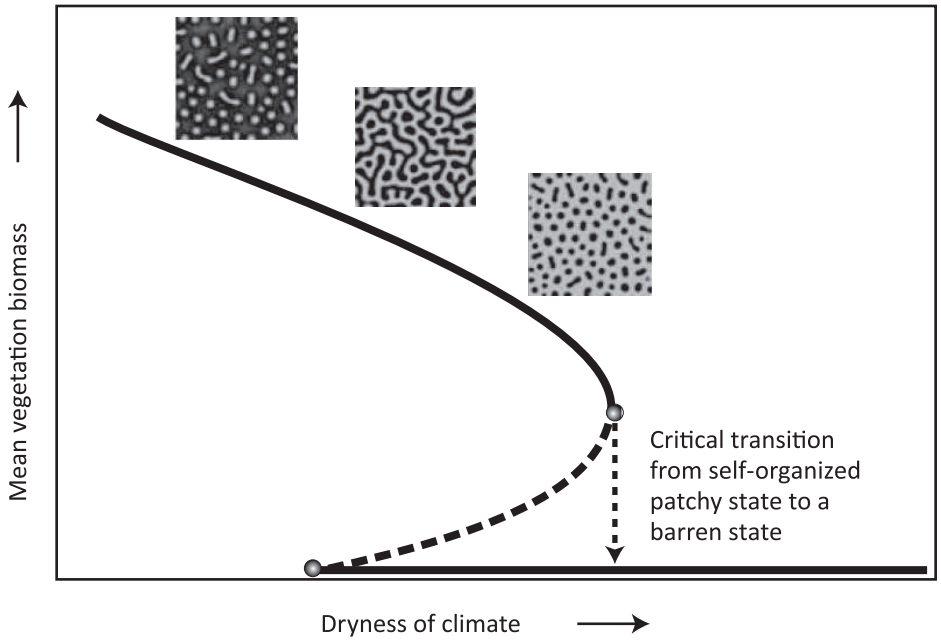

Figure 2.3 Ecosystems may undergo a predictable sequence of self-organized spatial patterns as they approach a critical transition. We show the modelled response of semi-arid vegetation to increasing dryness of the climate. Solid lines represent mean equilibrium densities of vegetation. The insets are maps of the pattern: the dark colour represents vegetation and the light colour represents empty soil. As the bifurcation point for a critical transition into a barren state is approached, the nature of pattern changes from maze-like to spots. [modified from Rietkerk et al. (2004)]

Climate

Interest in the possibility of critical transitions in the Earth system has been sparked by records of past climate dynamics revealing occasional sharp transitions from one regime to another (Alley et al. 2003). For instance, about 34 Myr ago the Earth changed suddenly from the tropical state in which it had been for many millions of years to a colder state in which Antarctica was glaciated, a shift known as the greenhouse–icehouse transition (Kump 2005; Liu et al. 2009; Tripati et al. 2005) (Figure 2.4). Also, glacial cycles tend to end with an abrupt warming (Luthi et al. 2008; Petit et al. 1999).

Uncertainty in reconstructing such dynamics remains considerable, and it is even more difficult to unveil the underlying mechanisms. Nonetheless, the sharpness of the shifts and the existence of positive feedbacks that, if strong enough, could cause self-propelling

change have led to the suggestion that these and other examples of rapid climate change could be explained as critical transitions (Alley et al. 2003; Lenton et al. 2008). Therefore, the reconstructed climate dynamics before such transitions are an obvious place to look for early-warning signals. In a recent analysis, a significant increase in autocorrelation was found in each of eight examples of abrupt climate change analyzed (Dakos et al. 2008) (Figure 2.4).

Another recent study suggests that flickering preceded the abrupt end of the Younger Dryas cold period (Bakke et al. 2009). Although the first part of this cold episode was quite stable, rapid alternations between a cold mode and a warm mode characterized the later part, and the episode eventually ending in a sharp shift to the relatively warm and stable conditions of the Holocene epoch (Clark et al. 2002). After examination of longer timescales, it has been suggested that the increasing Pleistocene climate variability may be interpreted as a signal that the near geological future might bring a transition from glacial–interglacial oscillations to a stable state characterized by permanent mid-latitude Northern Hemisphere glaciation (Crowley and Hyde 2008).

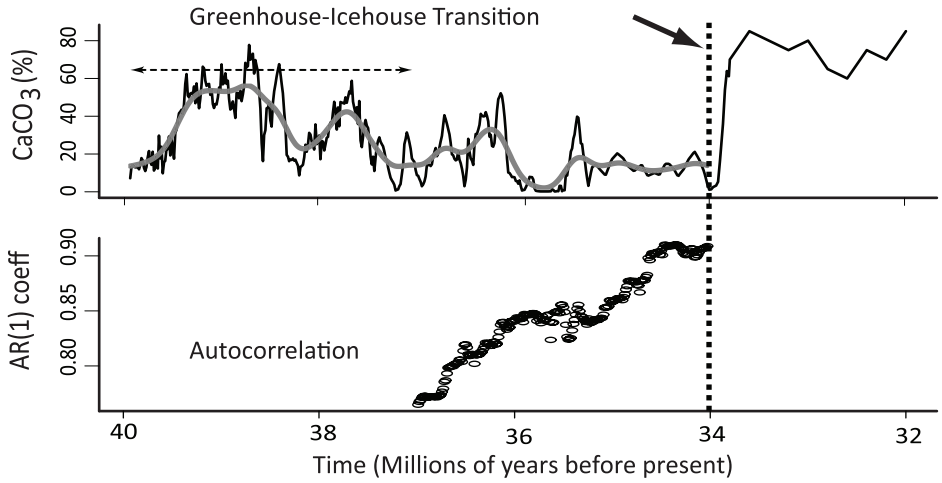

Figure 2.4 Critical slowing down indicated by an increase in lag-1 autocorrelation in climate dynamics. We show the period preceding the transition from a greenhouse state to an icehouse state on the Earth 34 Myr ago. The trends in the $CaCO_3$ concentration time-series removed by filtering before computing autocorrelation (AR(1) coefficient) are represented by the gray line. The horizontal dashed arrow marks the width of the moving window used to compute the autocorrelation. [modified from Dakos et al. (2008)]

Ecosystems

In ecology, critical transitions have become a major focus of research. The existence of alternative attractors has been demonstrated experimentally in lakes (Scheffer and van Nes 2007), and a large body of work now suggests that alternative stable states separated

by critical thresholds also occur in ecosystems ranging from rangelands to marine systems (Scheffer et al. 2001; Scheffer and Carpenter 2003). Work on early-warning signals in this field is just emerging. As mentioned earlier, in dry regions self-organization can lead to particular spatial patterns under some conditions. Here the complete loss of vegetation is an important transition, as recovery from the barren state may require more rain than is needed to preserve the last patches. There is good evidence to support the idea that a regular pattern characterized by spots of vegetation signals the proximity of a threshold to

BOX 2.3 | The relation between Critical slowing down, increased autocorrelation and increased variance

Critical slowing down will tend to lead to an increase in the autocorrelation and variance of the fluctuations in a stochastically forced system approaching a bifurcation at a threshold value of a control parameter. The example described here illustrates why this is so. We assume that there is a repeated disturbance of the state variable after each period Δt (that is, additive noise). Between disturbances, the return to equilibrium is approximately exponential with a certain recovery speed, λ. In a simple autoregressive model this can be described as follows:

$$x_{n+1} - \overline{x} = e^{\lambda \Delta t} (x_n - \overline{x}) + \sigma \varepsilon_n$$

$$y_{n+1} = e^{\lambda \Delta t} y_n + \sigma \varepsilon_n$$

Here y_n is the deviation of the state variable x of the equilibrium $\overline{x}$, ε_n is a random number from a standard normal distribution and σ is the standard deviation.

If λ and Δt are independent of y_n, this model can also be written as a first-order autoregressive (AR(1)) process:

$$y_{n+1} = \alpha y_n + \sigma \varepsilon_n$$

The autocorrelation $\alpha \equiv e^{\lambda \Delta t}$ is zero for white noise and close to one for red (autocorrelated) noise. The expectation of an AR(1) process $y_n = c + \alpha y_n + \sigma \varepsilon_n$ is

$$E(y_{n+1}) = E(c) + \alpha E(y_n) + E(\sigma \varepsilon_n) \rightarrow \mu = c + \alpha \mu + 0 \rightarrow \mu = \frac{c}{1-\alpha}$$

For c = 0, the mean equals zero and the variance is found to be

$$Var(y_{n+1}) = E(y_n^2) - \mu^2 = \frac{\sigma^2}{1-\alpha^2}$$

Close to the critical point, the return speed to equilibrium decreases, implying that λ approaches zero and the autocorrelation α tends to one. Thus, the variance σ tends to infinity. These early-warning signals are the result of critical slowing down near the threshold value of the control parameter.

such catastrophic desertification (Rietkerk et al. 2004). Other studies show how, in line with model predictions, vegetation-patch size distributions lose their scale-free structures and become characterized by truncated power laws as a transition to a barren state is approached (Kéfi et al. 2007a).

Early-warning signals are also being found for destabilization of exploited fish stocks. It has been shown that harvesting tends to lead to increased fluctuations in fish populations (Hsieh et al. 2006). This increase in variance is most likely due to increased intrinsic growth rates in the resulting populations, as older age classes are preferentially harvested and the younger fish have higher overall intrinsic rates of change (Anderson et al. 2008). Such higher growth rates lead to increased nonlinearity as they drive populations towards the critical transition from a stable to a cyclic or chaotic regime, as mentioned earlier.

Asthma attacks and epileptic seizures

Abrupt transitions in physiology include epileptic seizures and asthma attacks. In the case of asthma, it has been shown that human lungs can display a self-organized pattern of bronchoconstriction that might be the prelude to dangerous respiratory failure, and which resembles the pattern formation in collapsing dry-land vegetation (Venegas et al. 2005).

Epileptic seizures happen when neighboring neural cells all start firing in synchrony. Predicting such seizures far in advance remains very difficult (Mormann et al. 2007). However, before the seizure becomes noticeable several characteristic changes in neural activity can occur. For instance, minutes before an epileptic seizure, variance in the electrical signal recorded by electroencephalography may increase (McSharry et al. 2003) (Figure 2.5). More subtle changes (reduced dimensionality of the signal) occur up to 25 min before epileptic seizures, reflecting a continuous increase in the degree of synchronicity (and thus correlation) between neural cells (Elger and Lehnertz 1998). Also, hours before the seizure, mild energy bursts can occur in the brain followed by frequent symptomless seizures too small for the patients to notice (Litt et al. 2001). This resembles patterns of flickering in which smaller transient excursions to the vicinity of an alternative state precede the upcoming major shift.

Finance

The prediction of shifts in financial markets is a heavily researched area. In this field, the discovery of predictability quickly leads to its elimination, as profit can be made from it, thereby annihilating the pattern. As a result, although there is always some predictability that can be exploited by specialists (Brockner 1992; Lo et al. 2000), overall financial markets are notoriously difficult to predict (LeBaron 2000). Nonetheless, many papers in the financial literature show that market dynamics may contain information presaging major events (Bates 1991; Bates 1996; Hens and Schenk-Hoppe 2009). For instance, some events are preceded by measures of increased trade volatility (for example the spread between the value of put options and the value of call options (Bates 1991; Bates 1996)), but a 'volatility calm' before the abrupt change can also happen (Arvelund 2002; Bates 1991). A prominent volatility-based early-warning signal in financial markets is the VIX, or 'fear', index (Lo et al. 2000; Whaley 1993). There is also evidence of systematic

relationships in variance and first-order autocorrelation (Lebaron 1992), although lead–lag relationships tend to be erratic. Finally, increased spatial coherence may be an early-warning of major transitions. There is evidence that correlation increases across returns to different stocks in a falling market and patterns embodied in options prices may serve as a type of early-warning indicator (Hong and Stein 2003).

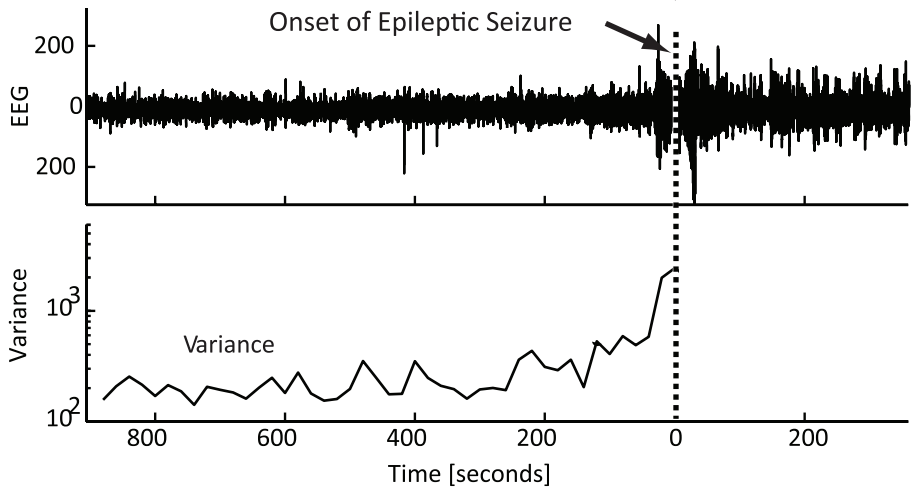

Figure 2.5 An example of the subtle changes in brain activity before an epileptic seizure that may be used as an early-warning signal. The epileptic seizure clinically detected at time 0 is announced minutes earlier in an electroencephalography (EEG) time-series by an increase in variance. [modified from McSharry et al. (2003)]

Outlook

As our overview shows, similar early-warning signals can appear in widely different systems: flickering may occur before epileptic seizures, the end of a glacial period and in lakes before they shift to a turbid state; self-organized patterns can signal an imminent transition in desert vegetation and in asthma; increased autocorrelation may indicate critical slowing down before all kinds of climatic transitions and in ecosystems; and increased variance of fluctuation may be a leading indicator of an epileptic seizure or instability in an exploited fish stock. Some of these complex systems are better understood than others. However, turning the reasoning around, it could be argued that the generic character of some early-warning signals suggests that these transitions may be somehow related to bifurcations, where universal laws of dynamical systems govern the pattern.

The theoretical basis of the work on early-warning signals in simple models is quite strong, and the first results from more elaborate models suggest that similar signals may arise in highly complex systems (Lenton et al. 2009). Nonetheless, more work is needed to find out how robust these signals are in situations in which spatial complexity, chaos and

stochastic perturbations govern the dynamics. Also, detection of the patterns in real data is challenging and may lead to false positive results as well as false negatives. False negatives are situations in which a sudden transition occurred but no early-warning signals could be detected in the behavior before the shift. This can happen for different reasons. One possibility is that the sudden shift in the system was not preceded by a gradual approach to a threshold. For instance, it may have remained at the same distance from the bifurcation point, but been driven to another stable state by a rare extreme event. Also, a shift that is simply due to a fast and permanent change of external conditions (Box 2.1 panel a of Figure) cannot be detected from early-warning signals. A second class of false negatives may arise from the statistical difficulty of picking up the early-warning signal. For instance, the detection of increased autocorrelation may require long time-series (Bence 1995). A third difficulty arises if the external regime of perturbations changes over time. This may distort or counteract the expected signals. False positives occur if a supposed early-warning signal is not the result of approaching a bifurcation. This may happen by chance or may result from a confounding trend within the system or in the external regime of perturbations.

Importantly, most of the indicators we have identified signal a wide class of impending transitions in complex systems. The same signals may even occur, albeit in a less pronounced way, as the system approaches a threshold that is not related to catastrophic bifurcations (Box 2.1 panel b of Figure) (Berglund and Gentz 2006). This has been shown for critical slowing down (van Nes and Scheffer 2007), and may also be true for autocorrelation and variance. Nonetheless, such non-catastrophic thresholds are related to the more spectacular catastrophic ones (Box 2.1), and systems may in fact move from one type of threshold to another. In conclusion, most early-warning signals are indicators of proximity to a broad class of thresholds, where small forces can cause major changes in the state of a complex system.

The idea that critical transitions across a range of systems may be related in the sense that they can be described by similar equations, implying similar possible bifurcations and early-warning signals, implies an exciting opportunity for connecting work across disciplines. However, there are many challenges to be overcome. For instance, filtering techniques for time-series (Box et al. 2008) are necessary to increase the sensitivity of indicators while preventing false positives (Dakos et al. 2008), but results depend on parameter choices in filtering (Dakos et al. 2008; Lenton et al. 2009). Therefore, it would be useful to build a set of reliable statistical procedures to test whether an increase in autocorrelation, for example, is significant. We note also that most of the signals we have discussed should still be interpreted in a relative sense. For instance, although autocorrelation is predicted to approach unity at a fold bifurcation, measurement noise will tend to reduce correlations. Also, perturbations will often trigger a transition well before a bifurcation point is reached. Thus, although a trend in the indicators may serve as a warning, the actual moment of a transition remains difficult to predict. A key issue when it comes to practical application is the question of whether a signal can be detected sufficiently early for action to be taken to prevent a transition or to prepare for one (Biggs et al. 2009b). Understanding spatial early-warning signals better might be particularly useful in this respect, as a spatial pattern contains much more information than does a

single point in a time-series, in principle allowing shorter lead times (Guttal and Jayaprakash 2009).

In any case, generic early-warning signals will remain only one of the tools we have for predicting critical transitions. In systems in which we can observe transitions repeatedly, such as lakes, rangelands or fields such as physiology, we may empirically discover where the thresholds are. Nonetheless, some extremely important systems, such as the climate or ocean circulation, are singular and afford us limited opportunity to learn by studying many similar transitions. Also, we are far from being able to develop accurate models to predict thresholds in most complex systems, ranging from cells to organisms, ecosystems or the climate. We simply do not understand all the relevant mechanisms and feedbacks sufficiently well in most cases. The generic character of the early-warning signals we have discussed here is reason for optimism, as they occur largely independently of the precise mechanism involved. Thus, if we have reasons to suspect the possibility of a critical transition, early-warning signals may be a significant step forwards when it comes to judging whether the probability of such an event is increasing.

Chapter 3

Spatial correlation as leading indicator of catastrophic shifts

Generic early-warning signals such as increased autocorrelation and variance have been demonstrated in time-series of systems with alternative stable states approaching a critical transition. However, lag times for the detection of such leading indicators are typically long. Here we show that increased spatial correlation may serve as a more powerful early-warning signal in systems consisting of many coupled units. We first show why from the universal phenomenon of critical slowing down, spatial correlation should be expected to increase in the vicinity of bifurcations. Subsequently, we explore the applicability of this idea in spatially explicit ecosystem models that can have alternative attractors. The analysis reveals that as a control parameter slowly pushes the system towards the threshold, spatial correlation between neighboring cells tends to increase well before the transition. We show that such increase in spatial correlation represents a better early-warning signal than indicators derived from time-series provided that there is sufficient spatial heterogeneity and connectivity in the system.

This chapter is based on the paper: V. Dakos, E. H. van Nes, R. Donangelo, H. Fort and M. Scheffer (2010). Spatial correlation as leading indicator of catastrophic shifts. *Theoretical Ecology* 3(3): 163-174. We would like to thank Sasha Panfilov and Nobuto Takeuchi for valuable discussions, as well as Sonia Kéfi, Andrea Downing, Reinette Biggs and Jordi Bascompte for their valuable comments.

Introduction

Abrupt extensive changes have been identified in a range of ecosystems (Scheffer et al. 2001). Some of these shifts are suggested to be critical transitions between alternative states (Scheffer and Carpenter 2003). Such critical transitions have been described, among others, for lakes (Carpenter 2005; Scheffer 1998), for marine and coastal environments (Daskalov et al. 2007; Petraitis and Dudgeon 1999), for terrestrial communities (Handa et al. 2002; Schmitz et al. 2006), and for semi-arid ecosystems (Narisma et al. 2007; Rietkerk et al. 2004).

Predicting critical transitions is a difficult task (Clark et al. 2001). However, recent theoretical work suggests that there may be generic leading indicators for critical transitions even when mechanistic insight is insufficient to build reliable predictive models (Scheffer et al. 2009). The underlying principle of most of these indicators is a phenomenon known in dynamical systems theory as 'critical slowing down' (Strogatz 1994). Critical slowing down occurs in most bifurcation points when the dominant eigenvalue characterizing the rates of change around the equilibrium becomes zero. This implies that approaching such critical points the system becomes slower in recovering from perturbations (Held and Kleinen 2004; van Nes and Scheffer 2007; Wissel 1984). In reality all systems are permanently subject to disturbances. It has been shown in models that in such situations one should expect that there is an increase in autocorrelation (Held and Kleinen 2004; Ives 1995; Kleinen et al. 2003) and in variance (Carpenter and Brock 2006) in the pattern of fluctuations as a bifurcation is approached.

A major drawback of such signals is that in practice real-time detection may come too late to take action, as long time-series of good quality and resolution are needed (Biggs et al. 2009b; Scheffer et al. 2009). In theory, spatial patterns may provide more powerful leading indicators, as they contain more information than a single data point in a time-series (Donangelo et al. 2010; Guttal and Jayaprakash 2009). Indeed, various studies have shown spatial signatures of upcoming transitions. For systems that have self-organized pattern formation, there are specific signals (Kéfi et al. 2007a; Rietkerk et al. 2004; von Hardenberg et al. 2001). However, these signals tend to be specific to the particular mechanism involved (Pascual and Guichard 2005) and cannot be generalized to other systems. In a stochastic extinction-colonization model, Oborny et al. (2005) showed that spatial variance of population densities increases near the critical extinction threshold. In similar stochastic spatial metapopulation models, spatial correlation increases prior to species extinction as a function of occupied patches (Bascompte 2001), transient time to extinction diverges near the spatial threshold (Gandhi et al. 1998; Ovaskainen et al. 2002) and the size of maximum patches declines as habitat fragmentation increases (Bascompte and Sole 1996). Recently it has been shown that rising variance accompanied by a peak in skewness preludes the transition of an underexploited resource to overexploitation in a spatial model with local alternative stable states (Guttal and Jayaprakash 2009).

Here we first explore whether critical slowing down might in theory generate spatial signals in spatially heterogeneous ecosystems that can go through a critical transition.

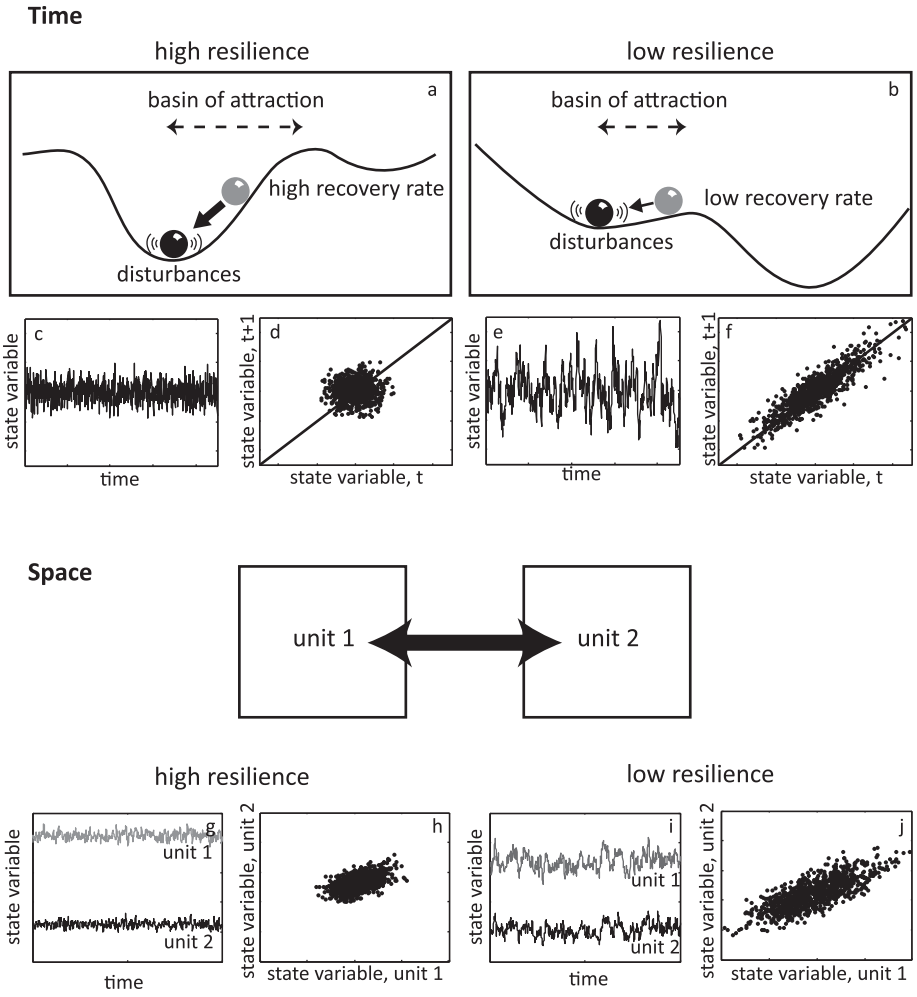

Figure 3.1 ***Time***: Balls and cups representation of the stability properties of a system exhibiting alternative stable states. (**a**) At high resilience, small disturbances to the equilibrium are counterbalanced by high recovery rates back to equilibrium. As a result, when monitoring the state variable in time, the collected time-series is characterized by low correlation between subsequent values (panels **c**, **d**). (**b**) At low resilience, the basin of attraction shrinks and the system is closer to the transition point. Small disturbances not only increase the chance of pushing the system to the alternative state, but they are not anymore effectively damped due to low recovery rates back to equilibrium. The resulting time-series is highly autocorrelated (panels **e**, **f**). ***Space***: Dynamics of two strongly connected units embedded in a hypothetical spatial system. When the system is far away from the transition (high resilience), dynamics in each unit are defined more by their own reaction processes than by dispersion (panel **g**) and appear weakly correlated (panel **h**). Close to the transition (low resilience), reaction processes are minimized due to critical slowing down and dispersion dominates (panel **i**). Units now are strongly correlated (panel **j**).

In particular, we propose a direct link between critical slowing down and increasing spatial correlation prior to a transition, analogous to what has been demonstrated in non-spatial systems (Scheffer et al. 2009). We show that an increase in spatial correlation can serve as an early-warning signal prior to a bifurcation point. Even though such divergence in long-range coherence has been shown in phase transitions (Fisher 1974; Solé et al. 1996; Stanley 1971), to our knowledge there is no work that investigates this phenomenon in spatially-explicit ecological models of alternative stable states as the ones we use in this study. Furthermore, we compare spatial and temporal correlation as leading indicators of transitions in three different spatially-explicit models and we show that their performance depends on the assumptions over the underlying connectivity and heterogeneity of the landscape.

Spatial consequences of critical slowing down

In models bifurcations represent thresholds where a tiny change in a parameter can lead to a qualitative change in the behavior of the system (Strogatz 1994). At such critical points the dominant eigenvalue characterizing the rates of change around the equilibrium becomes zero. This implies that approaching such bifurcation points, the system becomes increasingly slow in recovering from small perturbations back to its equilibrium. In the case of the classical fold bifurcation, the consequences can be seen intuitively from stability landscapes (Figure 3.1). The size of the basin of attraction around an equilibrium shrinks as the bifurcation point is approached by slowly tuning a control parameter (till the basin of attraction of one of the two equilibria disappears; Figure 3.1a, b). However, also the slopes of the stability landscape representing the return rate to equilibrium (engineering resilience) change. As the basin shrinks, these slopes become less steep before they eventually flatten out at the threshold. The corresponding smooth decline in return rates represented by eigenvalues happens in any continuous model approaching a fold bifurcation (Wissel 1984), and analysis of various models shows that such slowing down typically starts already far from the bifurcation point (Chisholm and Filotas 2009; van Nes and Scheffer 2007). If one exposes such a system to stochastic perturbations which are normally distributed and in the limit of the equilibrium so that the linear approximation still holds, slowing down implies that the state of the system at any given moment becomes more and more like its past state, as the return rate to equilibrium goes to zero at the bifurcation (Figure 3.1d, f).

What might be the consequence of critical slowing down in a system where we have many coupled units, each with alternative stable states? This may correspond for instance to a spatial grid of an ecosystem model with alternative stable states. If we assume that the conditions are different for each grid cell, i.e. the intrinsic equilibrium states of the units in isolation are different for each grid cell for instance due to different environmental conditions, then the diffusive exchange between the units will continuously tend to reduce such variation between cells. More precisely, the dynamics between two neighboring units (x_1 and x_2) will be governed by a reaction part (f) and a diffusion part governed by a diffusion rate (D):

$$\frac{dx_1}{dt} = f(x_1, p_1, c) + D(x_2 - x_1) \quad \text{(eq1)}$$

$$\frac{dx_2}{dt} = f(x_2, p_2, c) + D(x_1 - x_2) \quad \text{(eq2)}$$

where p_i is a parameter that defines heterogeneity between the two units and c is the control parameter that drives the system to the transition point. The Jacobian matrix of this system at equilibrium (x_1^*, x_2^*) is:

$$J = \begin{bmatrix} f'(x_1^*, p_1, c) - D & D \\ D & f'(x_2^*, p_2, c) - D \end{bmatrix},$$

with eigenvalues:

$$\lambda_1 = \frac{f'(x_1^*, p_1, c) + f'(x_2^*, p_2, c)}{2} - D + \frac{1}{2}\sqrt{\left(f'(x_1^*, p_1, c) - f'(x_2^*, p_2, c)\right)^2 + (2D)^2} \quad \text{(eq3)}$$

$$\lambda_2 = \frac{f'(x_1^*, p_1, c) + f'(x_2^*, p_2, c)}{2} - D - \frac{1}{2}\sqrt{\left(f'(x_1^*, p_1, c) - f'(x_2^*, p_2, c)\right)^2 + (2D)^2} \quad \text{(eq4).}$$

When connectivity is very low, we may assume that $D << f'(x_i^*, p_i, c)$ which renders the eigenvalues of the system equal to: $\lambda_1 \approx f'(x_1^*, p_1, c)$ and $\lambda_2 \approx f'(x_2^*, p_2, c)$. This assumption basically implies that the two units can be regarded as being disconnected. Under these conditions, each unit is governed by its own dynamics and shifts at a different critical threshold c_i. Changes in each unit are independent from each other. As a consequence one would expect to find no correlation between units.

When there is exchange between the units, units are no longer independent. If connectivity is strong, the critical thresholds at which each unit shifts converge ($c_1 \approx c_2 \approx c^*$). When the system is far away from the transition, units are governed by both 'reaction' and diffusion processes (eq3, eq4). Close to the transition point, 'reaction' within each unit becomes smaller due to critical slowing down ($f'(x_i^*, p_i, c^*) \rightarrow 0$). On the contrary diffusion is independent of the proximity to the transition but depends only on the gradient between the two units $(x_1^* - x_2^*)$. We may thus assume that at this point $D >> f'(x_i^*, p_i, c^*)$, and we may neglect $f'(x_i^*, p_i, c^*)$: the eigenvalues of the system approach $\lambda_1 \approx 0$ and $\lambda_2 \approx -2D$. This means that the system slows down each unit and diffusion will dominate, equalizing differences between units with rate $2D$ (the second eigenvalue characterizes the dynamics between the two units). Now, the state in a unit will be strongly dependent on that of its neighbor. As a result, units will become more strongly correlated close to the transition (Figure 3.1g-j).

Methods

Models description

We adapt three well-studied minimal models that can have alternative stable states (Table 3.1). The first model describes a logistically growing resource with fixed grazing rate (May 1977; Noy-Meir 1975). It describes the transition of an underexploited system to overexploitation as grazing pressure crosses a threshold. The second model describes the nutrient dynamics of a eutrophic lake (Carpenter et al. 1999). At low nutrient input rates, the lake remains oligotrophic through nutrient losses to sediment or hypolimnion. At increased nutrient loading, there is a high recycling of nutrients from the sediment or hypolimnion back to the water column due to lower oxygen levels and the lake may suddenly become eutrophic. The third model describes the transition of a clear water shallow lake dominated by macrophytes to a turbid water state where macrophytes are practically absent (Scheffer 1998). It models the interactions between macrophyte coverage and turbidity of a shallow lake.

By adding a dispersion term, we can extend the models in two dimensional space (Okubo 1980). As ecosystems are usually patchy, we assume that space is discrete and the dynamics take place in a $n \times n$ squared lattice which consists of evenly spaced coupled cells (Keitt et al. 2001; Van Nes and Scheffer 2005). Each cell can individually switch to its alternative state and is connected with its four neighboring cells. Connectivity is modeled as exchange of matter or biomass among neighboring cells mimicked through a simple diffusive process. Spatial heterogeneity in the landscape (e.g. topographic situation, local hydrological differences) is introduced in the model by randomly and independently setting a parameter $p_{i,j}$ in each cell (Table 3.1). We also assume there are random independent disturbances in each cell. Thus, the general form of our models is:

$$dX_{i,j} = f(X_{i,j}, p_{i,j}, c)dt + D(X_{i+1,j} + X_{i-1,j} + X_{i,j+1} + X_{i,j-1} - 4X_{i,j})dt + \sigma dW_{i,j} \qquad \text{(eq5)},$$

where f is the deterministic equation of the non-spatial model that governs the dynamics of the state variable $X_{i,j}$ at each cell as a function of parameter $p_{i,j}$ which introduces heterogeneity among cells, and as a function of c, the control parameter which causes each cell individually to switch between alternative states. D is the dispersion coefficient and $dW_{i,j}$ a white noise process independently added to each cell with a scaling factor σ (Table 3.1). To prevent edge effects we define periodic boundaries for the total lattice.

Models analysis

All simulations started with random initial conditions, where all cells were in the same state. We then increased a control parameter in small steps up till a critical value where the shift occurs. After each stepwise change in the control parameter we ran the model for 1,000 time steps to minimize transient effects. At the end of the 1,000 time steps, we used the last achieved local values of the state variables in each cell of the whole grid (50 $\times$ 50 cells) to calculate the spatial correlation of neighboring cells. This index was defined as the two-point correlation for all pairs of cells separated by distance 1, using Moran's co-

Table 3.1 Models, parameters and their values used in this study

Model and Parameter	Definition and Value
Overharvesting model (May, 1977)	
$dX_{i,j} = (a - bX_{i,j} + c\frac{X_{i,j}^p}{X_{i,j}^p + 1})dt + D(X_{i+1,j} + X_{i-1,j} + X_{i,j+1} + X_{i,j-1} - 4X_{i,j})dt + \sigma dW_{i,j}$	
$X_{i,j}$	resource biomass; state variable
K	carrying capacity, (10)
$r_{i,j}$	maximum growth rate, parameter introducing spatial heterogeneity at gridcell (i,j), (range: 0.6-1)
c	maximum grazing rate; control parameter, (1-3)
D	diffusion rate, (range: 0-1)
σ	SD of white noise, (0.1)
$dW_{i,j}$	white noise; uncorrelated in each gridcell (i,j)
Eutrophication model (Carpenter et al., 1999)	
$dX_{i,j} = (rX_{i,j}(1 - \frac{X_{i,j}}{K}) - c\frac{X_{i,j}^2}{X_{i,j}^2 + 1})dt + D(X_{i+1,j} + X_{i-1,j} + X_{i,j+1} + X_{i,j-1} - 4X_{i,j})dt + \sigma dW_{i,j}$	
$X_{i,j}$	nutrient concentration; state variable
α	nutrient loading rate; control parameter, (0.1-0.9)
r	maximum recycling rate, (1)
b_{ij}	nutrient loss rate; parameter introducing spatial heterogeneity at gridcell (i,j), (range: 0.8-1.2)
p	Hill coefficient, (8)
D	diffusion rate, (range: 0-1)
σ	SD of white noise, (0.01)
$dW_{i,j}$	white noise; uncorrelated in each gridcell (i,j)
Vegetation-Turbidity model (Scheffer, 1998)	
$dV_{i,j} = rV_{i,j}(1 - V_{i,j}\frac{h_E^p + E_{i,j}^p}{h_E^p})dt + D_V(V_{i+1,j} + V_{i-1,j} + V_{i,j+1} + V_{i,j-1} - 4V_{i,j})dt + \sigma dW_{Vi,j}$	
$E_{i,j} = \frac{E_o h_v}{h_V + V_{i,j}}$	
$E_{i,j}$	water turbidity; state variable
$V_{i,j}$	vegetation cover; state variable
$h_{E,ij}$	half-saturation turbidity constant, parameter introducing spatial heterogeneity at gridcell (i,j), (range: 1-3)
E_0	background turbidity; control parameter, (2-12)
r_V	maximum vegetation growth rate, (0.5)
h_V	half-saturation vegetation cover constant, (0.2)
p	Hill coefficient, (4)
D	diffusion rate, (range: 0-1)
σ	SD of white noise, (0.01)
$dW_{Vi,j}$	white noise; uncorrelated in each gridcell (i,j)

efficient (Legendre and Fortin 1989):

$$C_2(\delta) = \frac{n\sum_{i=1}^{n}\sum_{j=1}^{n} w_{i,j}(x_i - \bar{x})(x_j - \bar{x})}{W\sum_{j=1}^{n}(x_{i,j} - \bar{x})^2} \quad \text{(eq6)},$$

in which we associated a weight $w_{i,j}$ to each pair of cells (x_i, x_j) which takes the value of 1 for neighboring cells and 0 otherwise. W is the total number of pairs of neighboring cells. To test how parsimonious spatial correlation between neighboring cells for indicating the proximity to a transition is compared to spatial correlation between cells at higher distances, we also estimated spatial correlation at higher lags (δ up to 25). We quantified the increase of spatial correlation at higher distances by estimating the correlation length ψ from the exponential fit $exp(-\delta/\psi)$. The correlation length ψ describes the distance over which the behavior of a macroscopic variable is affected by the behavior of another (Solé et al. 1996). A growing correlation length ψ indicates that spatial correlation increases at longer distances.

Since we were interested in comparing changes in the spatial correlation between cells to changes in the temporal autocorrelation within cells (another potential early-warning signal), we also tracked 25 randomly chosen cells (1% of the total lattice) over the last 100 time steps of each run to estimate the temporal autocorrelation at-lag-1 (Held and Kleinen 2004). We thus used an equal amount of information for comparison of the spatial and temporal indicators: 1 $\times$ 2,500 cells versus 100 $\times$ 25 cells. We calculated temporal autocorrelation using the mean of the autocorrelation at-lag-1 estimated at each of the 25 sampled cells (see simulation scheme in Appendix Figure A3.1). To compare the performance of the spatial and temporal indicators, we quantified their trend using the nonparametric Kendall τ rank correlation of the control parameter and the spatial and temporal correlation estimates.

We explored three different levels of heterogeneity (Table 3.1): (1) no spatial heterogeneity ($p_{i,j}$ equal in all cells), (2) low spatial heterogeneity ($p_{i,j}$ drawn from a uniform distribution with low variance), and (3) high spatial heterogeneity ($p_{i,j}$ drawn from a uniform distribution with high variance). In each of these settings we studied the effect of different levels of connectivity (mimicked by the diffusive exchange term D=[0, 0.001, 0.0025, 0.005, 0.01, 0.025, 0.05, 0.1, 0.25, 0.5, 1]).

Since we are interested in signals that warn *before* the shift, we excluded the dynamics during the transition from our analysis. In spatial heterogeneous systems, different cells may shift at different times. Therefore it is not obvious how a threshold point should be determined. Here, we defined a threshold simply as the point when the first cell shifted to the alternative state (see Appendix Figure A3.2). This ensures that we are really focusing on early-warning signals rather than detecting changes that occur during the shift itself.

All simulations and statistical analyses were performed in MATLAB (v. 7.0.1). We solved the stochastic equations using an Euler-Murayama integration method with Ito calculus (Grasman 1999).

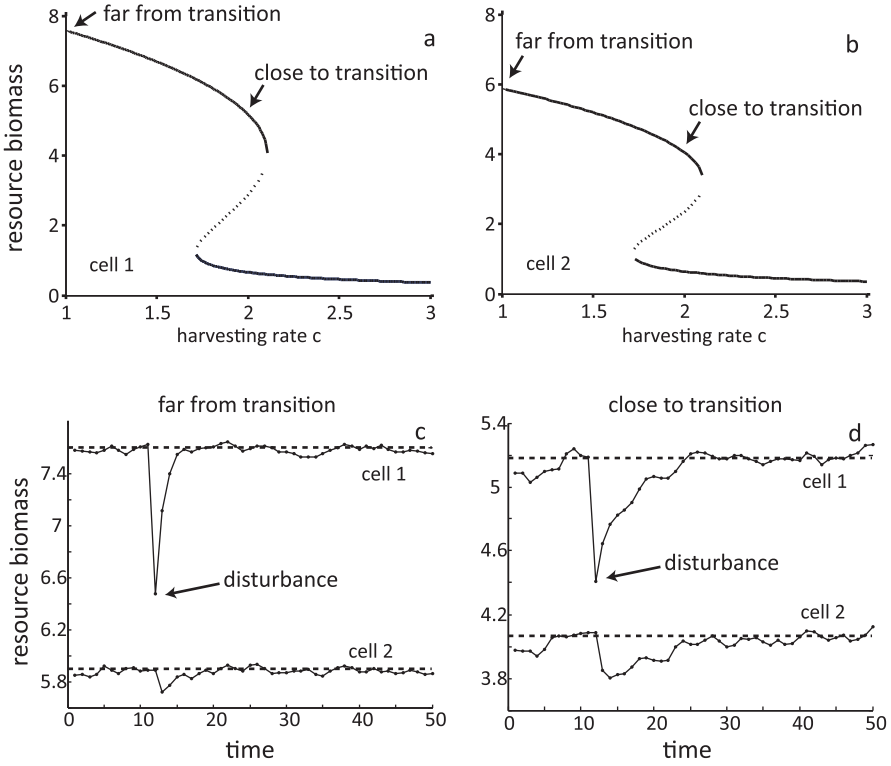

Figure 3.2 Overharvesting model by May (1977) implemented in a simplistic 2 cells spatial system. (**a**, **b**) Equilibrium values for resource biomass in both cells as a function of control parameter (harvesting rate *c*) that shifts the system from high resource biomass to low resource biomass. (**c**, **d**) Perturbation experiment (in both cases 15% reduction in biomass) showing the effect of "critical slowing down" in cell 1 for a highly connected system far and close to the transition. The dotted lines indicate the deterministic equilibrium value of the cell. (Parameters used: D=0.5 K_1=10, K_2=6 r=1, c=2 in **c**, c=1 in **d**).

Results

A simplified spatial scenario

To see how critical slowing down affects dynamics in space in a transparent way, we first implemented the overharvesting model of May (1977) in only two cells. In this oversimplified spatial scenario, the two cells have different carrying capacities and are harvested with the same rate. When connectivity is low, each cell shifts at a different

harvesting rate. When the system is strongly connected, the two cells shift at the same harvesting pressure (Figure 3.2a, b).

We tested whether critical slowing down occurs despite high connectivity by performing a perturbation experiment (van Nes and Scheffer 2007). Indeed, biomass in the perturbed cell 1 recovered slower before the transition compared to a situation far from the transition (Figure 3.2c, d). Note that, changes in cell 1 strongly affect dynamics of cell 2 (Figure 3.2c). This is in line with our theoretical prediction that close to the transition, units become less responsive to their own dynamics and more influenced by the dynamics of neighboring units. Also, it can be seen that there is a conspicuous increase in similarity as the system approaches the transition provided that there is sufficient connectivity (D) (Figure 3.3a) and spatial heterogeneity (δ) (Figure 3.3b).

Correlation in space and time

In the previous analysis we showed that critical slowing down causes the state of two cells to converge close to a transition. We now explore the effect of critical slowing down in the complete spatial models. Simulations show that indeed spatial correlation between neighboring cells increased prior to the transition in a wide range of conditions for all three models (see Appendix Figure A3.3). For example, in the vegetation-turbidity model spatial correlation between neighboring cells started to increase well before the shift (Figure 3.4a, b). As expected, with weakly connected cells (Figure 3.4c, d), spatial correlation between neighboring cells did not show a strong increase before the transition.

Interestingly, temporal autocorrelation performed in a somehow complementary way compared to spatial correlation (see also Appendix Figure A3.4); when connectivity was high, temporal autocorrelation showed a weaker trend with the control parameter (Kendall τ=0.26, $P<0.05$) than its spatial analog (Kendall τ=0.83, $P<0.05$) (Figure 3.4b). However, trends in temporal autocorrelation (Kendall τ=0.31, $P<0.05$) outperformed trends in spatial correlation when connectivity was low (Kendall τ=0.1, $P>0.05$) (Figure 3.4d).

To check how generic these results are, we systematically analyzed the trends in the spatial and temporal correlations up to the transition for a range of dispersion and heterogeneity conditions (Figure 3.5). The Kendall τ correlation statistic was used to quantify the strength of the trend of the correlation indicators for every level of dispersion rate. A higher value of this trend-statistic implies a more significant increase in the indicator prior to the transition. Despite some differences in the three models, two general patterns emerged: 1) high connectivity between patches favored a strong increase in the spatial correlation of neighbors, especially when there was inherent heterogeneity in the environment; 2) high environmental heterogeneity reduced the strength of the temporal correlation. The latter pattern is due to the fact that in this situation each cell shifts at a different level of the control parameter, implying that the autocorrelation measured at each cell is different, and consequently the estimate of their mean is noisy. Connectivity had no apparent effect on the trends in temporal autocorrelation.

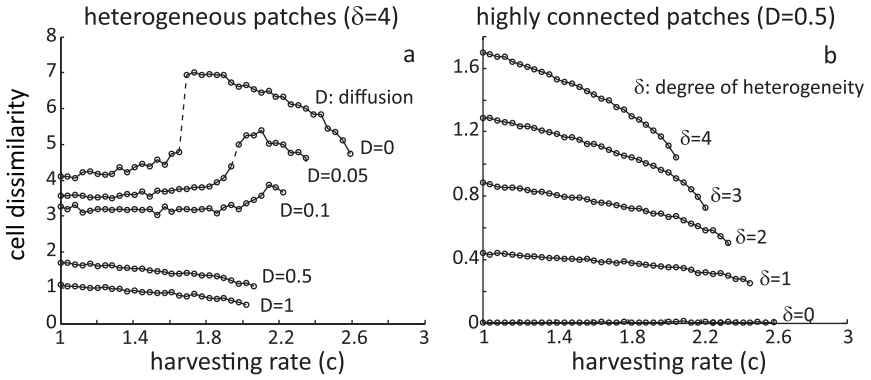

Figure 3.3 Effect of connectivity (dispersion rate *D*) and heterogeneity (δ defined as the difference in the carrying capacities K_i of the two cells) on the dissimilarity between neighbors for increasing levels of harvesting rate (*c*) in the 2 cell spatial overharvesting model by May (1977). (**a**) When connectivity is high (*D>0.1*) cells not only shift in sync, but they are becoming increasingly similar prior to the transition. (**b**) Such increase in similarity is greater the more inherently heterogeneous the cells are ($\delta > 0$).

We checked whether an increase in spatial correlation between neighboring cells for indicating the proximity to a transition is more parsimonious compared to changes in spatial correlation between cells at higher distances. We found that spatial correlation also at higher lags does indeed tend to increase prior to a transition, whereas after the transition the correlation is limited only to a few neighboring cells (see Appendix Figure A3.5a, b). Such increase in long range coherence is reflected in the growing correlation length ψ which can also serve as leading indicator of an imminent shift (Appendix Figure 3.5c). However, the almost 1:1 relationship between the trends of both signals strongly implies that spatial correlation between neighbors is a parsimonious indicator of an upcoming transition (Appendix Figure A3.6).

Discussion

Our analysis suggests that an increase in spatial correlation may be a leading indicator for an impending critical transition. Although we explored only three models explicitly, the fact that increased spatial correlation follows from the universal phenomenon of critical slowing down at bifurcations, implies that it may be a generic phenomenon for a wide class of transitions (van Nes and Scheffer 2007).

Our results also indicate that given the same number of data-points spatial correlation may generally outperform indicators derived from time-series as early-warning signal, corroborating to the suggestion that spatial indicators may be more reliable than temporal indicators (Guttal and Jayaprakash 2009). However we note that the performance of both

spatial and temporal indicators depends on the underlying connectivity and heterogeneity of the landscape. For instance, temporal autocorrelation is likely to be better only in homogeneous environments or extremely well 'mixed' (connected), systems which effectively start behaving as a single unit (see Appendix Figure A3.7).

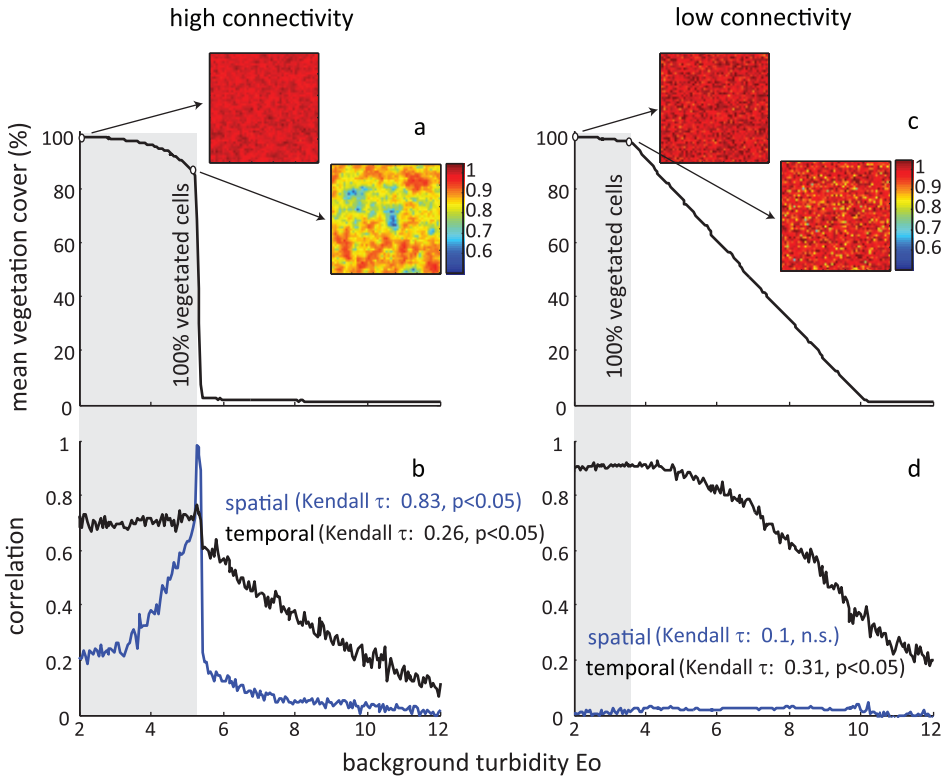

Figure 3.4 An example of the evolution of spatial and temporal correlation between neighboring cells in the vegetation turbidity model (Scheffer, 1998). Panels (**a**, **c**) show the spatial mean of the system's state variable following the slow change in the control parameter. The gray shaded area indicates the period before the system starts flipping. (**c**) Note the shift in the case of low connectivity is gradual, as each cell shifts almost independently from its neighbor. (**a**) The shift is abrupt when connectivity is high and the system reaches the transition globally. (**b**) Spatial correlation signals well in advance the shift of the lake to turbid conditions, outperforming the increase in temporal autocorrelation. (**d**) At low connectivity, spatial correlation hardly changes before the onset of transition, but the trend in temporal autocorrelation is stronger. Top panels are snapshots of the spatial distribution of vegetation cover far from the transition (high resilience), and just before the transition (low resilience). (Parameter values as in Table 3.1 for high heterogeneity in h_E).

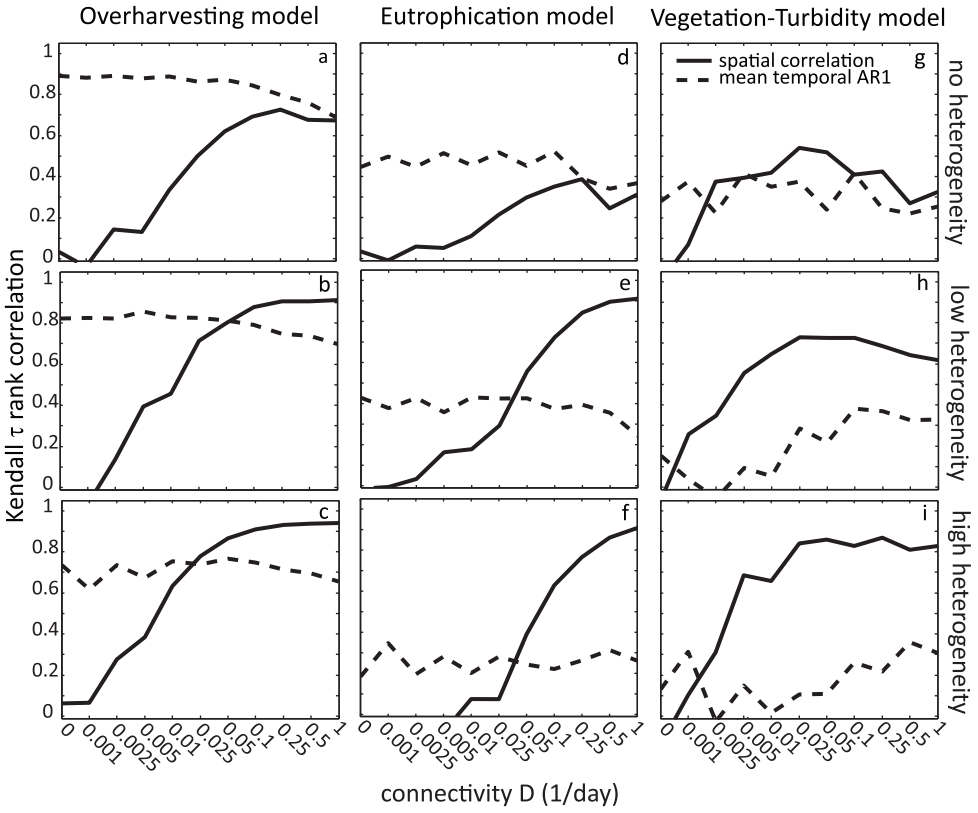

Figure 3.5 Summary of the Kendall τ rank correlation coefficients of the temporal and spatial leading indicators estimated for all dispersion levels and heterogeneity conditions for all three models. The Kendall τ statistic measures the strength of the trend of the leading temporal and spatial indicators before the shift of the spatial system. Significance levels for each statistic are summarized in Appendix Table A3.1.

Also, spatial correlation does not work well in systems with very little connectivity (Figure 3.4c, d). However, it should be noted that, if the environment is heterogeneous in such unconnected systems, temporal information from a single location will not be sufficient to warn for a critical transition on a large scale either, as the monitored patch might shift earlier or later than average. Thus, monitoring many patches is still required in such situations. A practical issue when it comes to optimizing monitoring strategies is that, using remote sensing, it may typically be much easier to obtain information for numerous points in space than for the same amount of points in time (e.g. 1,000 spatially spread sampling points versus 1,000 weekly measurements at the same spot). Still, even if spatial data are easier to obtain, the typical spatial and temporal resolution needed to acquire reliable estimates of the leading indicators remains an open question. This is because such scale will tend to be system specific. The spatial unit at which information is gathered in order to estimate spatial correlation will be determined by the scale to which processes in

the landscape operate. Similarly, temporal dynamics are governed by specific timescales. For instance, had we been monitoring plankton transitions we should be monitoring the dynamics in days (the generation time for most phytoplankton species).

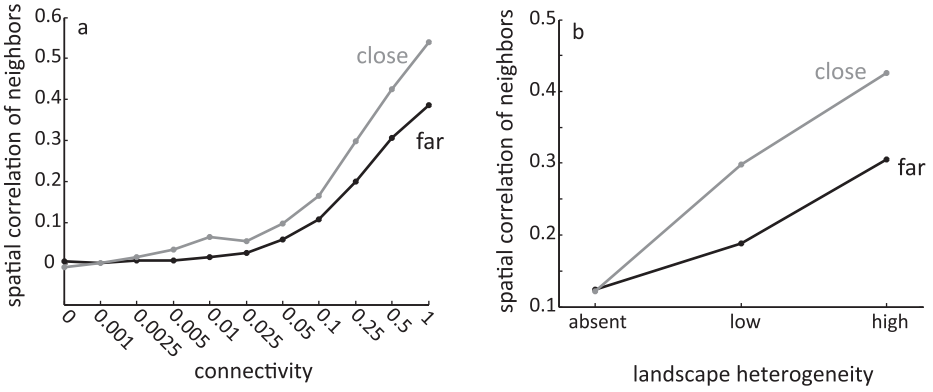

Figure 3.6 False positives in the performance of spatial correlation between neighbors for indicating the proximity to an upcoming transition in the overharvesting model of May (1977). (**a**) Spatial correlation increases as connectivity in the landscape becomes stronger both when the system is far (c=1) or closer to the transition (c=1.6) (Parameter values as in Table 3.1 for high heterogeneity in r). (**b**) Spatial correlation also increases as heterogeneity in the landscape becomes stronger regardless of the proximity to the transition (Parameter values as in Table 3.1 for D=0.5).

Clearly our analysis is merely a starting point when it comes to exploring the possibility of using an increase in spatial correlation as leading indicator for systemic shifts. In most cases the dispersal of seeds or animals is not only limited to neighboring cells as we assumed in our work. Guttal and Jayaprakash (2009) showed that the performance of spatial variance and spatial skewness as indicators of transitions in the same type of systems is insensitive to different dispersal patterns. We expect that the same will also hold for our results. Another simplified assumption in our models is that we have ignored that landscape characteristics are usually spatially correlated due to the underlying physical morphology or to the ecological memory that shapes the landscape (Peterson 2002). Therefore, for instance, dispersion rates are not expected to be constant across space. Nor growth rates of a particular resource will be uncorrelated in space. Instead connectivity will differ due to fragmentation in the landscape or there will be “islands” of high fertility where growth rates will be higher. We tested these two assumptions and we found that they do not affect the performance of spatial correlation as leading indicator of upcoming transitions (see Appendix Figure A3.8, A3.9).

One aspect to explore further is the likelihood of false positives (false alarms) or false negatives (no warning). For instance, it could well be that spatial correlation would also rise in situations which are unrelated to the proximity to a critical point (false alarms). As

we showed, spatial correlation is dependent on the existing connectivity and environmental heterogeneity. This means for instance that if connectivity increases (e.g. because of stronger currents, increased mixing etc), spatial correlation also becomes stronger (Figure 3.6a). Similarly, false alarms could result from changes in heterogeneity: if heterogeneity in the environment is accentuated as conditions change through time or as small scale disturbances increase patchiness in the landscape, this could potentially lead to an increase in spatial correlation producing a false warning of an impending shift (Figure 3.6b). Just as any early-warning signal, correlation is obviously likely to fail in providing early-warning (false negatives), if systems are hit by large disturbances. A global strong disturbance (compared to a local strong disturbance) may well tip the whole system to the alternative state, leaving no space for warning. To obtain a better feeling for the reliability of leading indicators, it would clearly be important to study their performance in more realistic scenarios of spatially correlated disturbances of multiple scales.

In this study, we explicitly explored only one class of models e.g. the ones that have a fold-bifurcation on a local level. In view of the connection to critical slowing down we expect spatial correlation to increase also prior to systemic shifts in systems with other bifurcations. For instance, the Hopf bifurcation, marking the transition of a stable to an oscillatory system is associated to critical slowing down (Chisholm and Filotas 2009) and so is the phenomenon of phase locking between coupled oscillators (Leung 2000).

On the other hand, sharp transitions are also described in systems with self-organized spatial patterns (Kéfi et al. 2007a; Rietkerk et al. 2004; von Hardenberg et al. 2001) for which it is unclear whether they display slowing down. In these systems Turing instability points give birth to regular pattern formation (HilleRisLambers et al. 2001) or long range correlations characterized by power law relationships emerge before the transition due to short range interactions (Pascual and Guichard 2005). Clearly, it would be worthwhile exploring the applicability of the correlation indicators presented in this work to a wider class of models.

Finally, we should acknowledge that although early-warning signals for regime shifts are potentially useful for managing transitions of real ecosystems, they still remain elusive in their application. Most of the proposed indicators are developed in simple ecological models and have not yet been tested in the field (Scheffer et al. 2009). Modeling exercises demonstrate that they may well fail to be used successfully in averting impending transitions (Biggs et al. 2009b; Contamin and Ellison 2009). One problem is the large amount of data needed (Carpenter et al. 2008; Dakos et al. 2008; Guttal and Jayaprakash 2008). Another drawback is that generic early-warning signals typically do not indicate the proximity to the critical threshold in absolute terms (van Nes and Scheffer 2007). Instead they can only be used to indicate a relative change of the system's resilience. Finally, there is the difficulty of moving from science to policy in a swift way (Biggs et al. 2009b; Scheffer et al. 2003). Management actions usually take years to implement due to institutional inertia or stakeholders' conflicting interests. Nonetheless, it is encouraging that there is an increasing number of examples where leading indicators have been identified for real systems (Scheffer et al. 2009), like the marine environment (Beaugrand et al. 2008), semi-

arid ecosystems (Kéfi et al. 2007a) or even climate (Dakos et al. 2008; Livina and Lenton 2007).

Our results resonate with earlier findings that long range coherence increases in percolating systems close to phase transitions (Pascual and Guichard 2005; Solé et al. 1996; Stanley 1971), suggesting that changes in spatial correlation may well turn out to be rather generic indicators of shifts in a variety of spatio-temporal systems, like the ones in this study with fold bifurcations. Potential applications might range from anticipating epidemic outbreaks (Davis et al. 2008) and the collapse of metapopulations (Bascompte and Solé 1996) to warning for epileptic seizures (Lehnertz and Elger 1998) or large scale climate transitions (Tsonis et al. 2007).

Appendix

Table A3.1 Kendall correlation statistics for the spatial and temporal correlation trend estimated in the three models analyzed in the main text. Values in bold are 2 tail significant (p<0.05).

dispersion	**no heterogeneity**		**low heterogeneity**		**high heterogeneity**	
Kendall τ correlation	spatial correlation	mean temporal AR1	spatial correlation	mean temporal AR1	spatial correlation	mean temporal AR1
Overharvesting model						
0	0.035	**0.889**	-0.037	**0.823**	0.062	**0.734**
0.001	-0.036	**0.880**	-0.075	**0.825**	0.066	**0.618**
0.0025	**0.142**	**0.890**	**0.137**	**0.823**	**0.278**	**0.736**
0.005	**0.132**	**0.878**	**0.393**	**0.857**	**0.385**	**0.675**
0.01	**0.335**	**0.889**	**0.456**	**0.827**	**0.633**	**0.755**
0.025	**0.498**	**0.861**	**0.712**	**0.824**	**0.780**	**0.738**
0.05	**0.620**	**0.871**	**0.800**	**0.814**	**0.866**	**0.765**
0.1	**0.692**	**0.844**	**0.877**	**0.792**	**0.910**	**0.747**
0.25	**0.726**	**0.796**	**0.905**	**0.746**	**0.932**	**0.712**
0.5	**0.675**	**0.761**	**0.906**	**0.739**	**0.938**	**0.695**
1	**0.674**	**0.690**	**0.912**	**0.697**	**0.939**	**0.654**
Eutrophication model						
0	0.035	**0.446**	-0.014	**0.429**	**-0.248**	**0.184**
0.001	-0.009	**0.497**	-0.006	**0.378**	-0.039	**0.347**
0.0025	0.059	**0.447**	0.033	**0.427**	**-0.207**	**0.196**
0.005	0.052	**0.514**	**0.163**	**0.358**	-0.047	0.282
0.01	0.110	**0.455**	**0.178**	**0.430**	-0.127	**0.202**
0.025	**0.214**	**0.517**	**0.293**	**0.425**	0.040	0.281
0.05	0.298	**0.452**	**0.557**	**0.426**	**0.251**	**0.243**
0.1	**0.350**	**0.522**	**0.723**	**0.374**	**0.544**	**0.221**
0.25	**0.387**	**0.391**	**0.843**	**0.394**	**0.709**	0.263
0.5	**0.244**	**0.340**	**0.896**	**0.355**	**0.834**	**0.313**
1	0.312	**0.368**	**0.911**	0.242	**0.885**	0.261
Vegetation-Turbidity model						
0	-0.108	0.281	-0.058	0.152	-0.135	0.131
0.001	0.068	0.375	**0.258**	0.039	0.102	**0.314**
0.0025	**0.374**	**0.225**	**0.347**	-0.052	**0.311**	-0.022
0.005	**0.396**	**0.418**	**0.554**	0.093	**0.687**	0.149
0.01	**0.419**	**0.352**	**0.649**	0.053	**0.658**	0.017
0.025	**0.540**	**0.377**	**0.730**	**0.287**	**0.842**	0.106
0.05	**0.520**	**0.241**	**0.726**	**0.218**	**0.859**	0.110
0.1	**0.411**	**0.417**	**0.726**	**0.381**	**0.827**	**0.262**
0.25	**0.426**	**0.245**	**0.686**	**0.370**	**0.870**	**0.217**
0.5	**0.272**	0.220	**0.643**	**0.326**	**0.810**	**0.362**
1	**0.326**	**0.256**	**0.617**	**0.330**	**0.828**	**0.308**

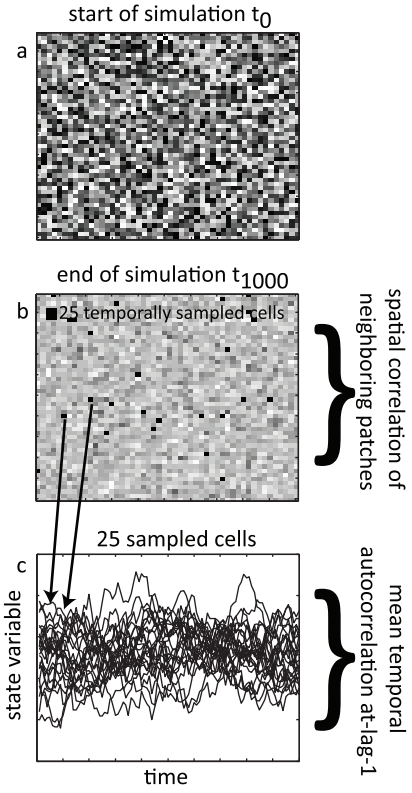

Figure A3.1 Schematic description of simulation scheme and sampling protocol for the estimation of the spatial and temporal correlation leading indicators.

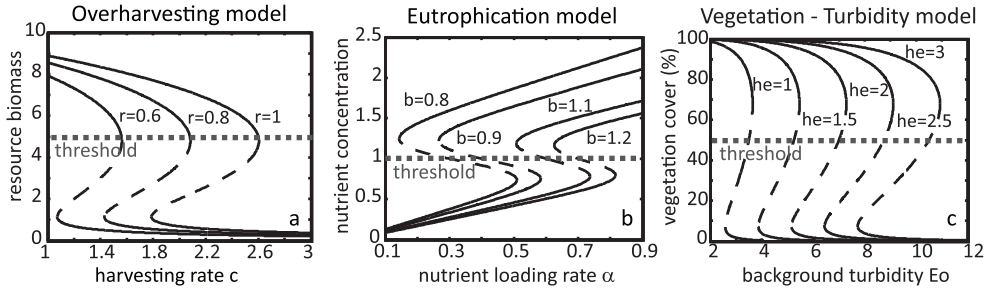

Figure A3.2 Bifurcation plots along the control parameter for all models used to define thresholds for assigning cells in one or the other stable state. In the overharvesting model (panel **a**), cells were considered underexploited if their biomass was higher 5. In the eutrophication model (panel **b**), patches with nutrient concentration below 1 were considered oligotrophic. In the vegetation turbidity model (panel **c**), patches with vegetation cover over 50% were considered vegetated.

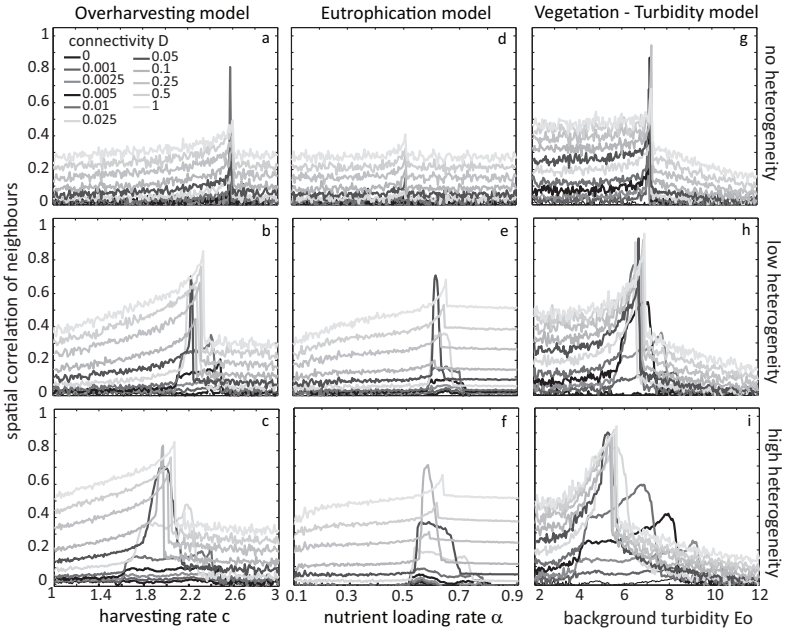

Figure A3.3 Spatial correlation as a function of control parameter for all levels of connectivity (*D*) in the three models analyzed in the main text.

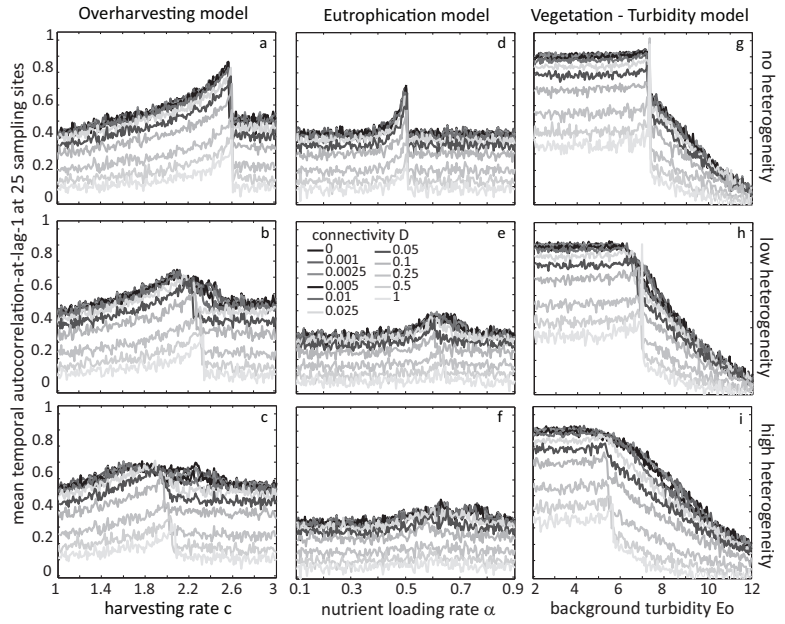

Figure A3.4 Mean temporal correlation of the 25 sampled cells as a function of control parameter for all levels of connectivity (*D*) in the three models analyzed in the main text.

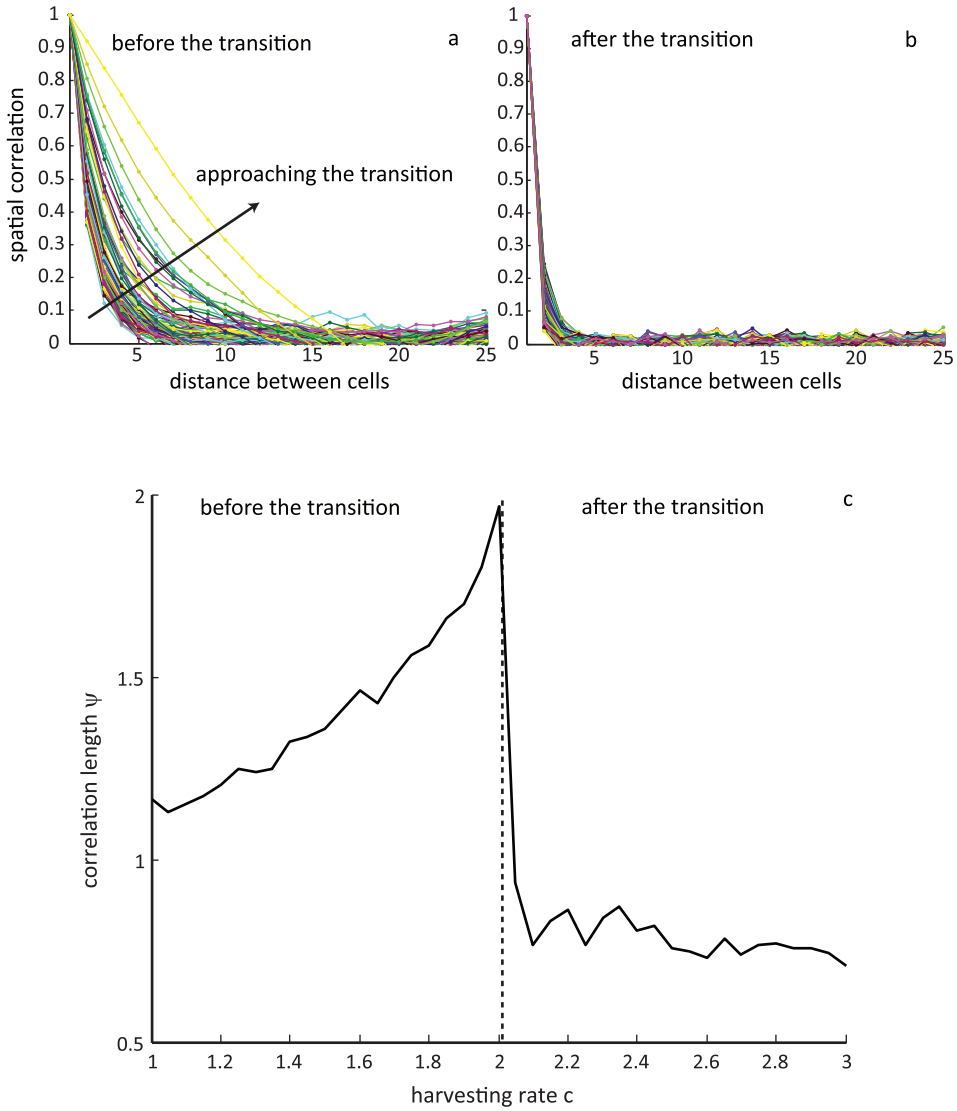

Figure A3.5 Spatial correlation estimated up to 25 cells distance (lags) in the overharvesting model of May (1977). (**a**) Each line in the correlogram corresponds to a value of the grazing rate *c* as the spatial system approaches the transition. The spatial correlation increases not only for the neighboring cells (lag 1) but extends up to approximately 15 cells distance before the shift. (**b**) After the transition the correlation is limited only to a few neighboring cells. (**c**) A growing correlation length ψ (estimated for each line in panels **a**, **b**) indicates increasing correlation at higher distances. (Parameter values as in Table 3.1 for D=0.5 and high heterogeneity in r)

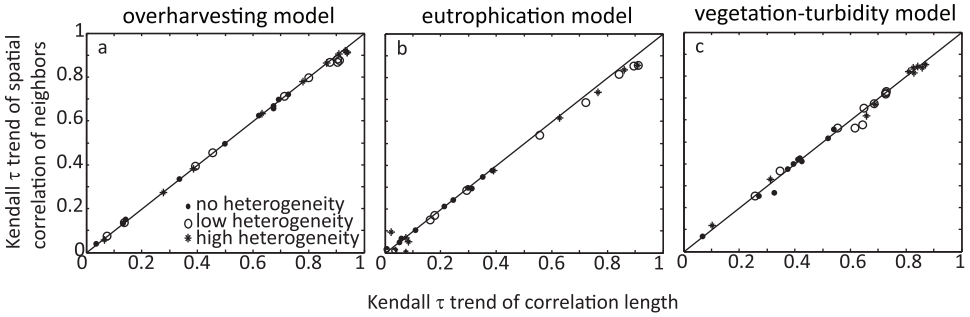

Figure A3.6 Kendall τ coefficients of the spatial correlation of neighbors and correlation length indicators estimated for all dispersion levels and heterogeneity conditions for all three models. The Kendall τ coefficient measures the strength of the trend of the spatial correlation and correlation length before the shift of the spatial system. The almost 1:1 relationship between the trends of both indicators strongly implies that spatial correlation between neighbors (lag 1) is a parsimonious indicator of an upcoming transition.

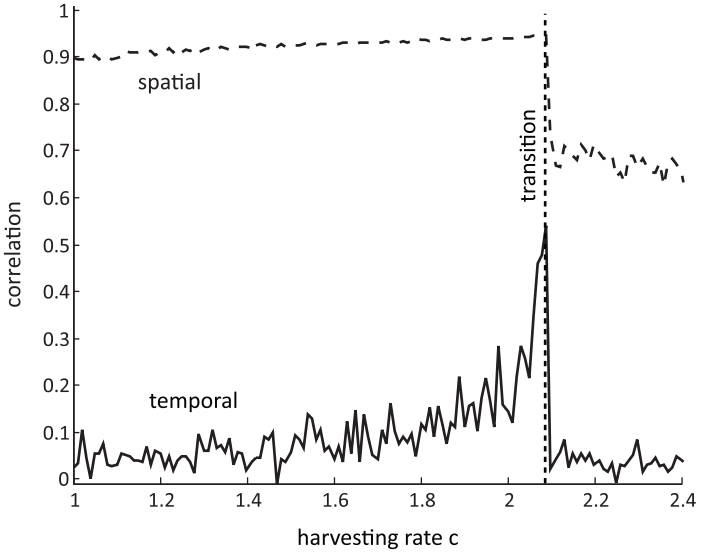

Figure A3.7 Spatial correlation of neighbors and mean temporal correlation of the 25 sampled cells as a function of the control parameter for an extreme high level of connectivity (D=100) in the overharvesting model with high heterogeneous conditions. As conjectured in the main text, in highly connected systems (due to high dispersal rates) spatial correlation is already high far away from the transition (≈0.897) and rises only slightly before the shift (≈0.946), indicating that its detection can prove problematic. Instead the rise in the temporal autocorrelation is much stronger.

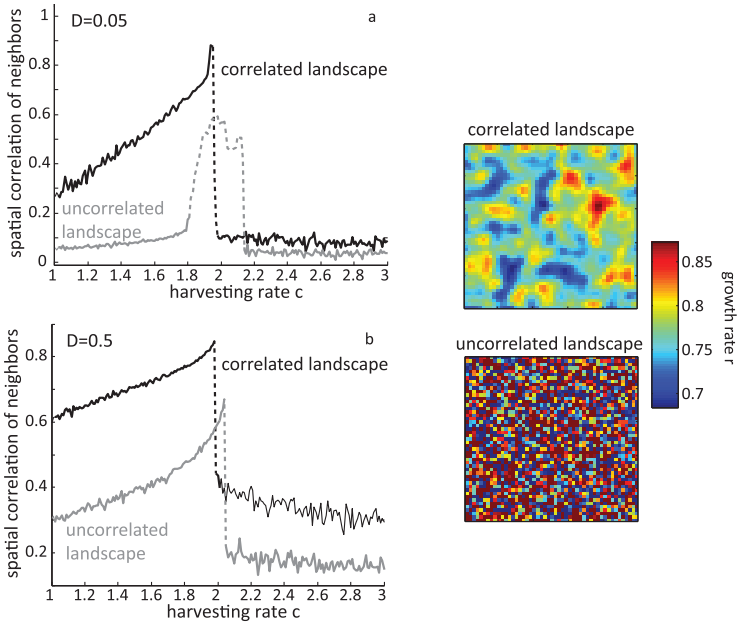

Figure A3.8 The evolution of spatial correlation of neighbors in correlated and uncorrelated landscapes for two levels of connectivity (*D*) in the overharvesting model. Spatial correlation is increasing prior to the transition in both correlated and uncorrelated landscapes. The shift is gradual in an uncorrelated landscape but abrupt when there is underlying correlation (panel **a**). Top panels are images of the spatial distribution of resource biomass growth rates *r*. Dotted line indicates the transition. (Parameter values as in Table 3.1 for high heterogeneity in *r*).

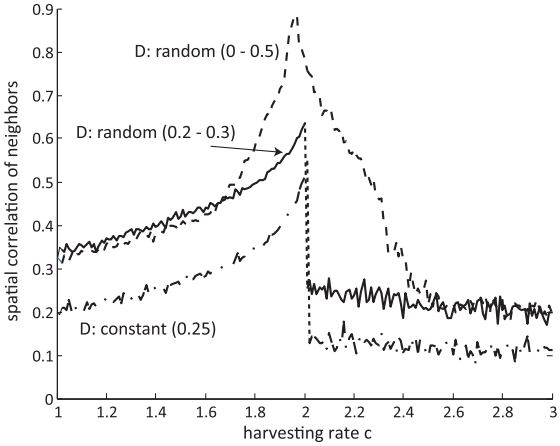

Figure A3.9 The evolution of spatial correlation of neighbors for different patterns of connectivity (*D*) in the overharvesting model. Dashed-dotted line: dispersion is equal to 0.25 across the landscape. Solid line: dispersion is randomly assigned between 0.2-0.3 (mean 0.25) across the landscape. Dashed line: dispersion is randomly assigned between 0-0.5 (mean 0.25) across the landscape. Spatial correlation of neighbors is increasing prior to the transition in all cases. (Parameter values as in Table 3.1 for high heterogeneity in growth rates *r*).

Chapter 4

How robust are early-warning signals for critical transitions?

Ecosystems close to a critical threshold may shift abruptly to alternative states. For ecosystem management it is important to predict such critical transitions. Recently it has been proposed to use rising autocorrelation and variance as indicators of approaching critical transitions. Here we explore the robustness of these indicators. We show both analytically and in simulations that variance may sometimes decrease close to a transition. This can happen when environmental factors fluctuate stochastically and the system becomes less sensitive to these factors near the threshold, or when critical slowing down reduces the system's capacity to follow high frequency fluctuations in the environment. In addition, when available data is limited, variance can be systematically underestimated due to the prevalence of low frequencies close to a transition. By contrast, autocorrelation increases always towards critical transitions. We provide examples of rising autocorrelation and simultaneously decreasing variance in time-series prior to ancient climate transitions.

This chapter is based on the paper: V. Dakos, E. H. van Nes, P. D'Odorico and M. Scheffer. How robust are early-warning signals for critical transitions? (submitted) We thank Steve Carpenter and William A. Brock for their valuable comments.

Introduction

Some systems may occasionally change quite abruptly to a contrasting state (Hare and Mantua 2000; Hughes 1994; Rietkerk et al. 2002; Scheffer et al. 2001). Theoretical studies have suggested that such shift may occur in systems with alternative stable states in which the conditions change gradually towards a critical point, called a bifurcation, where the system becomes unstable and shifts to the alternative state. It has been recently suggested that such shifts may be announced in advance by generic leading indicators for critical transitions (Scheffer 2009). This idea is based on the fact that systems tend to show a phenomenon known as 'critical slowing down' as they approach bifurcation points (Scheffer 2009; Strogatz 1994; Wissel 1984) where a tiny change in conditions can lead to a marked qualitative change in the behavior of a system. The term critical slowing down refers to the fact that near these points the return time to equilibrium upon a small perturbation increases strongly. To illustrate the principle, consider a system that exhibits alternative stable states over a range of conditions (Figure 4.1). Such system will undergo a critical transition at point F_1 when conditions (expressed by a control parameter p) cross a threshold (at $p = p_1$), and the system shifts to an alternative state (Figure 4.1a). The return rate to equilibrium upon a small perturbation can be approximated by the dominant eigenvalue of the Jacobian matrix of the linearized system (Pimm and Lawton 1977). This dominant eigenvalue smoothly declines to 0 as the system moves close to the critical threshold ($p \rightarrow p_1$) (Figure 4.1b). This means that the system will need increasingly more time to recover from a small perturbation as it comes closer to this critical point (van Nes and Scheffer 2007).

Now consider what will happen if one exposes such a system to a permanent stochastic regime of perturbations. Intuitively one can imagine that the loss of the system's tendency to return to its equilibrium may cause it to be simply pushed around by the stochastic perturbations. This effect can be seen in simulations in our example where the state of the system becomes more correlated to its past and drifts farther away from its equilibrium when the bifurcation is close (Figure 4.1f and d) compared to when the bifurcation is far (Figure 4.1e and d). Indeed, analytical arguments as well as simulations have suggested that close to a bifurcation one should expect critical slowing down to cause a rise in autocorrelation (Held and Kleinen 2004; Kleinen et al. 2003) and variance (Carpenter and Brock 2006) in stochastically forced systems.

While it is an attractive idea that such changes could be used as early-warning signals (or 'leading indicators') for critical transitions related to underlying bifurcations, the conditions under which this approach would be reliable are still poorly understood. Obviously, these leading indicators can only signal an upcoming transition if there is a gradual decrease in the dominant eigenvalue of the system. Thus, conditions should gradually move the system towards a bifurcation, if we want to be able to pick up a change in the leading indicators. Clearly, transitions between attractors induced by major perturbations, or chaotic dynamics far from local bifurcation points are unlikely to be picked up by such indicators. Even if the dominant eigenvalue decreases, statistical detection of the resulting change in dynamics can be challenging. Another, obvious source of false positives or negatives would be a systematic change in the external perturbation

regime over the period leading up to a shift (Scheffer et al. 2009). For instance, dynamics of a system under a regime of increasingly autocorrelated perturbations may appear increasingly autocorrelated, even if there is no approaching bifurcation.

Here we explore some more intricate mechanisms that may affect the way in which critical slowing down translates into autocorrelation and variance of fluctuations of a system. First, we ask whether the way in which the stochastic environmental perturbations act on the system would influence how an approaching bifurcation translates into autocorrelation and variance of the system dynamics. Thinking in terms of models, stochastic forcing can be applied directly to the state of the system (e.g., stochastically killing portions of a population), or to any of its parameters (e.g., temperature fluctuations affecting process rates). Most work so far has focused on the first aspect (Biggs et al. 2009b; Brock and Carpenter 2006; Brock et al. 2006; Carpenter et al. 2009; Dakos et al. 2010; Guttal and Jayaprakash 2008; Guttal and Jayaprakash 2009; but see Carpenter et al. 2006, 2008). In this paper, we first examine how perturbations on parameters may impact the behavior of the leading indicators compared to the case of direct perturbations on the system state. For these two situations we derive simple analytical approximations for autocorrelation and variance as functions of the proximity to a bifurcation, and we compare the results to estimates of autocorrelation and variance derived from numerical simulations. We also discuss how sensitive estimators of autocorrelation and variance may be to limitations of our current time-series techniques. Lastly, we use two examples of ancient climate transitions to show how patterns in autocorrelation and variance may deviate prior to a shift.

Methods and Models

Perturbations of the state of a system

To derive analytical expectations for autocorrelation and variance let us assume that the dynamics of a system are described by a continuous stochastic equation

$$dx = f(x,p)dt + \sigma dW \qquad \text{(eq1)},$$

where $f(x,p)$ is the deterministic part of the system and dW is the stochastic driver represented by a white noise process of mean zero and magnitude σ^2.

When a small perturbation ε pushes the state of the system a tiny bit away from equilibrium x^* (for which $f(x^*,p)=0$), the system returns to equilibrium with a rate approximately equal to the dominant eigenvalue $\lambda(x^*,p)$ of the linearized system:

$$d\varepsilon = \lambda(x^*,p)\varepsilon dt + \sigma dW \qquad \text{(eq2)},$$

where $\lambda(x^*,p)$ is negative if x^* is stable.

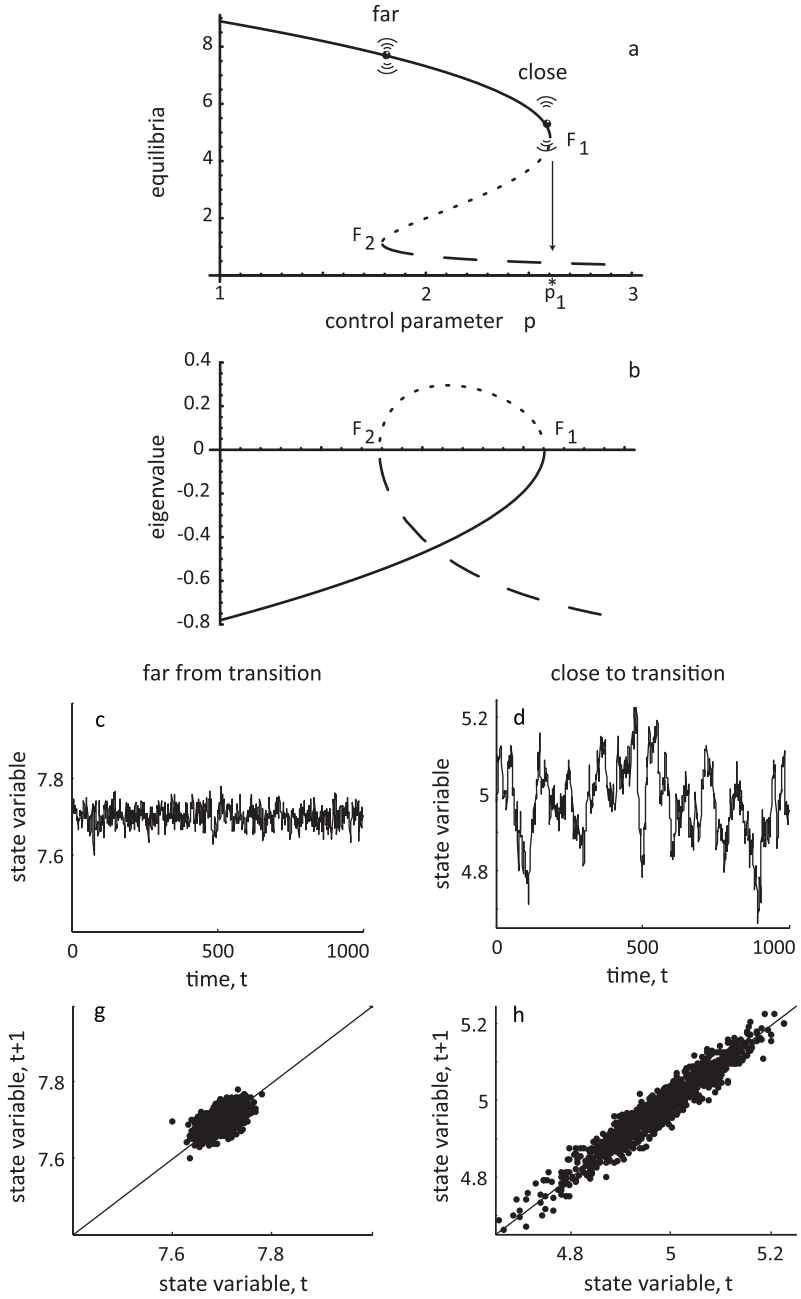

Figure 4.1 An example of a system undergoing a critical transition through a fold bifurcation F_1, when control parameter p reaches a threshold value p_1. (**a**) Stable and unstable equilibria as function of control parameter p. (**b**) Eigenvalues of stable and unstable equilibria (dotted lines denote unstable equilibria). (**c-f**) Sampled realizations and their first-lag correlations of a stochastically perturbed system: far from the bifurcation (panel **c**, **e**) and close (panel **d**, **f**) to it.

Equation 2 has the explicit solution (Gardiner 2003): $\varepsilon_t = \varepsilon_0 e^{\lambda(x^*,p)t} + \sigma \int_0^t e^{\lambda(x^*,p)(t-s)} dW(s)$, where the temporal variable s is integrated between time 0 (when $\varepsilon_t=\varepsilon_0$) and time t. Autocorrelation ρ_ε and variance ${\sigma_\varepsilon}^2$ of ε_t are given by $\rho_\varepsilon = e^{\lambda(x^*,p)|t-s|}$ and $\sigma_\varepsilon^2 = \frac{\sigma^2}{2\lambda(x^*,p)}(e^{2\lambda(x^*,p)t} - 1)$ respectively (Gardiner 2003).

For sufficiently long time-series ($t \to \infty$), we can derive approximate expressions for autocorrelation at-lag-1 and variance (Gardiner 2003), which explicitly depend on the responsiveness of the system as determined by the dominant eigenvalue $\lambda(x^*,p)$ (and, thus, by the proximity to a critical transition):

$$\rho_\varepsilon(1) = e^{\lambda(x^*,p)} \qquad \text{(eq3)}$$

$$\sigma_\varepsilon^2 = -\frac{\sigma^2}{2\lambda(x^*,p)} \qquad \text{(eq4).}$$

Perturbations of parameters representing processes

When environmental stochasticity is affecting processes in the system, we may model that by assuming that one of the parameters p of the system $dx=f(x,p)dt$ becomes a random parameter with mean p^*. If we consider that for average p^* an equilibrium x^* exists (i.e., $f(x^*,p^*)=0$), then the evolution of small disturbances around equilibrium x^* can be approximated by the linearized system (Ripa and Heino 1999):

$$dx = f_x(x^*,p^*)(x-x^*)dt + f_p(x^*,p^*)(p-p^*)dt \qquad \text{(eq5).}$$

Assuming that $\varepsilon=x-x^*$ and $z=p-p^*$, where z is a Gaussian random variable with mean zero and magnitude σ^2, equation 5 can be rewritten as:

$$d\varepsilon = \lambda(x^*,p^*)\varepsilon dt + f_p(x^*,p^*)\sigma dW \qquad \text{(eq6)}$$

where $\lambda(x^*,p^*)$ is the eigenvalue of the system for average parameter p^*, $f_p(x^*,p^*)$ is the partial derivative of f with respect to the parameter p that is affected by environmental noise, and dW is a stochastic term of zero mean and unit variance that represents the random variable z. In this case, the effect of stochastic perturbations on the state of the system depends on $f_p(x^*,p^*)$. The factor $f_p(x^*,p^*) = \left.\frac{\partial f}{\partial p}\right|_{x^*}$ reflects the sensitivity of the system to changes in the parameter p: in other words it reflects how the system is modulating (scaling) the magnitude of perturbations to produce an effect on its state.

Following the same steps as above, autocorrelation at-lag-1 is the same as equation 3, however variance is now also a function of $f_p(x^*,p^*)$:

$$\sigma_{\varepsilon}^2 = -\frac{\sigma^2 f_p(x^*,p^*)^2}{2\lambda(x^*,p^*)} \quad \text{(eq7).}$$

Importantly, given that $f_p(x^*,p^*)$ may change if a control parameter brings the system closer to a bifurcation, variance may be amplified or dampened as the system approaches the bifurcation. By contrast, autocorrelation remains solely dependent on the dominant eigenvalue $\lambda(x^*,p^*)$.

Simulation experiments

We tested our theoretical approximations of autocorrelation and variance in a well-studied model that describes the shift of a harvested resource to overexploitation (May 1977; Noy-Meir 1975). Resource biomass *x* grows logistically and is harvested according to

$$dx = (rx(1-\frac{x}{K}) - c(\frac{x^2}{x^2+h^2}))dt + f_p(x,p)\sigma dW \quad \text{(eq8)}$$

where *r* is the growth rate, *K* is the population's carrying-capacity, *h* is the half-saturation constant and *c* is the grazing rate. When *c* reaches a certain threshold value (c ≈ 2.604), the system undergoes a critical transition through a fold bifurcation. When environmental noise is affecting directly the state variable *x*, white noise is added through a stochastic term *dW* with magnitude σ^2. When environmental noise affects the parameters, *dW* is scaled by $f_p(x,p)$, which reflects how stochastic forcing translates into changes in the state; scaling factors $f_p(x,p)$ for growth rate *r*, grazing rate *c*, and carrying-capacity *K* are $f_r(x) = x(1-\frac{x}{K})$, $f_c(x) = -\frac{x^2}{x^2+h^2}$, and $f_K(x) = \frac{rx^2}{K^2}$ respectively.

We started simulations from equilibrium and slowly increased grazing rate *c* until the system shifted to overexploitation. After each stepwise change of grazing rate, we ran the model for 500 time steps. We used these 500 time steps to estimate autocorrelation at-lag-1 and variance (expressed as standard deviation) for each level of grazing rate *c*. We estimated autocorrelation at-lag-1 by fitting a first-order autoregressive model using package *arfit* in MATLAB (Schneider and Neumaier 2001). We repeated this for 200 simulations and used average estimates for both indicators.

Time-series analysis

We estimated autocorrelation at-lag-1 and standard deviation prior to transition for two ancient climate records. The first transition is the end of the Younger Dryas (Clark et al. 2002). The second record represents the sudden change of the earth from a tropical state without ice caps to a state with ice caps around 34 million years ago (Tripati et al. 2005).

We estimated the leading indicators in both records prior to transition applying an overlapping moving window of half the size of the record after detrending with a Gaussian kernel smoothing function. Full details on the methods for the time-series analysis can be found in Dakos et al. (2008).

All simulations and statistical analyses were performed in MATLAB, R (http://www.r-project.org/), and Mathematica. We solved the stochastic equations using an Euler-Murayama integration method with Ito calculus in 36 integration steps for each time step. Parameter values used were r=1, K=10, h=1, c=[1, 3], σ=0.1, unless otherwise indicated. Both climate time-series represent climate data proxies and were downloaded from the World Data Center for Paleoclimatology, National Geophysical Data Center, Boulder, Colorado (http://www.ncdc.noaa.gov/paleo/data.html).

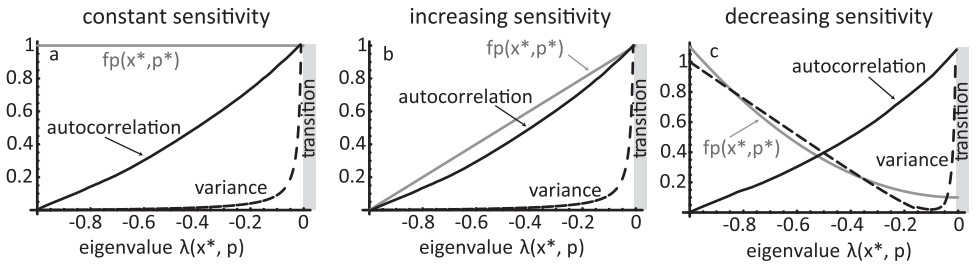

Figure 4.2 Analytically predicted trends in autocorrelation at-lag-1 $\rho(1)$ and variance σ_ε^2 prior to a zero-eigenvalue transition depending on the sensitivity $f_p(x^*,p^*)$ of the system to noise. (**a**) Constant sensitivity $f_p(x^*,p^*)$ of the system to a parameter. (**b**) Increasing sensitivity $f_p(x^*,p^*)$ of the system to a parameter towards the transition. (**c**) Decreasing sensitivity $f_p(x^*,p^*)$ of the system to a parameter towards the transition. (Autocorrelation at-lag-1 $\rho(1)$ based on equation 3; variance σ_ε^2 based on equation 7 with σ^2 = 1 rescaled to the interval 0-1).

Results

Our theoretical approximations illustrate that autocorrelation at-lag-1 should depend only on the dominant eigenvalue characterizing the return rate to equilibrium of the system upon perturbations, regardless of whether environmental noise acts on the state or the parameters of the system. This means that as the system undergoes a transition when $\lambda(x^*,p) \rightarrow 0$, autocorrelation at-lag-1 in idealized situations is expected to reach 1 (equation 3) (Held and Kleinen 2004; Ives et al. 2003). When perturbations affect the state of the system directly, variance is also predicted to increase gradually before the bifurcation (equation 4) (Brock and Carpenter 2006; Carpenter and Brock 2006) (Figure 4.2a). However, when environmental stochasticity acts on a parameter of the system, the effect on variance is modulated by the system's sensitivity to that parameter, $f_p(x^*,p^*) = \left.\frac{\partial f}{\partial p}\right|_{x^*}$. Therefore, under a constant environmental noise regime, variance in the fluctuations of the state may either increase or decrease as the system approaches a

bifurcation (equation 7). Nonetheless, at the bifurcation itself, variance should approach infinity as long as the sensitivity of the system to the disturbed parameter is not zero (i.e. $f_p(x^*,p^*)^2>0$).

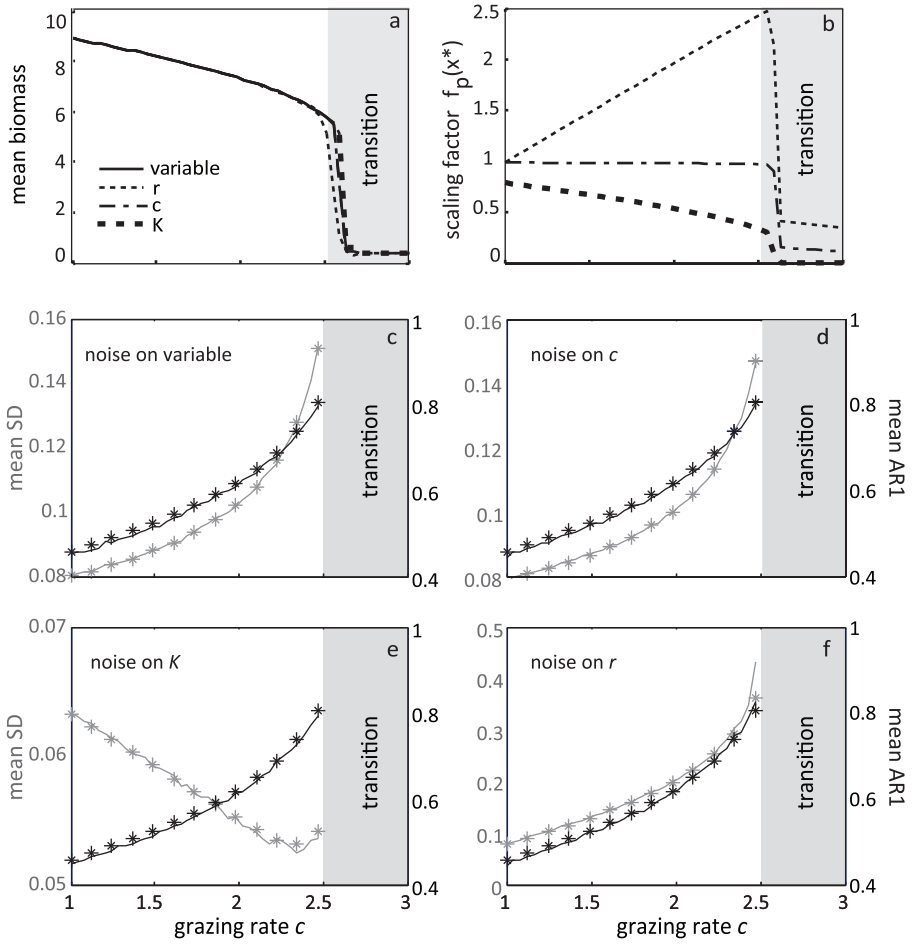

Figure 4.3 Trends in leading indicators for simulated data from a model of a logistically growing plant population ('resource') driven slowly to a catastrophic collapse through gradually increasing grazing rates. The model is exposed to environmental stochasticity affecting the state variable, grazing rate *c*, carrying capacity *K*, or growth rate *r*. (**a**) Mean biomass at increasing grazing rate. (**b**) The analytically derived scaling factor representing how strongly a perturbation of a parameter affects the state. (**c-f**) Analytical and numerical estimates of autocorrelation and variance for stochastic forcing of the state or different parameters (asterisks: analytical estimates; lines: numerical estimates; black lines: autocorrelation at-lag-1; gray lines: variance).

Figure 4.2 illustrates this effect. If the sensitivity of the system to the disturbed parameter stays constant or increases towards the bifurcation, variance will typically increase over a range prior to transition (Figure 4.2b). However, the opposite can occur, if the sensitivity of the system to the disturbed parameter is shrinking as the system is approaching the transition (Figure 4.2c). Autocorrelation at-lag-1 is insensitive to this effect (Figure 4.2).

Numerical simulations support these theoretical predictions (Figure 4.3). In the overgrazing model, trends in variance towards the bifurcation point depend on the way in which the sensitivity to the affected parameter (scaled by $f_p(x^*,p^*)$) changes as the system approaches the bifurcation. While noise on most parameters has a similar effect to noise applied directly to the state (Figure 4.3c, d), noise on the carrying-capacity *K*, leads to an opposite trend in variance over much of the trajectory of the system towards the bifurcation (Figure 4.3e). Only very close to transition, the effect of critical slowing down overwhelms the effect of the decreasing trend in sensitivity (cf. Figure 4.2c). The simulations also illustrate that, as expected, autocorrelation at-lag-1, is insensitive to the way in which environmental noise affects the system (Figure 4.3c-f).

Filtering effects of slowness

In addition to the potential effect of decreasing sensitivity to parameters, there is a quite different mechanism that may in some situations mute variance as the system approaches a bifurcation. This is related to the very nature of critical slowing down. Consider an overall slow system (Figure 4.4). When environmental stochasticity directly affects the system's state variables, the system is as if it were "pushed" around the fixed equilibrium (Figure 4.4a gray line). By contrast, when noise affects parameters, one can think of the system as 'tracking a fluctuating equilibrium' (in this case driven by a fluctuating carrying-capacity *K*) (Figure 4.4a black line). Now, if the system is inherently slow (i.e. has low rates of change), it will hardly follow the fluctuations in the equilibrium and as a result its state may vary only little over time (Figure 4.4b black line). As critical slowing down will only aggravate the already limited capacity of the system to track the fluctuating environment, it will 'freeze' the state of the system even more as it approaches the bifurcation. As our simulations illustrate, this may smother even the increase of variance just before the bifurcation (Figure 4.4c, d). Again, autocorrelation is insensitive to this effect. It will increase prior to the shift regardless of the responsiveness of the system, even though in such inherently slow systems autocorrelation is obviously always very large (Figure 4.4e, f).

Examples from climate dynamics

In light of these results, we explored how estimated variance changed in the periods leading up to ancient climate shifts that we analyzed for autocorrelation trends earlier (Dakos et al. 2008). Although all time-series show an increase in autocorrelation leading up to the shifts, we found no consistent trends in variance (see Figure A4.1 in Appendix). As an example we show two transitions where autocorrelation at-lag-1 increased before the shift (Figure 4.5c, f), but variance did not show a consistent trend ir even decreased systematically prior to the transition (Figure 4.5b, e).

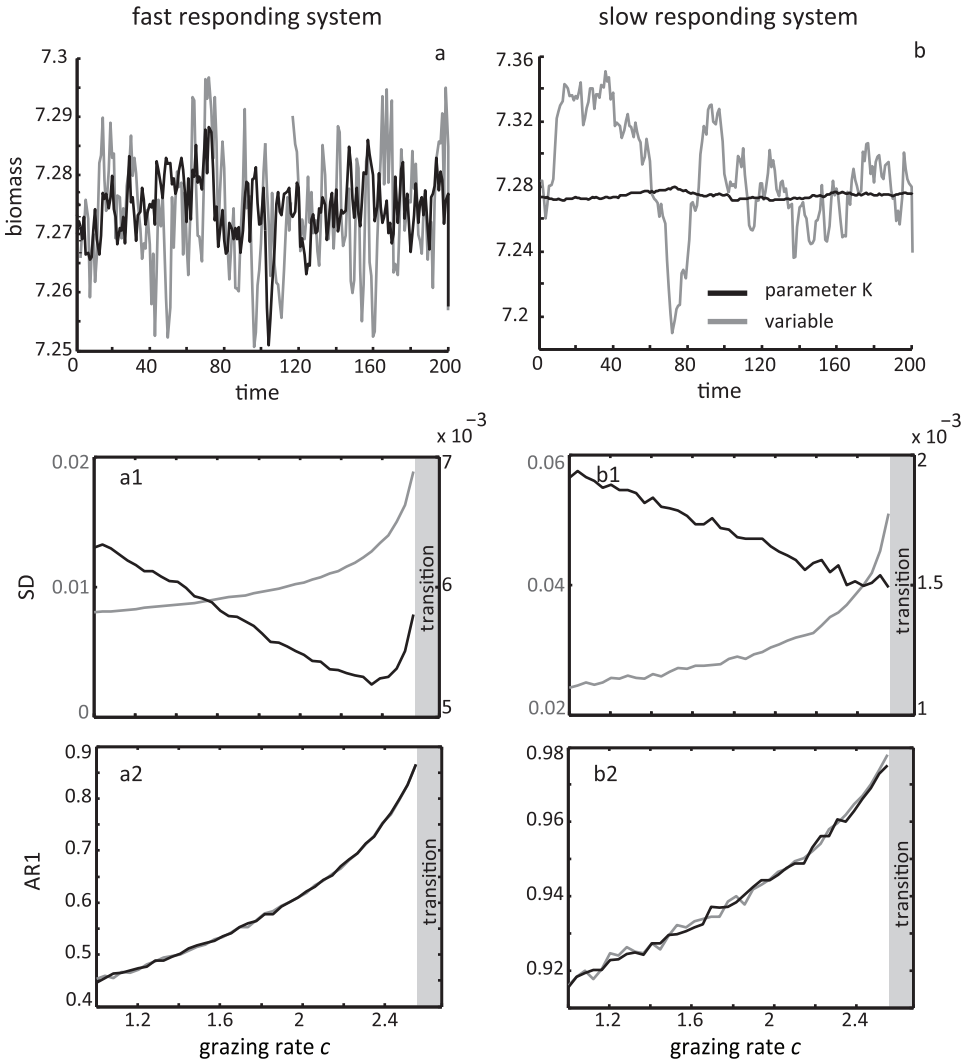

Figure 4.4 Simulations illustrating how slowing down can reduce the sensitivity of a system to high frequency fluctuations in the environment, preventing variance from rising in the vicinity of a bifurcation point. (**a**) Behavior of a fast responding system where environmental noise is affecting either the state of the system (black line) or a parameter (in this case carrying capacity *K*, gray line). Variance first drops and rises only before the transition (panel **a1**). Autocorrelation rises prior to transition independently from the source of environmental stochasticity (panel **a2**). (**b**) Behavior of a slow-responding system. This system is less able to track the constantly changing equilibrium. Slowing down, further "freezes" the system, preventing variance to rise in the vicinity of the bifurcation point (panel **b1**). Autocorrelation at-lag-1 is rising in a slow responding system independently from the source of environmental stochasticity (panel **b2**).

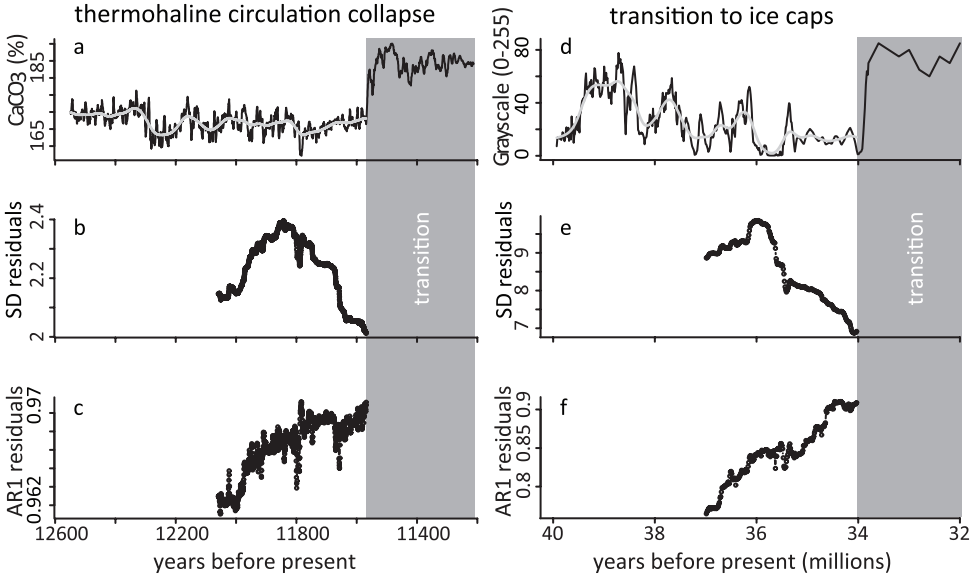

Figure 4.5 Examples of two ancient transitions in the climate record. (**a**) The exit from the Younger Dryas after the collapse of the thermohaline circulation, and (**d**) the onset of ice caps after a period of a warm earth with no ice on the poles. We estimated variance (panels **b**, **e**) and autocorrelation at-lag-1 (panels **c**, **f**) of the residuals after detrending using a Gaussian smooth function (gray line). Gray area denotes the period after the onset of the shift.

Discussion

The use of indicators of critical slowing down, to sense the risk of upcoming critical transitions in real world systems is an exciting prospect. Rising variance and autocorrelation are among the prime candidate indicators. However, while autocorrelation appears a relatively robust indicator, our results suggest that there can be particular conditions under which variance may decrease instead of rise prior to a transition. Specifically, this can happen if environmental stochasticity affects the 'equilibrium' rather than the state of the system, and the effect can be aggravated if the systems inherent rates of change are slow relative to the frequency characteristics of the forcing regime.

It remains difficult to judge how common distortions of the basic effect of critical slowing down on variance will be in practice. Obviously, stochastic perturbations will usually affect a system in multiple ways simultaneously. This may well tend to cause an overall increase of variance in most situations. Indeed, simulations with a lake ecosystem model subject to multiple sources of stochasticity suggest that an increase of variance may dominate the pattern (Carpenter and Brock 2006; Carpenter et al. 2008). On the other hand, in systems with multiple thresholds where interacting transitions may be at play, variance may be muffled prior to a shift (Brock and Carpenter 2010). Additionally, on a less fundamental

level, estimated variance may decrease with critical slowing down purely due to limitations of our data analysis techniques. As the fluctuations of the system become increasingly dominated by low frequencies close to a transition, there is a high chance of missing part of this variability simply because our time-window for estimating variance is limited, and also because there is an increasing risk that local detrending techniques filter out this slow part of the variability (see Appendix A4.1). Clearly, these issues are somehow more easily addressed than the fundamental mechanisms that may cause real (rather than perceived) variance to decrease towards a bifurcation. Nonetheless, it may be important to maintain a search image for these phenomena.

It is interesting that with respect to the factors we explored, rising autocorrelation appears a robust indicator of critical slowing down. Of course this is not to say that it will be a flawless indicator in practice. Our results are based on the assumption that the linear approximation of equation 2 sufficiently describes the underlying process of the system. This means that we can accurately measure critical slowing down (or $\lambda(x^*,p)$ in equation 2) using autocorrelation. In case the approximation is imprecise (as it may be in most practical cases), a quite long generated signal may be required to estimate the dominant eigenvalue from autocorrelation. This is not necessary when measuring variance, which in principle can be done with fewer data. Moreover, as mentioned in the introduction there is a series of situations in which no critical slowing down can be expected prior to a radical shift in the state of a system, and even if there is an underlying slowing down, systematic trends in the stochastic regime forcing the system may distort any pattern in correlation or variance. For instance, large magnitude perturbations can cause a shift already far from the bifurcation point (Guttal and Jayaprakash 2007; Scheffer et al. 2009), or they can dominate the behavior of the system completely as studied in the literature of so-called 'noise-induced transitions' (Horsthemke 2006). In such cases neither variance nor autocorrelation are expected to rise before major changes in the systems dynamics (see Appendix A4.2). Thus, identifying potential leading indicators in systems dominated by high levels of noise merits further study.

Another challenging problem in real-world situations is the long time-series needed to detect indicators of critical slowing down. The resulting large lag times, combined with potentially high costs of intervening and large uncertainty will make it hard to have decision makers act in a timely fashion (Biggs et al. 2009b; Contamin and Ellison 2009). In this light, the fact that spatial information may indicate critical slowing down with much shorter lag times (Carpenter and Brock 2010; Dakos et al. 2010; Donangelo et al. 2010; Guttal and Jayaprakash 2009) is of great importance. Interestingly, the fundamental mechanism that translates critical slowing down into rising temporal autocorrelation will also cause spatial correlation to increase (Dakos et al. 2010). In addition, other spatial pattern changes may indicate an upcoming systemic transition in a range of systems (Kéfi et al. 2007a; Rietkerk et al. 2004). However, as in the leading indicators from time-series, we are just starting to understand the underlying mechanisms.

Clearly, while the fundamental principle of critical slowing down is known in physics already for a long time, the search for practical leading indicators of critical transitions in ecology and earth science has just started. Although it is illustrative to demonstrate

particular model situations in which some indicators do not work (Ditlevsen and Johnsen 2010; Hastings and Wysham 2010), in this phase it may be especially useful to try to understand on a more fundamental level what are the limitations of different indicators. Undoubtedly, there exists a family of issues related to model identification and statistical estimation that affect our ability to detect generic early-warning signals. Although much remains to be explored in this field, it seems likely that, rather than a silver bullet approach we will need to develop a toolkit of indicators and a good understanding of when each of them might be most useful. When it comes to variance, it clearly remains an attractive candidate, as it is a straightforward characteristic that can in principle be easily measured. On the other hand, our results suggest a search image for situations in which it may not work as an indicator of critical slowing down.

Appendix

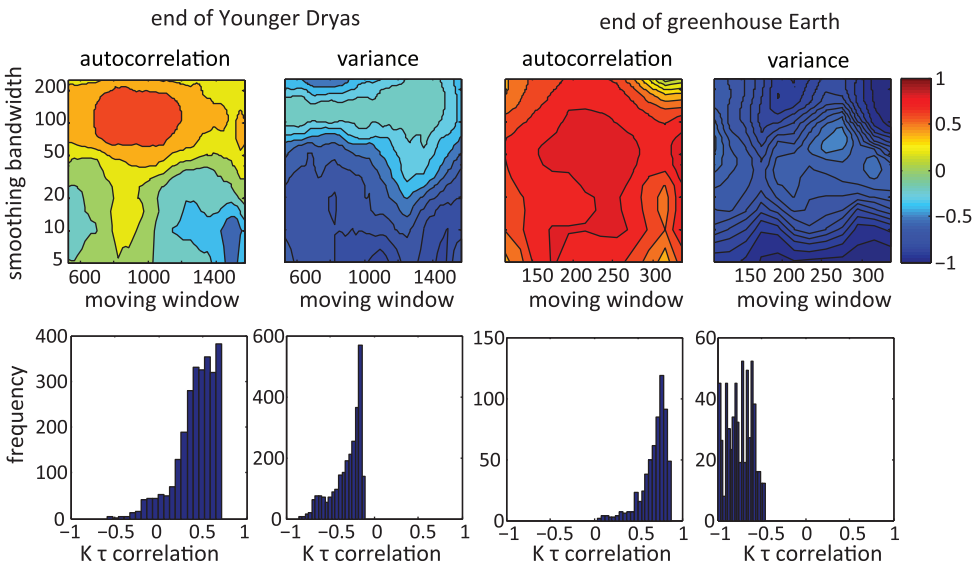

Figure A4.1 Sensitivity analysis on the trends in autocorrelation and variance prior to transition in the two paleoclimate records presented in the main text, for a range of moving windows and smoothing bandwidths. Autocorrelation shows a positive trend (positive Kendal τ coefficient) for both records, while variance is always decreasing prior to transition.

Appendix A4.1: Deviations in the performance of leading indicators when measured in time-series due to methodological issues

In this work, we have assumed that we can accurately estimate autocorrelation and variance in time-series produced by a system as it approaches a critical transition. In practice, there are important limitations to our data analysis capacity. Below we demonstrate how methodological issues in the analyses of time-series can also cause deviations in the estimates of leading indicators and in particular variance. For this we use a simple first-order autoregressive model $\tilde{z}_{t+1} = \phi\, \tilde{z}_t + \varepsilon_t$, where $\tilde{z}$ is the deviation of the process from some mean μ ($\tilde{z} = z - \mu$) and ε_t an error term. Variance is given by $\sigma_\phi = \frac{\sigma_\varepsilon^2}{(1-\phi^2)}$ and autocorrelation by $\rho_1 = \phi$ (Box 2008). In this model, the approach to a critical transition occurs when ϕ reaches 1 (random walk). As ϕ tends to 1 lower frequencies start to dominate and both variance and autocorrelation rise.

Effects of detrending on estimators

One aspect that we have to deal with is the occurrence of trends in our time-series. If at some point a trend kicks in, this will cause autocorrelation as well as variance to rise, even if there is no upcoming bifurcation at all. To avoid such 'false positives' detrending is required. However, detrending itself can also affect the results in unwanted ways. For example, if detrending is done relatively on a sufficiently fine scale that it removes major ups and downs in the time-series (Figure A4.2e), it may actually remove low frequencies fluctuations that carry important information. As close to transition low frequencies increase at the cost of higher frequencies, detrending may in fact cause the estimated variance to decrease as a result. As illustrated by our simulations (Figure A4.2), this may lead to a decrease in estimated variance (Figure A4.2c, d), even if real variance increases. Autocorrelation is not sensitive to this effect (Figure A4.2g, h).

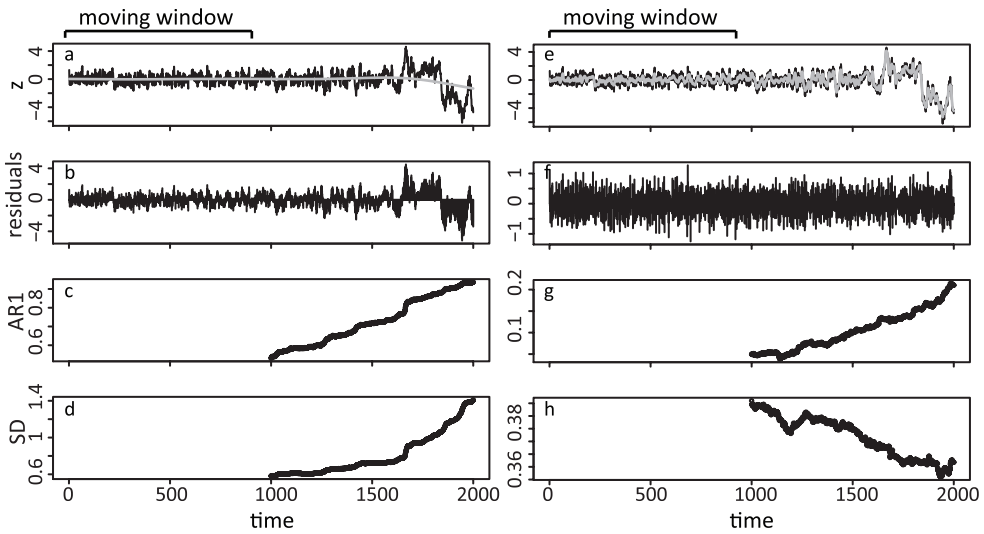

Figure A4.2 Time-series generated by a first-order autoregressive process approaching random walk. (**a**) Gaussian detrending accurately filtering out low frequencies (e.g. through detrending using a broad bandwidth (=500)). (**b**) Residuals after detrending **c**) Autocorrelation at-lag-1 increases. (**d**) Variance increases. (**e**) Gaussian detrending effectively filtering out low frequencies (e.g. through detrending using a narrow bandwidth (=6)). (**f**) Residuals after detrending (**g**) Autocorrelation at-lag-1 increases. (**h**) Variance decreases. (detrending and estimation of variance and autocorrelation with moving window size 50% of time-series, after Dakos et al. (2008); time-series generated with increasing coefficient ϕ from 0.5 to 0.99 in 10 steps, error mean zero and error variance 0.25; Gray line corresponds to Gaussian detrending).

Effects of limited time windows on estimators

Another related distortion may arise from the fact available time-series may not be long enough to allow accurate estimates of how characteristics of the fluctuations in the

system change as the system approaches a bifurcation. In practice, moving time windows used to estimate change in variance and autocorrelation will always be limited. As critical slowing down causes low frequencies to start dominating the fluctuations in the system, a limited moving window will cause both autocorrelation and variance to show a fluctuating trend prior to transition (Figure A4.3b, c). More interestingly, the limited moving window may lead to a weak increasing trend in estimated variance compared to autocorrelation (Figure A4.3b, c).

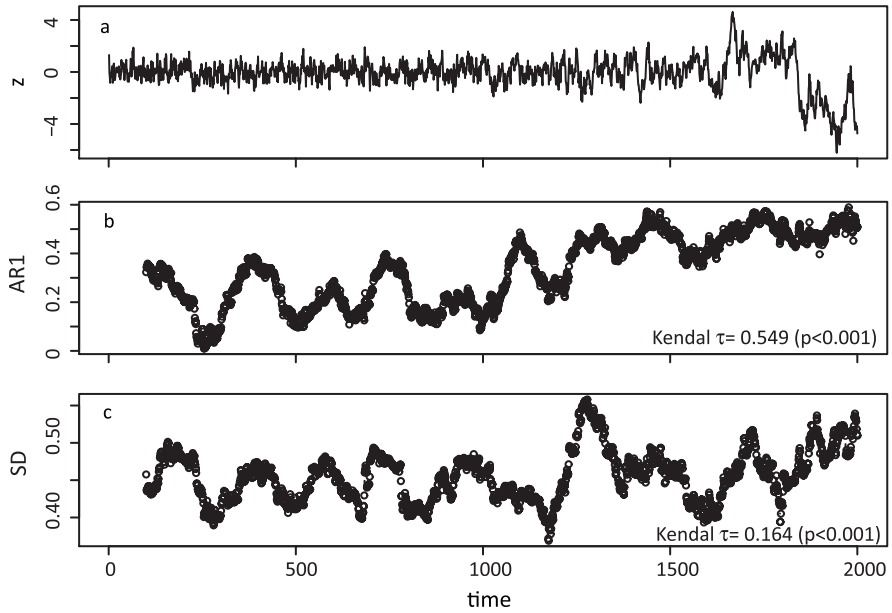

Figure A4.3 (**a**) Time-series generated by a first-order autoregressive process approaching random walk. The limited size of the moving window causes fluctuating trends in both autocorrelation at-lag-1 and variance. However, autocorrelation at-lag-1 (panel **b**, Kendall τ = 0.549 *p<0.001*) shows an overall positive trend compared to variance (panel **c**, Kendall τ = 0.164 *p<0.001*). (Detrending and estimation of variance and autocorrelation with moving window size of 100 points; trend removal with a Gaussian filter performed within the moving window with bandwidth = 10; time-series generated with increasing coefficient ϕ from 0.5 to 0.99 in 10 steps, error mean zero and error variance 0.25)

Appendix A4.2: Leading indicators in the case of noise-induced transitions

In this study, we restricted ourselves to the case where the magnitude of perturbations is relatively weak. In the case of strong perturbations on the state of a bistable system, it has been shown that the system jumps between the alternative attractors (Guttal and Jayaprakash 2007). Such phenomenon is defined as flickering and it has been suggested as an indicator of an approaching transition (Brock and Carpenter 2010; Scheffer et al. 2009).

Things, however, are different when the magnitude of perturbations affecting processes of the system becomes really strong. In that case, qualitative changes in the preferential states of the system may occur. This means that new states may appear, which do not correspond to the deterministic equilibria of the system (*noise-induced transitions*) (Horsthemke 2006). These new states are not equilibria in the strict sense of the word, but rather modes in the stationary probability distribution of the system state. The question that has not yet been explored is whether leading indicators would still work in the case of such noise-induced transitions.

For this, we consider a system in which a noise-induced transition occurs when noise magnitude exceeds a critical value, while no bifurcation exists in the deterministic counterpart of the system. To this end, we use the case of a linearly harvested population that grows logistically (May 2001):

$$\frac{dx}{dt} = rx(1-\frac{x}{K}) - cx \qquad \text{(eqA1)}$$

where K is the carrying capacity, r and c are growth and harvest rate parameters, respectively. With no noise, this system exhibits only one stable state ($x^*=K(1-c/r)$ for $r>c$), and undergoes no bifurcation. We consider the case in which r is a Gaussian stochastic parameter with mean r_0 and variance σ^2. In this case equation A1 becomes

$$dx = (r_0 x(1-\frac{x}{K}) - cx)dt + x(1-\frac{x}{K})\sigma dW \qquad \text{(eqA2)}$$

where the effect of environmental noise on the system dynamics is determined by factor $f_r(x) = x(1-\frac{x}{K})$ (see also main text). The solution of equation A2 provides the stationary probability distribution $p_s(x)$ of x. The maxima and minima of $p_s(x)$ are shown in Figure A4.4a as a function of noise intensity. In the absence of noise (i.e. σ=0) the system has a unimodal probability distribution that corresponds to the equilibrium of the deterministic part of equation A2. As σ exceeds a critical value (σ_c=1.18), the probability distribution becomes bimodal: now two modes are present (at x=0 and x>0, Figure A4.4a). Under such strong noise regime (σ=3), the bimodal distribution collapses to a unimodal distribution at which a population shifts to extinction, when harvesting rate c reaches a critical value (Figure A4.4b). The question is whether this transition – that is possible only under a strong noise regime – can be anticipated by an increase in autocorrelation and variance as the control parameter c approaches the critical point (c≈0.8). To answer this question we carried out numerical simulations using as initial conditions the nontrivial mode of the system paying particular attention to avoid measuring flickering (the repeated switches between the modes of the two probability distributions). Therefore, we considered only fluctuations of the state variable that remained within the probability distribution of the nontrivial equilibrium. We did this by truncating each simulation to the point at which x dropped below the dashed line in Figure A4.4b. We repeated this for 1,000 simulations and estimated the average variance and average autocorrelation at-lag-1. We found that

both variance and autocorrelation decrease as the system approaches the critical point (Figure A4.4c, d). Our results demonstrate that in the case of noise-induced transitions leading indicators may fail to signal the approaching transition.

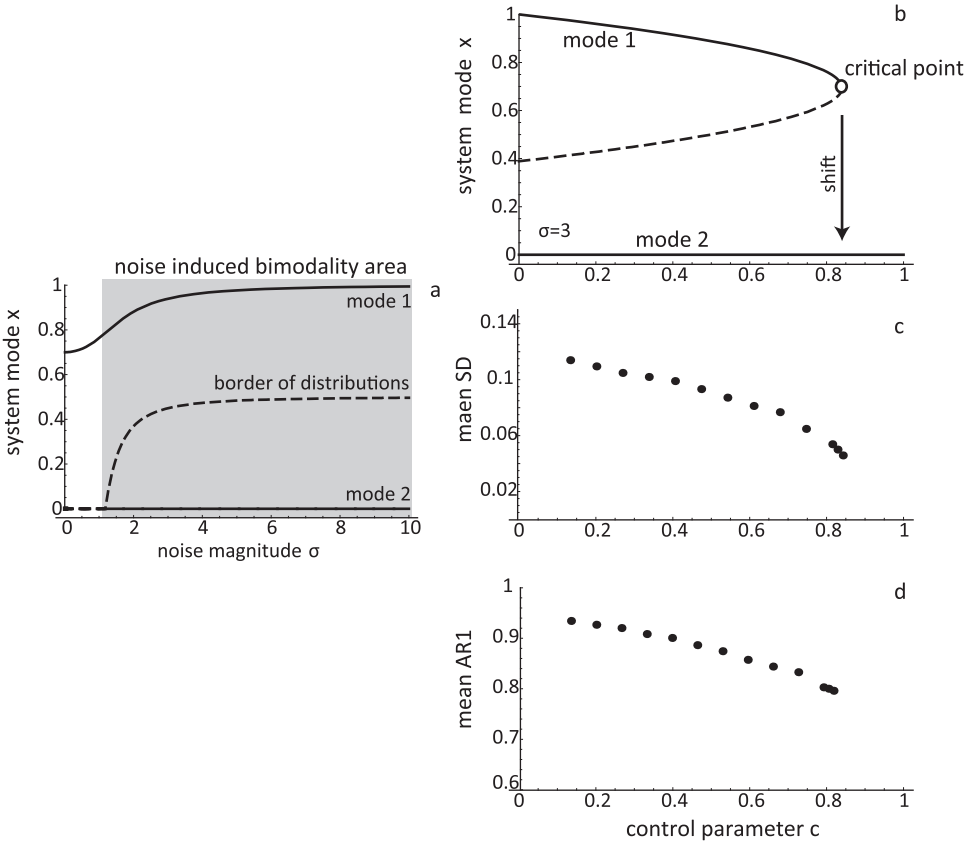

Figure A4.4 (**a**) Modes of stationary distribution of state variable x of equation A2 as a function of noise magnitude σ. Bimodality emerges only when noise magnitude exceeds a critical value (r_0=1, K=0.3, σ=1.18, noise-induced transition). (**b**) Bifurcation diagram for a noise-induced bimodal system (σ=3) as a function of control parameter harvest rate c. (**c**) Average variance (estimated as standard deviation), and d) Average autocorrelation at-lag-1 (AR1) prior to the transition. (Solid lines: stable modes of stationary distributions; dashed lines: borders between stationary distributions of modes)

Chapter 5

Slowing down in spatially patterned ecosystems at the brink of collapse

Predicting the risk of critical transitions such as the collapse of a population is important in order to direct management efforts. In any system that is close to a critical transition, recovery upon small perturbations becomes slow, a phenomenon known as 'critical slowing down'. It has been suggested that such slowing down may be detected indirectly through an increase in spatial and temporal correlation and variance. Here, we tested this idea in arid ecosystems, where vegetation may collapse to desert due to increasing water limitation. We used three models that describe desertification, but differ in the spatial vegetation patterns they produce. In all models, recovery rate upon perturbation decreased before vegetation collapsed. However, in one of the models, slowing down failed to translate into rising variance and correlation. This is caused by the regular self-organized vegetation patterns produced by this model. This finding implies an important limitation of variance and correlation as indicators for critical transitions. However, changes in such self-organized patterns themselves are a reliable indicator of an upcoming transition. Our results illustrate that while critical slowing down may be a universal phenomenon at critical transitions, its detection through indirect indicators may have limitations in particular systems.

This chapter is based on the paper: V. Dakos, S. Kéfi, M. Rietkerk, E. H. van Nes and M. Scheffer. Slowing down in spatially patterned ecosystems at the brink of collapse. *American Naturalist* (in press). We thank Ilka Hoof for reading and commenting on the paper, and Sergio Rinaldi for valuable discussions on bifurcation theory.

Introduction

There is growing evidence that some ecosystems may occasionally undergo catastrophic transitions to alternative states (Scheffer et al. 2001): coral reefs can be overgrown by fleshy algae and shift to a degraded state (Knowlton 2004); shallow lakes may flip from a macrophyte dominated clear-water state to a turbid-water state due to eutrophication (Scheffer 1998) and arid ecosystems may lose their perennial vegetation and turn into desert due to increasing aridity or overgrazing (MA 2005; Reynolds et al. 2007).

Close to a critical threshold for such catastrophic transitions, the resilience (*sensu* Holling 1973) of an ecosystem becomes small in the sense that only a small perturbation is needed to tip the ecosystem to an alternative state. Intuitively, such loss of resilience can be understood as the shrinking of the basin of attraction around the equilibrium state of the ecosystem (Figure 5.1a, b). Unfortunately, our knowledge of most ecosystems or other system is insufficient to predict critical thresholds, while at the same time it is difficult to measure resilience directly (Carpenter 2003). In view of these limitations, an alternative approach has been recently proposed (Scheffer et al. 2009).

The idea is to use generic properties of critical thresholds (in mathematical jargon, bifurcation points) to develop early-warning indicators that can be used as indirect indicators of resilience (Scheffer et al. 2009). These indicators are simple statistical properties that can be measured directly by monitoring the state variables of the system, and they all behave in predictable ways prior to transitions regardless of the details of the system. In other words, theory suggests that we can identify the risk of an upcoming transition by monitoring characteristics such as population abundances, nutrient concentrations, or vegetation cover in any system be it a coral reef, a lake, or a savanna ecosystem.

The fact that these indicators change predictably prior to critical transitions is related to the return rate to equilibrium after a perturbation that goes to zero at most bifurcations. To see what this means intuitively, note that when the basin of attraction shrinks, it also becomes flatter (Figure 5.1a, b). This implies that the monitored state variable of the system - such as macrophyte cover in a lake - returns more slowly to equilibrium after a small perturbation (Figure 5.1b) (Wissel 1984). This phenomenon, known as critical slowing down (Strogatz 1994), has major consequences for the transient behavior of the system. A system will take longer to recover from a disturbance when it is close to a critical threshold (van Nes and Scheffer 2007) (Figure 5.1a1, b1). If the system is subjected to stochastic perturbations there are also systematic changes in its fluctuations. First, it will resemble its previous state more closely when it is close to a critical threshold (Held and Kleinen 2004; Ives 1995) (Figure 5.1a2, b2). Second, the state of the system will fluctuate more widely around its equilibrium close to transition (Carpenter and Brock 2006; Van Nes and Scheffer 2003) (Figure 5.1a3, b3). Usually, but not necessarily, the basin of attraction also becomes asymmetric close to a transition (Figure 5.1a, b) (Scheffer et al. 2009). Such asymmetry causes the state of the system to spend more time in the flatter part of the attraction basin (Figure 5.1a4, b4). As a result the distribution of system states becomes skewed nearby a transition (Guttal and

Jayaprakash 2008). While most of the work on leading indicators has focused on the analysis of time-series, the temporal indicators that signal approaching shifts have spatial equivalents as well. This means that we can also measure leading indicators using spatial information for systems such as the distribution of abundances of metapopulations in a fragmented habitat, or the distribution of vegetation over a landscape. In such cases, spatial correlation may rise (Dakos et al. 2010), spatial variance may increase (Donangelo et al. 2010; Guttal and Jayaprakash 2009), and spatial skewness will often peak (Guttal and Jayaprakash 2009) before a spatially connected system goes through a systemic shift to an alternative state.

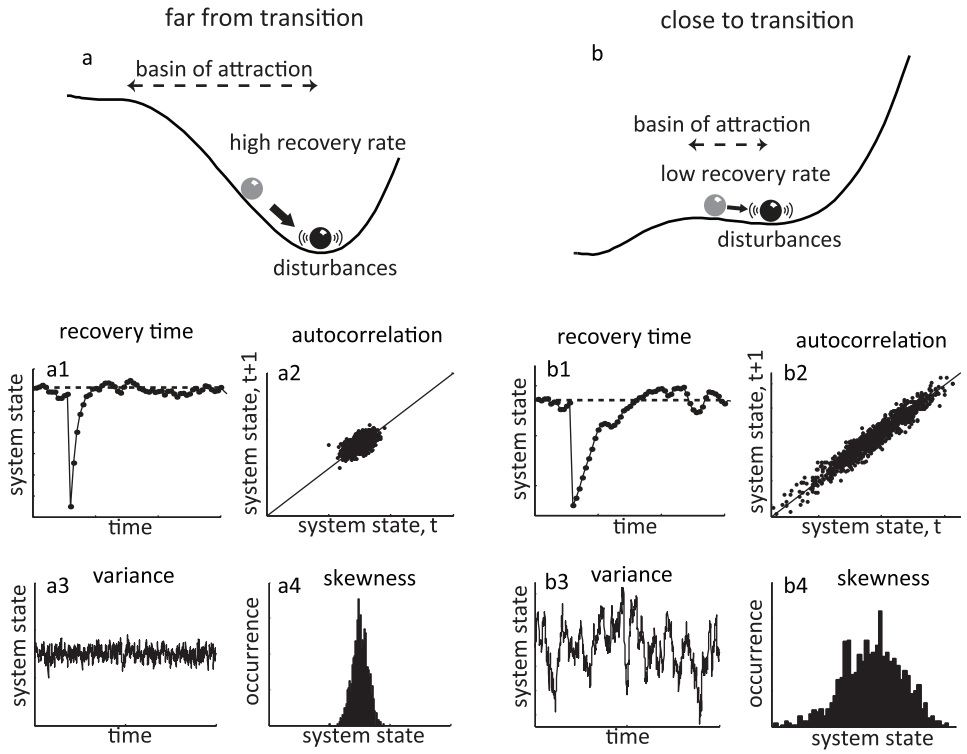

Figure 5.1 Balls and cups representation of the basin of attraction of a system with alternative stable states. (**a**) Far from transition the state of the system lies in a broad basin of attraction. Small disturbances to equilibrium are damped by high recovery rates back to equilibrium. As a result the time to recover from a disturbance is short (**a1**). When monitoring the state of the system in time, the collected time-series is characterized by low correlation between subsequent values (**a2**), low variance (**a3**), and low skewness (**a4**). (**b**) Close to transition the basin of attraction shrinks and may become asymmetric. Small disturbances increase the chance of shifting to the alternative state and they are not anymore effectively damped due to low recovery rates back to equilibrium. The time to recover from a disturbance now is long (critical slowing down) (**b1**), and the collected time-series is characterized by high correlation between subsequent values (**b2**), high variance (**b3**), and high skewness (**b4**).

So far, most of these indicators have been tested in relative simple models where a specific type of critical transition occurs (i.e. a fold or transcritical bifurcation) (Carpenter and Brock 2006; Guttal and Jayaprakash 2008; van Nes and Scheffer 2007). In such simple models the indicators work well. There are, however, other cases of critical transitions for which it is not yet clear whether these indicators would successfully work (Hastings and Wysham 2010; Scheffer et al. 2009). Spatially explicit ecosystems with pattern formation are such case (Rietkerk et al. 2004).

Pronounced examples of such patterned ecosystems come from arid ecosystems where we can find a mosaic of vegetated patches and bare soil (Aguiar and Sala 1999). Climate change and human pressure may cause these systems to turn into barren deserts (Reynolds et al. 2007) with considerable consequences on the livelihoods of more than 25% of the world's population. Specific models have shown that the collapse of vegetation to bare soil can be a critical transition (Rietkerk et al. 2002). Depending on the spatial mechanisms that dominate in arid ecosystems, particular changes in spatial patterns may signal if vegetation is close to collapsing into bare ground. A class of models stressing local facilitation predicts changes in the size distribution of vegetation patches prior to desertification (Kéfi et al. 2007a; Kéfi et al. 2011). Another class of models stresses that when resources accumulate in the vicinity of vegetation but are depleted elsewhere (Rietkerk et al. 2002), regular self-organized patterns occur. In these models, pattern shapes are predicted to change in specific ways before the collapse to a desert state (Rietkerk et al. 2004; von Hardenberg et al. 2001). Remarkably, the universal phenomenon of critical slowing down, and the way this may translate into the generic leading indicators of correlation and variance, has not been studied in such spatially patterned systems so far. Obviously, combining generic and specific leading indicators in this type of spatial systems can advance our ability to anticipate critical transitions.

Here, we address this gap in our understanding of the predictability of critical transitions in spatially patterned models using arid ecosystems as an example. First, we explore whether critical slowing down occurs before the collapse to desertification in these models. We then estimate both spatial and temporal early-warning indicators and compare them to the specific pattern-based indicators found in these systems when approaching a critical transition.

Methods

Three models of desertification: spatial mechanisms, patterns and transitions

We analyzed three existing models that describe spatial dynamics of vegetation in arid ecosystems. All models may undergo a critical transition to a desert state, but they differ in the type of patterns they exhibit. All transitions are associated to hysteresis. This means that restoring environmental conditions to values before the transition does not lead to recovery of vegetation. Below we describe the mechanisms, transitions and patterns encountered in each model.

Table 5.1 Models, parameters and their values used in this study.

Model and Parameter	Definition, Value and Unit

'local-positive feedback' model (modified from Guttal & Jahaprakash, 2007)

$$\frac{dw_{i,j}}{dt} = R - w_{i.j} - \lambda w_{i.j} B_{i.j} + D(w_{i+1.j} + w_{i-1.j} + w_{i.j+1} + w_{i.j-1} - 4w_{i.j}) + \sigma_w dW_{i,j} \qquad (1a)$$

$$\frac{dB_{i.j}}{dt} = \rho B_{i.j}(w_{i.j} - \frac{B_{i.j}}{B_c}) - \mu \frac{B_{i.j}}{B_{i.j} + B_O} + D(B_{i+1.j} + B_{i-1.j} + B_{i.j+1} + B_{i.j-1} - 4B_{i.j}) + \sigma_B dW_{i,j} \qquad (1b)$$

$w_{i,j}$	water moisture level in each gridcell (i,j), mm
$B_{i,j}$	vegetation biomass in each gridcell (i,j), g
D	exchange rate, 0.05 d^{-1}
λ	water consumption rate by vegetation, 0.12 g^{-1} d^{-1}
ρ	maximum vegetation growth rate, d^{-1}
B_c	vegetation carrying capacity, 1 g
μ	maximum grazing rate, 2 d^{-1}
B_O	half saturation constant of vegetation consumption, 1 (-)
R	mean annual rainfall, range: 0.8 - 2 mm d^{-1} **(control parameter that determines the collapse of vegetation at a critical value)**
σ_w	standard deviation of white noise on water moisture, 0.01
σ_B	standard deviation of white noise on vegetation biomass, 0.25
$dW_{i,j}$	white noise; uncorrelated in each gridcell (i,j)

'local-facilitation' model (Kéfi et al, 2007)

$$w_{\{0,+\}} = (\delta\rho_+ + (1-\delta)q_{+|0})(b - c\rho_+) \qquad (2a)$$

$$w_{\{-,0\}} = r + f\,q_{+|-} \qquad (2b)$$

$$w_{\{+,0\}} = m \qquad (2c)$$

$$w_{\{0,-\}} = d \qquad (2d)$$

$w_{\{0,+\}}$	colonization probability of an unoccupied site
$w_{\{-,0\}}$	regeneration probability of a degraded site
$w_{\{+,0\}}$	mortality probability of an occupied site
$w_{\{0,-\}}$	degradation probability of an unoccupied site
ρ_+	density of vegetated sites
$q_{i\|j}$	clustering vegetation intensity probability of finding a site j in state i (+,0,-)
m	mortality probability of a vegetated site, 0.1 (-)
f	local facilitation strength: maximum effect of a neighboring vegetated site on the regeneration of a degraded site, 0.9 (-)
β	'intrinsic seed production rate per vegetated site' x 'survival probability' x 'germination probability'
ε	establishment probability of seeds on {o}-site in a system without competition
b	b (=β*ε) measures the severity of the environmental conditions. A lower b value reflects a higher aridity level, range: 0.3 - 1 (-) **(control parameter that determines the collapse of vegetation at a critical value)**
δ	fraction of seeds globally dispersed, 0.1 (-)
g	competitive effect of the global density of {+}-sites on the establishment of new individuals
c	β*g, 0.3 (-)
r	regeneration probability of a {-}-site without vegetated sites in its neighborhood, 0.0001 (-)
d	degradation probability of {o}-sites, 0.2 (-)

Table 5.1 continued

'scale-dependent feedback' model (modified from Rietkerk et al., 2002)

$$\frac{\partial P}{\partial t} = cg_{\max}\frac{W}{W+k_1}P - dP + D_p\Delta P + \sigma dW \qquad (3a)$$

$$\frac{\partial W}{\partial t} = \alpha O\frac{P+k_2W_O}{P+k_2} - cg_{\max}\frac{W}{W+k_1}P - r_wW + D_w\Delta W + \sigma dW \qquad (3b)$$

$$\frac{\partial O}{\partial t} = R - \alpha O\frac{P+k_2W_O}{P+k_2} + D_O\Delta O + \sigma dW \qquad (3c)$$

P	plant density, g m^{-2}
W	soil water, mm
O	surface water, mm
c	conversion of water uptake to plant growth, 10 g mm^{-1} m^{-2}
g_{max}	maximum specific water uptake, 0.05 mm g^{-1} m^{-2} d^{-1}
k_1	half-saturation constant of specific plant growth and water uptake, 5 mm
D_p	plant dispersal, 0.1 m^{-2} d^{-1}
α	maximum infiltration rate, 0.2 d^{-1}
k_2	saturation constant of water infiltration, 5 g m^{-2}
W_O	water infiltration rate in the absence of plants, 0.2 (-)
r_w	specicific water loss due to evaporation and drainage, 0.2 d^{-1}
D_w	diffusion coefficient of soil water, 0.1 m^2 d^{-1}
D_O	diffusion coefficient of surface water, 100 m^2 d^{-1}
d	specific loss of plant density due to mortality, 0.25 d^{-1}
Δ	Laplacian operator for diffusion
R	rainfall, range: 0.05 - 2 mm d^{-1} **(control parameter that determines the collapse of vegetation at a critical value)**
σ	standard deviation of white noise, 0.01
dW	white noise

The first model is based on the vegetation model by Guttal and Jayaprakash (2007) and Shnerb et al. (2003) (Table 5.1, eqs 1a-b). We made this model spatially explicit by defining it as a stochastic lattice differential equation model (LDE) (Chow et al. 1996). In such a model, space is represented by a two dimensional lattice of coupled patches (Keitt et al. 2001; van Nes and Scheffer 2005). In each patch, vegetation *B* grows logistically and has a loss rate due to grazing. Vegetation growth depends on water availability *w*. When annual rainfall decreases, water scarcity reduces vegetation growth. At some point, vegetation growth cannot compensate for losses to grazing, and a patch shifts to its alternative overgrazed desert state. Biomass and water are exchanged between neighboring patches at rate *D*. Therefore a patch with high biomass will have the tendency to 'leak' biomass to its neighboring sites, which results in a positive effect on its neighbors (in terms of biomass gain) but in a negative effect on the site itself (Figure 5.2a1). If this diffusive effect is very strong, differences between patches tend to be smoothed out and the ecosystem as a whole remains in a homogeneously vegetated state (Figure 5.2a2), until conditions force all patches to flip to the desert state through synchronized 'fold bifurcations' at each patch (Figure 5.2a3) (van Nes and Scheffer 2005). (Bifurcations are parameter values where the qualitative behavior of a system

changes fundamentally.) The important mechanism in this model is a positive feedback that causes each patch to have alternative stable states (undergrazed vegetated state or overgrazed desert state). For this reason, in the rest of the paper we refer to this model as *'local-positive feedback'* model.

The second model is a stochastic cellular automaton (CA) (Kéfi et al. 2007b) (Table 5.1, eqs 3a-c) with discrete time steps. An ecosystem is represented by a lattice composed of cells, which can only be in one of three states: vegetated (+), empty (o) or degraded (-). Empty cells are cells whose soil is still fertile. Degraded cells are cells with eroded soil unsuitable for recolonization. The basic processes in this model are captured by four transformations: colonization of empty cells, mortality of vegetation, degradation of empty cells, and regeneration of degraded cells. Each of these four transformations can occur with a certain probability at each time step (Table 5.1, eqs 2a-d). The colonization and regeneration probabilities of a patch are positively affected by the presence of vegetation in its four neighboring cells (Figure 5.2b1). Because of this facilitating effect we will refer to this model hereafter as the *'local-facilitation'* model. The facilitation leads to the formation of clusters of vegetated gridcells and these patches have size distributions that can be described by a power law (Figure 5.2b2) (Kéfi et al. 2007a; Kéfi et al. 2011). The size of the clusters is dependent on the ecological conditions (such as rainfall or grazing pressure). Under favorable conditions giant clusters span the lattice from one edge to the other (Kéfi et al. 2011). The point where these giant clusters break down is called the 'percolation point'. When conditions become even harsher, a transition point is reached where all vegetation goes extinct (Figure 5.2b3).

The third model is a stochastic version of a partial differential equations model (PDE) describing the dynamics of vegetation biomass, soil water and surface water (HilleRisLambers et al. 2001; Rietkerk et al. 2002) (Table 5.1, eqs 3a-c). Plants, *P*, grow depending on soil water availability and are lost due to mortality or grazing. Surface water, *O*, is supplied by rainfall and lost due to infiltration in the soil and runoff. Soil water, *W*, is surface water that infiltrated in the soil after rain events and is taken up by plants or lost by runoff. Plants, soil water and surface water are all assumed to diffuse in two-dimensional space. In this model, the infiltration rate of water in the soil is higher in areas with vegetation than in bare soil, leading to accumulation of water under vegetation and to its depletion further away: a scale-dependent feedback. In other words, vegetation has a local-positive effect on itself and on its immediate surroundings, but a negative effect further away (Figure 5.2c1). For this reason, in the rest of the paper, we refer to this model as *'scale-dependent feedback'* model. This scale-dependent feedback leads to the formation of regular vegetation patterns (Figure 5.2c2, c3), through a so-called 'Turing instability' (Turing 1952). At the Turing instability the feedback is just strong enough to form patterns (HilleRisLambers et al. 2001; Rietkerk et al. 2002; von Hardenberg et al. 2001). Patterns show a distinct sequence of shapes from gaps to labyrinths and to spots with decreasing rainfall. When water availability becomes limited, vegetation cannot sustain itself and the ecosystem undergoes a second transition point: that of collapse into desert (Figure 5.2c3).

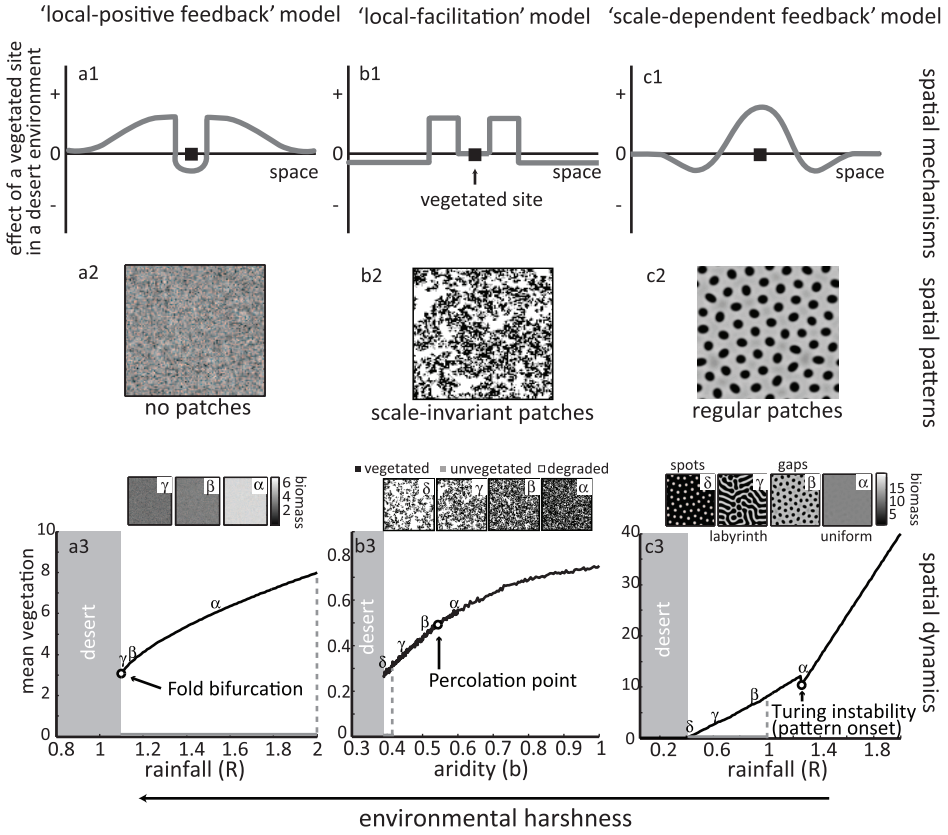

Figure 5.2 Schematic representation of the effect of vegetation on its environment, the patterns formed, and the dynamics of vegetation as function of environmental harshness. (**a**) 'Local-positive feedback' model: (**a1**) a vegetated site with high vegetation biomass has positive effect on its environment but negative effect on itself due to 'leak' of biomass to neighboring sites. The positive effect diminishes with distance. (**a2**) No patches form, only irregular clustering of biomass. (**a3**) Spatial vegetation mean biomass with decreasing rainfall *R*. (**b**) 'Local-facilitation' model: (**b1**) a vegetated site has positive effect at its direct vicinity with no cost on itself. (**b2**) Irregular vegetation patches form. (**b3**) Spatial vegetation density (fraction of vegetation sites occupied) with decreasing aridity *b*. (**c**) 'Scale-dependent feedback' model: (**c1**), a vegetated site has positive impact on itself and its surroundings, but negative feedback further away because local accumulation of water means that is depleted further away. (**c2**) Regular vegetation patterns form. (**c3**) Spatial vegetation mean density with decreasing rainfall *R*. Regardless of the spatial mechanisms in each model, there is a critical point at which vegetation collapses (gray shaded area). (Fold bifurcation: point at which total vegetation shifts to desert; Percolation point: break-up of giant cluster that spans the whole lattice; Turing instability: onset of regular pattern formation. Embedded panels are spatial snapshots of vegetation before desertification. Dotted gray lines indicate the hysteresis loop present in all systems.)

Simulations and analyses

Parameter values of the three models and their units are given in Table 5.1. We used parameter values such that the transition of vegetation to desertification is discontinuous ('catastrophic'). In all models, we assumed homogeneous conditions, i.e. parameter values are the same everywhere in space. For each model, we selected a parameter that describes aridity (see Table 5.1), as this drives desertification in arid ecosystems. In the *'local-positive feedback'* and *'scale-dependent feedback'* models the level of aridity is directly determined by rainfall (parameter *R*, low rainfall leads to low vegetation growth), whereas in the *'local-facilitation'* model aridity is indirectly determined by the establishment probability of new vegetation (parameter *b*, high aridity leads to low vegetation establishment). In all models we changed these control parameters in small steps. We started simulations from a complete vegetated state in all models. We discarded transients and continued the simulations in each step using the last stationary state as initial condition. We repeated this until the control parameters reached a critical threshold at which vegetation collapsed.

We first examined whether critical slowing down occurs before all transition points in all models. As there are no formal analytical solutions for all transitions that could enable us estimate critical slowing down by the dominant eigenvalue of the system (Scheffer et al. 2009), we followed a numerical approach (van Nes and Scheffer 2007). After the ecosystem reached equilibrium, we removed 10% of the total vegetation biomass, cover or density according to model, and estimated the recovery time to equilibrium (with an accuracy of 0.01%) by simulation. We did this along the whole pathway to collapse of vegetation for all models.

For the calculation of the spatial indicators, we used equilibrium values of vegetation biomass, cover or density according to model for each level of control parameter up to collapse of vegetation. In the case of the *'local-facilitation'* model, we first determined the vegetation cover by summing the vegetated cells using a *4*×*4*-cells non-overlapping moving filter along the lattice. We estimated spatial correlation between neighbors, spatial variance, and spatial skewness. Spatial correlation between-neighbors was defined as the two-point correlation for all pairs of neighboring cells using Moran's coefficient (Legendre and Fortin 1989). Skewness was estimated as the third moment about the mean, $\frac{E(x-\mu)^3}{\sigma^3}$, where μ is the mean of x, σ is the standard deviation of x, and *E(.)* is the expectation operator.

In addition to spatial indicators, we also followed the evolution of temporal correlation, variance and skewness. To this end, for each level of control parameter, we estimated autocorrelation at-lag-1, variance, and skewness of total vegetation biomass, cover or density from the last 1,000 points of the produced time-series. We calculated autocorrelation at-lag-1 by fitting an autoregressive model of first order using the *arfit* package in MATLAB (Neumaier and Schneider 2001). To compare the performance of both spatial and temporal indicators, we quantified their trends using the nonparametric Kendall τ rank correlation of the control parameter and the spatial and temporal

correlation estimates. A Kendall τ coefficient that was significantly different from zero (p<0.025) specified whether the indicators increased or decreased before each transition point.

All simulations and statistical analyses were performed in MATLAB v7.1.0246 (The Mathworks). We solved the stochastic equations of the *'local-positive feedback'* model in a *100×100* cells lattice using an Euler-Murayama integration method with Ito calculus. We used a stochastic asynchronous update algorithm for the *'local-facilitation'* model in a *400×400* cells lattice. The *'scale-dependent feedback'* model was implemented in a *128×128* cells lattice and solved using a semi-implicit method (Janssen et al. 2008). The stochastic part of the *'scale-dependent feedback'* model was solved using an Euler-Murayama integration method with Ito calculus. We assumed periodic boundaries in all models.

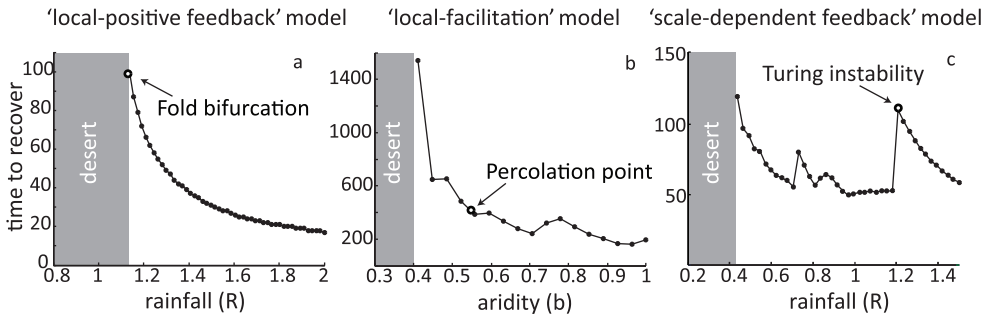

Figure 5.3 Critical slowing down approximated by recovery time before the collapse of vegetation in all three models. Recovery time was estimated by a pulse perturbation experiment as the time for mean plant density to recover back to equilibrium after a 10% reduction in plant densities in the whole lattice. [Results based on simulations in a *64x64* lattice for the *'local-positive feedback'* and *'scale-dependent feedback'* models. All other parameters as presented in the main text.]

Results

Critical slowing down prior to transitions

We first checked whether critical slowing down was present before each transition point in all models. In all models we found an increase in time needed for recovery as the ecosystem approached the critical point of collapse to a desert state (Figure 5.3). Similarly, recovery times increased before the Turing instability point in the *'scale-dependent feedback'* model (Figure 5.3c). All these points belong to the type of transitions where critical slowing down is expected to occur: they represent 'local' bifurcations of stable equilibria that become unstable (Dakos et al. 2010; Judd and Silber 2000; Kéfi et al. 2007a). Interestingly, critical slowing down occurred also before the vegetation collapse in the *'scale-dependent feedback'* model, despite the fact that this

transition represents a more complicated kind of bifurcation. Specifically it corresponds to a 'global' bifurcation where a stable spatial periodic attractor (the regular vegetation patterns) collapses to a uniform desert state. Obviously the percolation point in the *local facilitation* model cannot be detected by critical slowing down as this point does not correspond to a bifurcation that would imply a change in the stability of the ecosystem.

Spatial leading indicators prior to transitions

For the transitions where critical slowing down was at play, we tested whether spatial correlation, variance and skewness also increased (see Table A5.1 in the Appendix). In the *'local-positive feedback'* model, all of these spatial indicators showed clear positive trends before the transition (Figure 5.4a1-3) similar to those observed in previous studies (Dakos et al. 2010; Guttal and Jayaprakash 2009). Close to collapse, slowly decaying fluctuations of vegetation resulted in an increase in spatial variance. As these fluctuations took place in an increasingly asymmetric basin of attraction, spatial skewness changed as well (it became negative because vegetation biomass distributions skewed towards low biomass values).

In the *'local-facilitation'* model, the three spatial indicators behaved more-or-less the same as in the *'local-positive feedback'* model (Figure 5.4b1-3). Far from the transition, environmental conditions sustained large areas of vegetation cover leading to low spatial variance (Figure 5.4b1). Spatial skewness was negative, as distributions of vegetation cover were skewed towards low values (Figure 5.4b2). As aridity increased, areas of high vegetation cover broke into smaller parts: vegetation cover distributions became symmetric and, therefore, variance increased and skewness became zero. Approaching the transition skewness turned positive, because now, areas of high vegetation cover became scarce. Variance of vegetation cover also rose towards the transition only to drop just before the shift. Spatial correlation between-neighbors gradually increased up to the transition (Figure 5.4b3). As expected no special change occurred before the percolation point. In addition to spatial correlation, variance and skewness, changes in patch size distributions also indicated proximity to desertification (Figure 5.5a).

In the *'scale-dependent feedback'* model, the onset of pattern formation at the Turing instability point was again announced by an increase in spatial correlation between-neighbors and variance (Figure 5.4c1-3) as would be expected in view of the critical slowing down we found (Figure 5.3c). Spatial skewness, remained constant (Figure 5.4c2), as there is no alternative attractor (bare ground) before the onset of pattern formation. Despite the presence of critical slowing down, spatial correlation or variance did not increase prior to the collapse of vegetation in the *'scale-dependent feedback'* model (Figure 5.4c1-3). There was an increase in spatial skewness. However, this was driven by the increasing number of bare cells in the lattice due to gradual loss of vegetation rather than due to an asymmetric basin of attraction. Spatial variance stayed high as patterns evolved from gaps to labyrinths, but decreased when spots emerged and dropped just before the ecosystem turned into desert (Figure 5.4c1). Spatial

correlation of vegetation density was high and dropped only close before the collapse, when the regularity in the shape of the patterns became weaker (Figure 5.4c3). While spatial correlation and variance did not change as the ecosystem approached this transition, the sequence in the shape of vegetation patterns clearly indicated the upcoming collapse (Figure 5.5c).

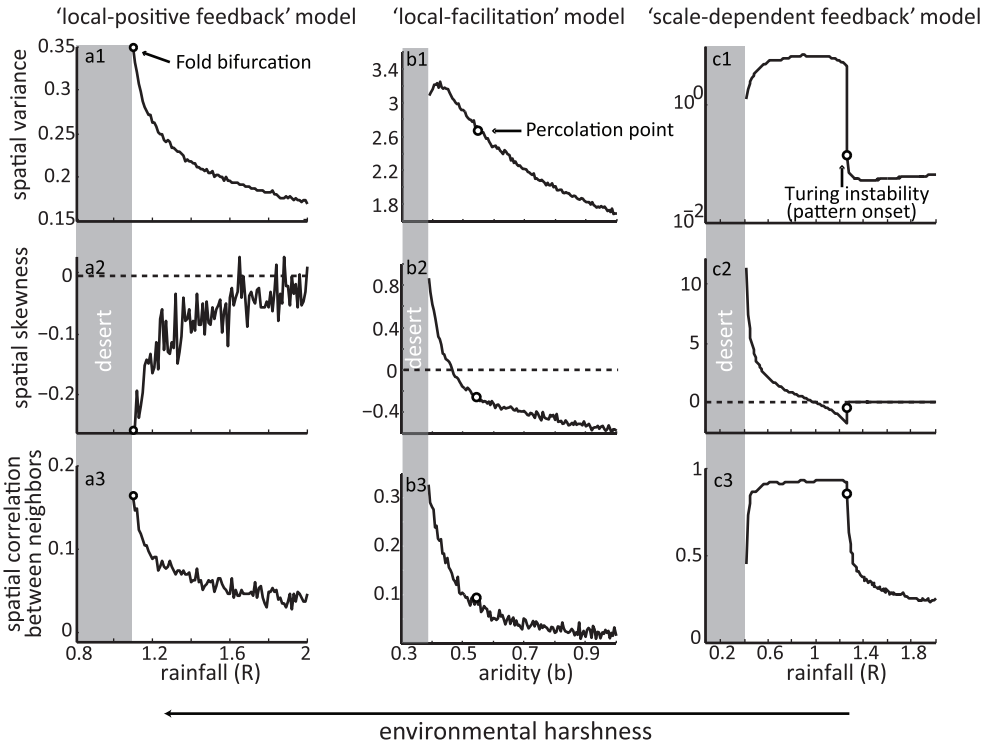

Figure 5.4 Spatial variance, spatial skewness, and spatial correlation between neighbors as function of increasing harshness in the environment up to desertification (gray shaded area). Spatial indicators are estimated using final values of all cells at the end of the simulation for each level of the control parameter (rainfall in 'local-positive feedback' and 'scale-dependent feedback' models; aridity in 'local-facilitation' model). Open circles indicate: (**a1-3**) the point at which vegetation shifts to barren state in the 'local-positive feedback' model (Fold bifurcation); (**b1-3**) the point at which patches of vegetation that span the lattice from one edge to the other disappear in the 'local-facilitation' model (Percolation point); (**c1-3**) the onset of regular vegetation patterning in the 'scale-dependent feedback' model (Turing instability).

Temporal leading indicators prior to transitions

In addition to spatial correlation, variance and skewness, we estimated temporal autocorrelation (at-lag-1), variance and skewness for the total vegetation cover in all models (Figure 5.6). In the *'local-positive feedback'* and *'local-facilitation'* models, auto-

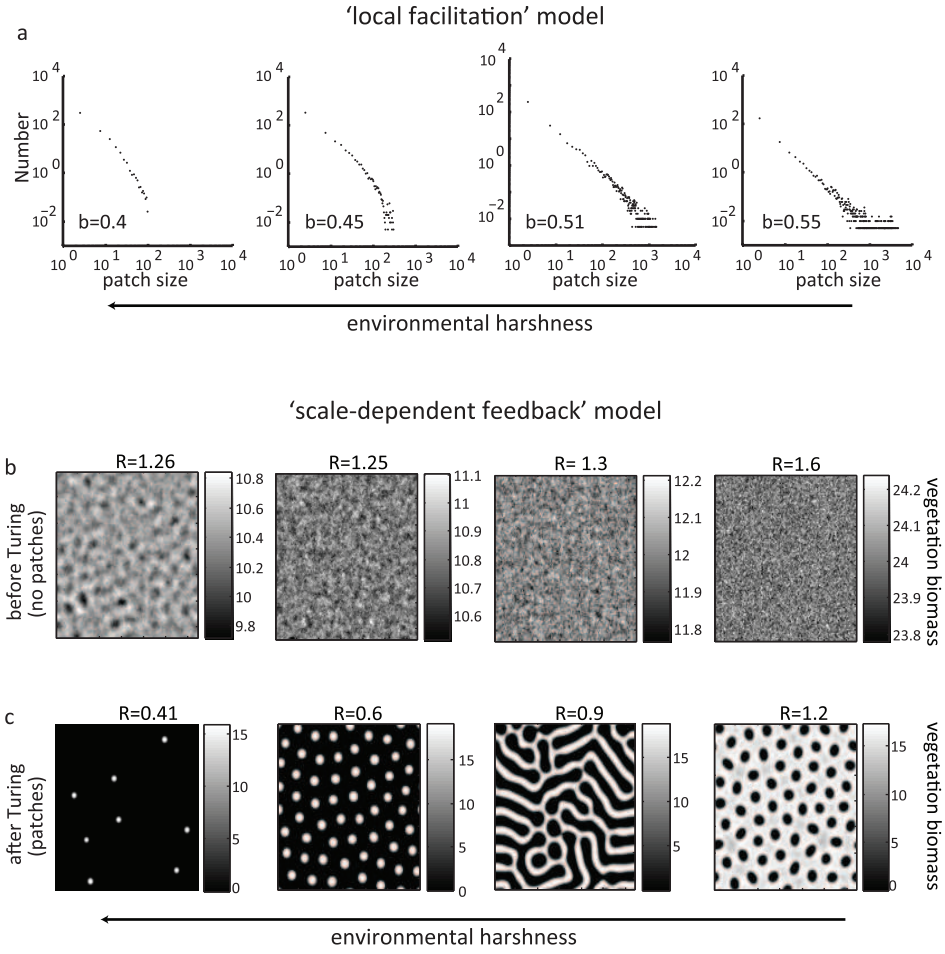

Figure 5.5 System-specific indicators. (**a**) 'Local-facilitation' model: Evolution of patch size distributions. As conditions become harsher, big vegetated patches disappear and their distribution is characterised by a truncated power law. Statistical properties of the changing distributions are summarized in Figure A5.1 in the Appendix. (**b**) 'Scale-dependent feedback' model: Spatial configuration of vegetation before the Turing instability for decreasing rainfall (R). Note the slight emergence of patterns before the Turing instability (R ≈ 1.25, scale in all panels is comparable). (**c**) After the Turing there is a specific sequence of pattern shapes: gaps, labyrinth, spots and the gradual loss of spots till the system collapses.

correlation (at-lag-1) and variance increased towards the transition (Figure 5.6a1, a3, b1, b3). Temporal skewness did not change in any of the two models (Figure 5.6a2, b2). In the *'scale-dependent feedback'* model, all temporal indicators failed to signal upcoming desertification (Figure 5.6c1-3). Peaks in variance of total vegetation density after the Turing instability occurred almost when patterns changed from gaps to labyrinths to

spots (Figure 5.6c1). Similarly but less clearly, peaks in skewness after the Turing instability were related to transitions in the sequence of patterns (Figure 5.6c2). Autocorrelation (at-lag-1) after the Turing instability remained high and fluctuated slightly as more cells became bare before the transition (Figure 5.6c3). Interestingly, the onset of pattern formation at the Turing instability was preceded by increasing autocorrelation (at-lag-1) (Figure 5.6c3). Variance and skewness, however, showed no trend (Figure 5.6c1, c2).

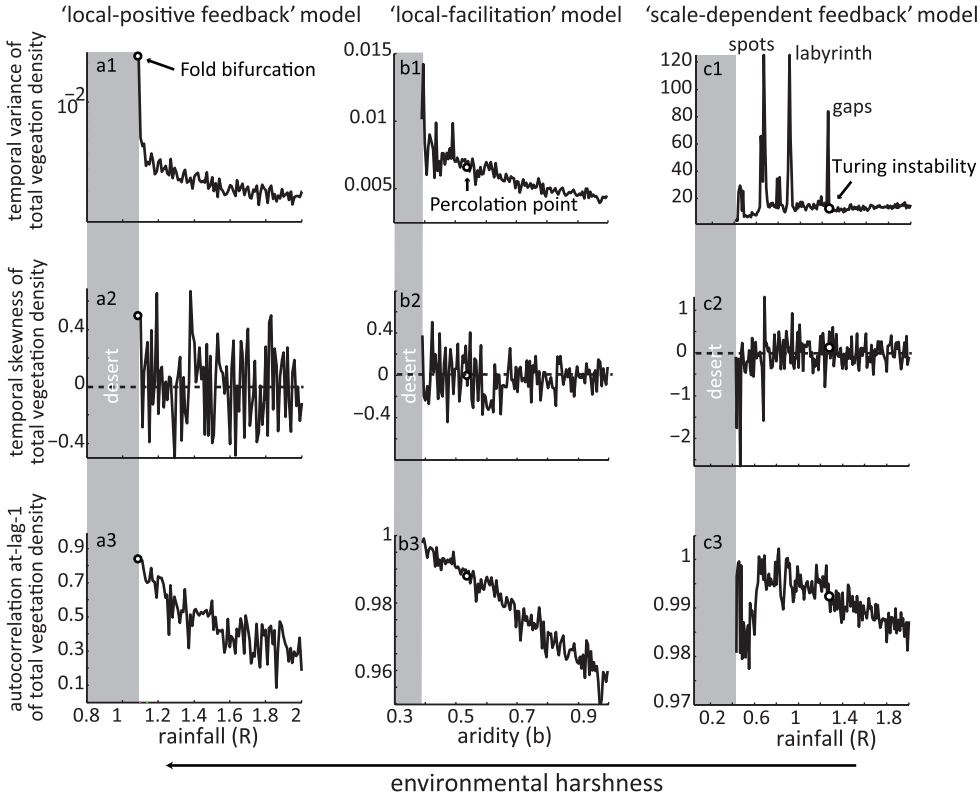

Figure 5.6 Temporal variance, temporal skewness, and temporal autocorrelation (at-lag-1) as a function of increasing harshness in the environment up to desertification (gray shaded area). Temporal indicators are estimated from the last 1,000 points of total vegetation biomass, cover or density for each level of control parameter (rainfall in *'local-positive feedback'* and *'scale-dependent feedback'* models; aridity in *'local-facilitation'* model). Open circles indicate: (**a1-3**) the point at which vegetation shifts to barren state in the *'local-positive feedback'* model (Fold bifurcation); (**b1-3**) the point at which patches of vegetation that span the lattice from one edge to the other disappear in the *'local-facilitation'* model (Percolation point); (**c1-3**) the onset of regular vegetation patterns in the *'scale-dependent feedback'* model (Turing instability).

Discussion

Critical transitions are large self-propelling changes in the state of a system induced by small changes in external conditions (Scheffer 2009). Given that critical transitions occur unexpectedly and may have drastic and irreversible consequences, the ability to estimate their risk is of utmost societal and economic importance. Early-warning signals for critical transitions offer such opportunity (Scheffer et al. 2009). If detected early in advance (Biggs et al. 2009b), they can help to navigate away from unpleasant surprises.

It has been suggested that the universal phenomenon of critical slowing down close to critical transitions will in practice translate into early-warning signals, i.e. a rise in correlation and variance (Scheffer et al. 2009). In this study, we show that this is not always true. We found that the shift of arid ecosystems to desert in a *'scale-dependent feedback'* model with self-organized regular patterns is not announced by a rise in correlation or variance despite the fact that critical slowing down does happen. This was the only exception. We found a rise in correlation and variance in space (and less clearly in time) to precede the collapse of vegetation in the two other arid ecosystem models we used. Moreover, we identified similar signatures before the onset of pattern formation that mark the transition of a complete vegetation cover to regular patches of vegetation in the *'scale-dependent feedback'* model (Table 5.2).

The failure of correlation and variance to announce the shift to desert in the *'scale-dependent feedback'* model suggests that there may be considerable deviations in the behavior of generic indicators in this or similar classes of spatially organized systems when compared to the other two model systems we studied. These deviations appear to be associated with the presence of self-organized regular patterns, which are a consequence of the way feedbacks operate in space for these classes of systems.

In the *'local-positive feedback'* model, spatial processes are governed by diffusion between neighboring sites (Figure 5.2a1). Close to transition, random losses of vegetation in each site take longer to be compensated; the vegetation dynamics slow down and diffusion starts to dominate the patterns. As a result, each site becomes more influenced by biomass dispersed from its neighbors (Dakos et al. 2010). Such strong neighbor effects lead to increasing spatial clustering of vegetation (Figure 5.2a2). This translates into elevated correlation and variance before a transition.

In the *'local-facilitation'* model, regeneration of a degraded site depends on the presence of vegetation next to it (Figure 5.2b1). When aridity increases, colonization of empty sites by vegetation becomes more difficult ("slows down") and just as in the '*local positive feedback'* model the regeneration of vegetation in the degraded sites will be influenced more strongly by the presence of vegetated neighbors. As a result, local facilitation becomes the dominant force that leads to clustering around existing irregular patches (Figure 5.5a), again translating into an increase in correlation and variance prior to transition to desertification.

Table 5.2 Summary of the performance of leading indicators in the three models used.

Indicator	Model				
	‘local-positive feedback’	'local-facilitation'		‘scale-dependent feedback’	
	up to transition point	up to percolation point	from percolation to transition point	up to Turing instability	from Turing instability to transition point
Critical Slowing Down	+	+	+	+	+
Generic					
Spatial correlation	+	+	+	+	fails
Spatial variance	+	+	+	fails	fails
Spatial skewness	+	+	+	fails	+
Temporal correlation	+	+	+	+	fails
Temporal variance	+	+	+	fails	fails
Temporal skewness	fails	fails	fails	fails	fails
System-specific					
Patch size distributions	not applicable (no patches)	+	+	not applicable (no patches)	not applicable (one size patches)
Pattern shapes	not applicable (no patches)	not applicable (irregular patterns)	not applicable (irregular patterns)	not applicable (no patterns)	+

Things work differently in the *'scale-dependent feedback'* model with its distinct regular vegetation patterns (Figure 5.2c). High regularity of the patterns simply translates into high correlation and variance. As rainfall decreases towards the shift, patterns change in shape, but their regularity remains high and so does correlation and variance. Only just before the transition when the regularity of the patterns starts breaking up, correlation and variance decrease.

Although regular pattern formation appears to mask the performance of variance and correlation as leading indicators in the *'scale-dependent feedback'* model, the shape of the patterns themselves reveals much information on the proximity to the upcoming transition (Rietkerk et al. 2004). This may be true for the entire class of ecosystems that exhibit self-organized pattern formation, ranging from bogs (Eppinga et al. 2009) to mussel beds (van de Koppel et al. 2005). Similar pattern-based indicators specific to certain classes of systems may be deviations in power laws in systems with scale-invariant patches (Pascual and Guichard 2005), such as the ones produced by the *'local-facilitation'* model (Figure 5.5a) (Kéfi et al. 2007a). Although such pattern-based indicators may sometimes be enough to announce specific types of transitions, combining them with correlation and variance may help to reduce the possibility of false alarms. For example, changes in the statistical properties of patch size distributions (such as a decrease in skewness of patch sizes, see Appendix Figure A5.1) together with an increase in skewness of vegetation cover (Figure 5.4b2) may yield a more robust indicator of an approaching transition than any of those indicators alone. More importantly, pattern-based and generic indicators complement each other. In systems with self-organized regular patterns, changes in the shape of the patterns can be used for announcing desertification (Figure 5.5c), whereas generic indicators (in particular spatial correlation) can signal the onset of pattern formation: the transition to the appearance of the first degraded sites in the ecosystem (Figure 5.4c3).

The failure of the correlation and variance to signal collapse in systems with self-organized regular patterns suggests that there may be more cases in which these indirect indicators of resilience can fail to signal the risk of upcoming transitions. Obviously, we cannot expect such leading indicators to signal the proximity of transitions that are not associated to critical slowing down (Scheffer et al. 2009). However, our results show that even if critical slowing down is present, it may not be reflected by rising correlation or variance. By contrast, the recovery time required for the system to return to equilibrium after a disturbance appears to be a robust indicator of critical slowing down (Figure 5.3). Indeed, recent work on a similar model system with pattern formation confirms that recovery time upon disturbance increases before desertification (Bailey 2011).

In conclusion, recovery time upon local perturbation experiments may be the most generic and robust indicator of critical slowing down before a transition (van Nes and Scheffer 2007). While elevated correlation and variance may often serve as indirect indicators of critical slowing down, the presence of self-organized regular patterns can suppress change in such indicators. In this particular situation, changes in the patterns themselves are the best indicator of an upcoming transition.

Appendix

Supplementary Statistics

Table A5.1 Kendall τ rank correlation statistics for spatial and temporal leading indicators estimated in the all models. Asterisks indicate significant trends (p<0.025).

	'local-positive feedback'	'local-facilitation'		'scale-dependent feedback'	
Kendall τ rank correlation	up to transition point	up to percolation point	from percolation to transition point	up to Turing instability	from Turing instability to transition point
Spatial Indicators					
correlation	0.768*	0.702*	0.940*	0.912*	-0.741*
variance	0.975*	0.973*	0.798*	-0.631*	-0.360*
skewness	-0.610*	0.880*	0.986*	-0.025	1.000*
Temporal Indicators					
correlation	0.654*	0.819*	0.654*	0.524*	-0.176*
variance	0.686*	0.755*	0.301*	-0.446*	-0.214*
skewness	0.041	0.108	0.147	-0.013	-0.167

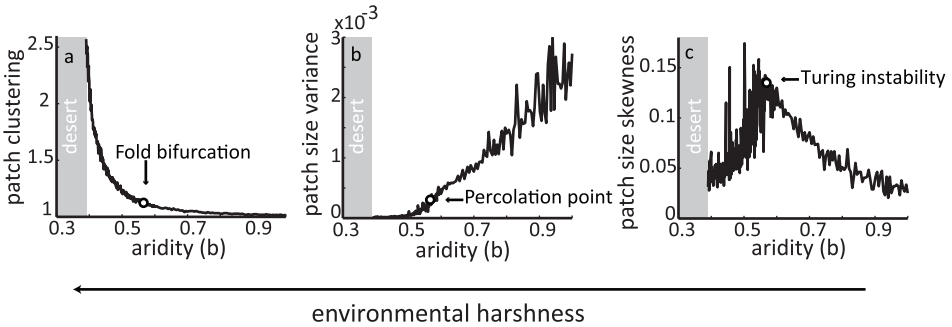

Figure A5.1 Statistical properties of patch size distributions in the *'local-facilitation'* model. (**a**) Spatial clustering increased (clustering was estimated as $\frac{q_{+|+}}{\rho_+}$ where $q_{+|+}$ is the conditional probability of finding a vegetated cell next to a vegetated cell and ρ_+ the fraction of vegetated cells in the total grid (van Baalen 2000)). (**b**) Patch size variance declined up to the transition point. (**c**) Patch size skewness exhibited a dual behavior: it rose till the percolation point as the number of large patches decreased and the number of small patches increased. After the percolation point, skewness dropped as the large patches broke down into small ones. The lack of vegetated patches in the *'local-positive feedback'* model and the regularity of the patches in the *'scale-dependent feedback'* model makes such estimation not feasible in these two models.

Chapter 6

Slowing down as an early-warning signal for abrupt climate change

In the Earth's history, periods of relatively stable climate have often been interrupted by sharp transitions to a contrasting state. One explanation for such events of abrupt change is that they happened when the earth system reached a critical tipping point. However, this remains hard to prove for events in the remote past, and it is even more difficult to predict if and when we might reach a tipping point for abrupt climate change in the future. Here we analyze eight ancient abrupt climate shifts and show that they were all preceded by a characteristic slowing down of the fluctuations starting well before the actual shift. Such slowing down, measured as increased autocorrelation, can be mathematically shown to be a hallmark of tipping points. Therefore, our results imply independent empirical evidence for the idea that past abrupt shifts were associated to the passing of critical thresholds. Since the mechanism causing slowing down is fundamentally inherent to tipping points, it follows that our way to detect slowing down might be used as a universal early-warning signal for upcoming catastrophic change. As tipping points in ecosystems and other complex systems are notoriously hard to predict in other ways, this is a promising perspective.

This chapter is based on the paper: V. Dakos, M. Scheffer, E. H. van Nes, V. Brovkin, V. Petoukhov and H. Held (2008). Slowing down as an early warning signal for abrupt climate change. *Proceedings of the National Academy of Sciences* (PNAS), 105(38): 14308-14312. We thank the IPL institute for providing opportunity for interdisciplinary cooperation, Steve Carpenter and William Brock for insightful discussions on early-warning signals in time-series, and Cajo ter Braak for statistical advice.

Introduction

The relative constancy of the climate over the past 10,000 years is exceptional in view of the large variability found in reconstructions of almost all periods before. Particularly noteworthy in the records of past climate dynamics are occasional sharp transitions from one state to another. Such transitions happened at various time-scales (Alley et al. 2003). For instance, about 34 million years ago the earth changed suddenly from the tropical state in which it had been for hundreds of millions of years to a state with ice-caps, a shift known as the greenhouse-icehouse transition (Kump 2005; Tripati et al. 2005) (Figure 6.1a). A prominent feature of the climate cycles that followed is the abrupt termination of most glacial periods (Petit et al. 1999) (Figure 6.1c, e, g, i). Zooming in on a finer time-scale shows that there are sharp shifts too. A well known example is the Younger Dryas period, when just after the recovery from the last glacial maximum the climate at Greenland relapsed to very cold conditions for many centuries and then suddenly jumped back to a more than ten degrees warmer state (Clark et al. 2002) (Figure 6.1m). An even more recent abrupt climate shift is the sudden shift of North Africa from a savanna-like state with scattered lakes to a desert state about 5,000 years ago (deMenocal et al. 2000) (Figure 6.1o).

Proposed explanations for these and other examples of abrupt climate change usually invoke the existence of thresholds in external conditions where the climate system is particularly sensitive, or even has a tipping point (Lenton et al. 2008), similar to that of a canoe where one leans over too much to one side. In models such tipping points correspond to bifurcations (Kuznetsov 1995) where at a critical value of a control parameter an attractor becomes unstable, leading to a shift to an alternative attractor. The underlying mechanism causing such extreme sensitivity at particular thresholds is typically a positive feedback. The earth system is notoriously riddled with such positive feedbacks (Lawton 2001; Rial et al. 2004; Woodwell 1998). Unfortunately, the explanations for abrupt climatic change in the past remain rather hypothetical as they are difficult to test. Even if the proposed mechanisms seem plausible, our capacity to model these systems accurately is too limited to conclude with reasonable certainty that tipping points are involved. This is particularly worrisome in view of the possibility of hitting upon a tipping point as current climate change proceeds. Although most climate scientists would acknowledge that possibility, we are simply unable to predict if and when future climate change might bring us to a critical threshold (Alley et al. 2003). Even though climate models are rapidly improving, the chances that we will soon be able to predict potential tipping points with sufficient accuracy seem negligible. A similar situation exists in ecology where the existence of thresholds for catastrophic shifts has been shown for a range of systems (Scheffer et al. 2001), but prediction of such shifts has remained elusive.

In the face of our limited mechanistic insight it would be invaluable to have another way to find out whether past abrupt climate change was related to the crossing of critical thresholds, and to know if parts of our current climate system may be approaching such a threshold. A possible clue that we explore here, is to use the theoretical finding that, as a rule, dynamical systems become ‘slow’ when a critical point is approached as conditions are gradually changing. In technical terms the mechanism is that the maximum real part of

the eigenvalues of the Jacobian matrix tends to zero as a bifurcation point is approached (Strogatz 1994). As a result the dynamical system becomes increasingly slow in recovering from small perturbations (Strogatz 1994; van Nes and Scheffer 2007; Wissel 1984).

Although an ideal way to test if a system is slowing down (van Nes and Scheffer 2007) would be to study its response to small experimental perturbations, this is obviously of little use for analyzing past climate change. An alternative is to interpret fluctuations in the state of a system as its response to natural perturbations. Slowing down should then simply be reflected as a decrease in the rates of change in the system, and therefore as an increase in the short-term autocorrelation in the time-series (Ives 1995). Various authors have elaborated methods to detect slowing down associated to a shift in model-generated time-series of the thermo-haline circulation (Held and Kleinen 2004; Kleinen et al. 2003; Livina and Lenton 2007). Kleinen et al. (2003) analyzed spectral properties, and Held and Kleinen (2004) focused on autocorrelation as a statistic to detect slowing down before the transition. Livina and Lenton (2007) suggested an approach inspired by a technique for detecting long-term memory in a time-series. Despite the interest in this field, so far no significant signs of slowing down before a shift have been shown on real data.

Here we analyze the change in autocorrelation in time-series of eight ancient events of abrupt climate change reconstructed from geological records (Figure 6.1, see Methods section) to examine if the climate system slows down when a critical threshold is approached. Since we are interested in the possibility of using such information as an early-warning signal we used only data from before the actual transition (shaded bands in Figure 6.1) to scan for slowing down. Details of the time-series and the identification of the period before the shift can be found in the Appendix (Table A6.1).

Methods

Data sources

We used examples of climatic transitions that have been widely interpreted as significant shifts in the climate record and for which underlying positive feedbacks have been suggested as mechanistic explanation. We have not pre-selected the examples on the basis of preliminary results from our own analyses. The time-series used represent climate data proxies derived from different sources. All were downloaded from the World Data Center for Paleoclimatology, National Geophysical Data Center, Boulder, Colorado, (http://www.ncdc.noaa.gov/paleo/data.html). The terrigenous dust record was accessed from (http://www.ldeo.columbia.edu/~peter/Resources/data.html) the personal webpage of P.B. deMenocal. Full details on the data records used are given in Table A6.1 of the Appendix.

Data selection

We used only points in the record that correspond to the period prior to the transition (Table A6.1). The exact transition points were determined by eye and all were roughly

equal to those cited in the original papers where the records appeared. We have chosen the transition points conservatively, in the sense that we avoided including points that were part of the transition itself. This is important, as due to increased serial correlation inclusion of such points would bias the estimate of our slowing down indicator. In a few cases, double values for the same date occurred in the original files. Those were averaged to provide a single value for each chronology.

Interpolation

We used linear interpolation to transform the climate records to time-series with equidistant data. This allows us to use the time-series analysis approaches suggested earlier for detecting slowing down (Held and Kleinen 2004; Ives et al. 2003; Kleinen et al. 2003) on real reconstructed climate records.

Detrending

To filter out long trends and to achieve stationarity we subtracted a Gaussian kernel smoothing function from the data and used the remaining residuals for the estimation of the autoregressive coefficient at lag 1. We chose a bandwidth in such a way that we do not over-fit while still removing the long-term trends visible in the records. The same treatment was applied also to the simulated time-series and the original records without interpolated points (see Table A6.2 and A6.3). Figure A6.2 in the supplement shows the interpolated, filtered time-series and the resulting residual time-series of Figure 6.1a, m, i of the main text for visual inspection.

Autocorrelation

The autocorrelation at lag 1 was computed by fitting an autoregressive model of order 1 (AR1 model of the form $x_{t+1}=\alpha_1 x_t+\varepsilon_t$, by an ordinary least squares (OLS) fitting method) applied on the data points within a sliding window of fixed size up to the transition point. In each case we took a sliding window of half the size of the interpolated time-series. We tested for evidence of slowing down by estimating the nonparametric Kendal rank-correlation τ statistic on the estimates of the autoregressive coefficients α_1 (details in Appendix).

Model generated time-series

We used a stochastic one dimensional energy balance climate model forced by relative incoming radiation to simulate data of ocean temperature that reflect a transition to an icehouse earth (Fraedrich 1978) (Figure 6.2a). The thermo-haline circulation dynamics are generated by the CLIMBER-2 climate model of intermediate complexity (Figure 6.2c). The data series on desertification in Western North Africa (Figure 6.2e) was produced using a stochastic version of the climate box model (Brovkin et al. 1998) forced by reconstructed solar irradiance and atmospheric CO_2 concentration. See Appendix for the model details.

Surrogate data

For each time-series we tested the likelihood of obtaining our computed trend statistics (Kendall's τ rank correlation) by chance, using 1,000 surrogate time-series of the same length as the filtered simulated and real data in three different ways. Firstly, we bootstrapped our data sets by shuffling the original residual time-series and picking data with replacement to generate surrogate records of similar distribution (mean and variance). Secondly, we produced a surrogate time-series that had the same Fourier spectrum and amplitudes as the original sets (Theiler et al. 1992). Lastly, we created surrogate data sets produced by an autoregressive model of order 1 with the same variance, mean and autocorrelation at lag 1 with the residuals time-series starting from the same initial value as in the original series (Theiler et al. 1992). For each surrogate set, we computed the trend detection statistic. We then calculated the probability that our estimates of the trend statistic would be observed by chance as the fraction of the 1,000 surrogate series scoring the same value or a higher one. The probability distributions for the model and data trend statistic as well as details on how we produced the surrogate sets are summarized in the Appendix (see Table A6.4, Figure A6.3).

Results and Discussion

Evidence for critical slowing down

In all examples of abrupt climate change we analyzed, autocorrelation showed an increase in the period before the shift (Figure 6.1 lower panels in each pair), suggesting that these climate systems did indeed slow down before the abrupt change, as expected theoretically for systems approaching a tipping point. All the trends were significant as measured by the Kendall rank correlation coefficient τ, but the strength of the correlation varied among cases. There was a marked increase in slowing down before the end of the greenhouse Earth (Figure 6.1b), the end of the Younger Dryas (Figure 6.1n) and the end of glaciation I (Figure 6.1j). Autocorrelation moderately increased before the end of glaciation IV, III and the desertification of North Africa (Figure 6.1d, f, p), whereas the end of the Bølling-Alleröd (Figure 6.1l) and the end of glaciation II (Figure 6.1h) showed weak signs of slowing down. We explored the likelihood that our method would find such results by chance, i.e. without an underlying critical slowing down causing the pattern, by studying the occurrence of trends in computer generated surrogate time-series (see Methods section). The approach was to generate large numbers of randomized time-series with characteristics similar to the analyzed stretches of climate series before episodes of abrupt change, and see in how many cases our analysis would find an increase in autocorrelation by chance. These analyses (see Appendix, Table A6.4 and Figure A6.3) indicated that the probability of finding the increase in autocorrelation detected in the data by chance is very low for the three transitions that showed the strongest slowing down (end of greenhouse Earth, end of Younger Dryas, and end of glaciation I).

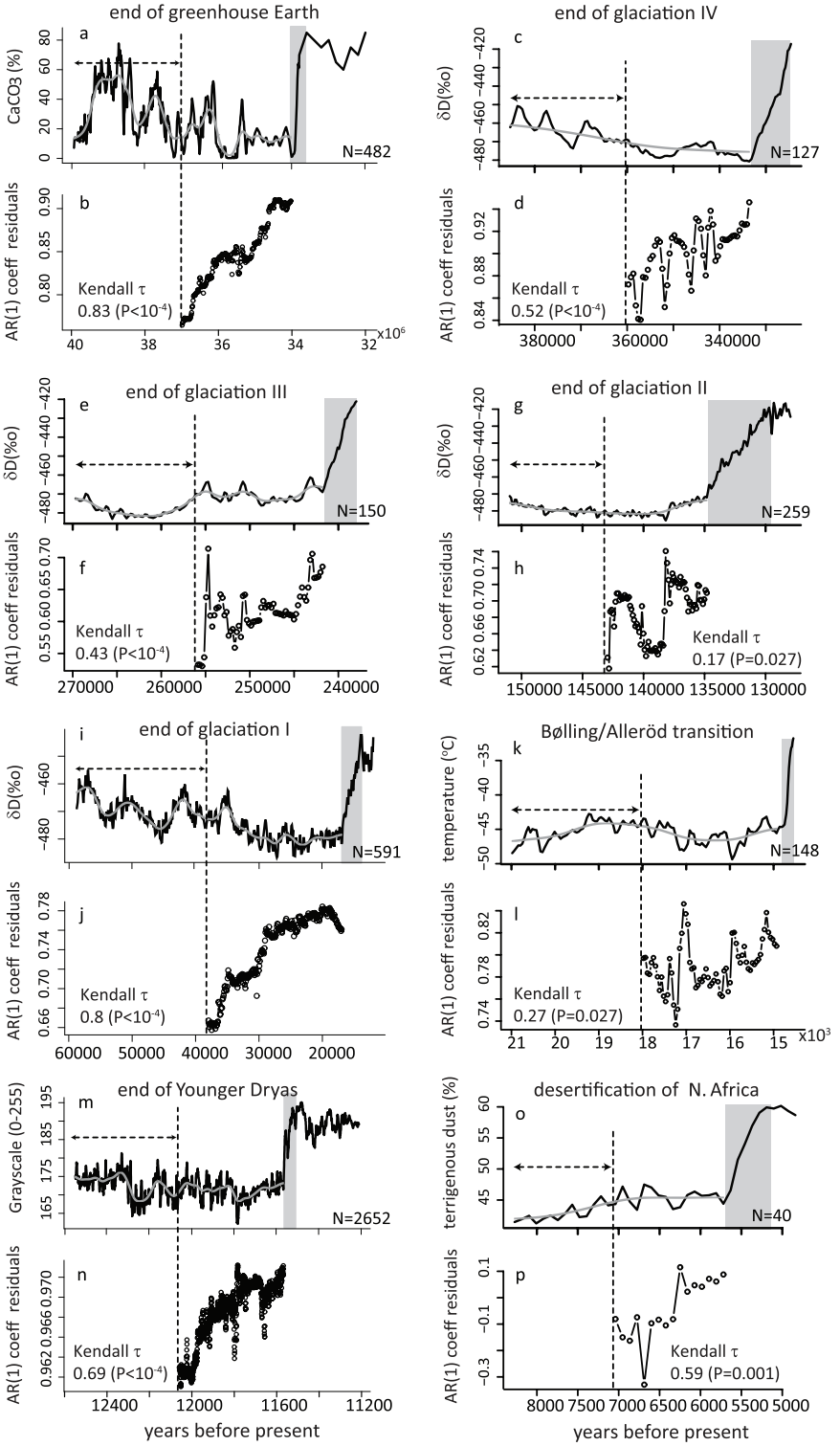
end of greenhouse Earth
a
CaCO3 (%)
N=482
b
AR(1) coeff residuals
Kendall τ
0.83 (P<10-4)
x10^6
end of glaciation IV
c
δD(‰)
N=127
d
AR(1) coeff residuals
Kendall τ
0.52 (P<10-4)
end of glaciation III
e
δD(‰)
N=150
f
AR(1) coeff residuals
Kendall τ
0.43 (P<10-4)
end of glaciation II
g
δD(‰)
N=259
h
AR(1) coeff residuals
Kendall τ
0.17 (P=0.027)
end of glaciation I
i
δD(‰)
N=591
j
AR(1) coeff residuals
Kendall τ
0.8 (P<10-4)
Bølling/Alleröd transition
k
temperature (°C)
N=148
l
AR(1) coeff residuals
Kendall τ
0.27 (P=0.027)
x10^3
end of Younger Dryas
m
Grayscale (0-255)
N=2652
n
AR(1) coeff residuals
Kendall τ
0.69 (P<10-4)
years before present
desertification of N. Africa
o
terrigenous dust (%)
N=40
p
AR(1) coeff residuals
Kendall τ
0.59 (P=0.001)
years before present

Figure 6.1 (previous page) Eight reconstructed time-series of abrupt climate shifts in the past: (**a**) the end of the greenhouse Earth, (**m**) the end of the Younger Dryas, (**k**) the Bølling-Alleröd transition, (**o**) the desertification of North Africa, (**i**) the end of the last glaciation and (**g**, **e**, **f**) the ends of earlier glaciations. In all cases the dynamics of the system slow down before the transition, as revealed by an increasing trend in autocorrelation (lower panels **b**, **d**, **f**, **h**, **j**, **l**, **n**, **p**). The gray bands identify transition phases. The arrows mark the width of the moving window used to compute slowness. The smooth gray line through the time-series is the Gaussian kernel function used to filter out slow trends. Data in (**a**) come from tropical Pacific sediment core records, data in (**m**) are from the Cariaco basin sediment, data in (**k**) come from the Greenland GISP2 ice core, data in (**o**) from the sediment core ODP Hole 658C off the West coast of Africa, and data presented in (**c**, **e**, **g**, **i**) are from the Antarctica Vostok ice core (full details in Appendix Table A6.1).

These records have the most detailed data (all > 450 data points). The other time-series are much less detailed (all < 150 data points), and our surrogate data analyses suggest higher probabilities of finding the observed trends by chance in those cases. The lower number of points in some of the series, obviously makes the results less reliable, not only because of the small number of points per se, but also because the resolution can be insufficient to capture the short-term autocorrelation. This is especially so in the case of the desertification of North Africa, where the points are spaced almost a century apart which may well be too short to capture the interactive dynamics of vegetation and monsoon supposed to drive the dynamics. The scarcity of points in the record (Np=30 prior to the transition) results in residuals of alternating positive and negative values and in estimates of the autoregressive coefficient α_1 that show a negative autocorrelation (Figure 6.1p).

To weigh the combined uncertainties, and look at the overall picture, we computed the probability of finding the complete set of P-values by chance, using Fisher's combined probability. This combined probability appears to be very small (P<0.003) irrespective of the approach taken to generate surrogate data (Table A6.4).

Robustness of results to the choice of methods

The results obviously depend upon choices made in the data processing (see Methods section). Two important parameters are the bandwidth used in the function for filtering and the size of the sliding window used to compute the autocorrelation. We performed an extensive analysis of the sensitivity of outcomes to the choice of these parameters for our three longest time-series. The results indicate that the observed increase in autocorrelation before the climate shifts is a rather robust outcome. Actually, this analysis shows that we could have obtained more significant trends by tailoring these parameters for the specific series (Figure A6.4). We also explored whether interpolation used to generate equidistant data for the time-series analyses might have caused spurious trends in autocorrelation. Estimates of autocorrelation on the non-interpolated data gave roughly similar results (Table A6.3) (see also Appendix).

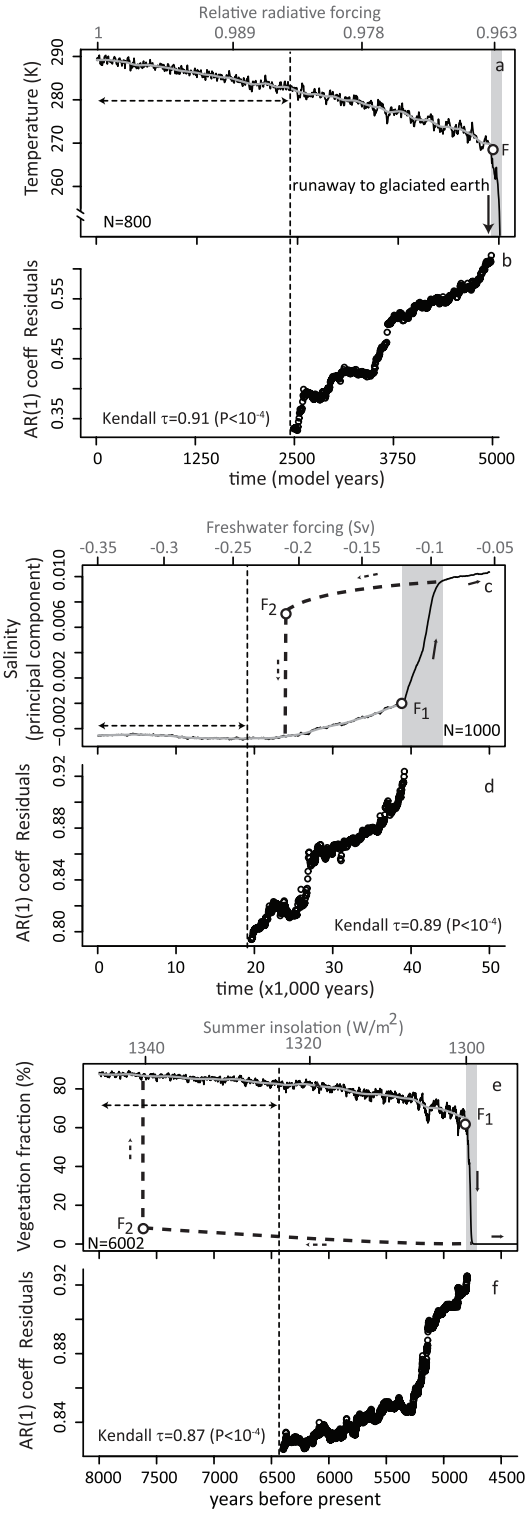
Relative radiative forcing
1
0.989
0.978
0.963
Temperature (K)
290
280
270
260
a
F
runaway to glaciated earth
N=800
b
AR(1) coeff Residuals
0.55
0.45
0.35
Kendall τ=0.91 (P<10-4)
0
1250
2500
3750
5000
time (model years)
Freshwater forcing (Sv)
-0.35
-0.3
-0.25
-0.2
-0.15
-0.1
-0.05
Salinity
(principal component)
0.010
0.006
0.002
−0.002
c
F2
F1
N=1000
d
AR(1) coeff Residuals
0.92
0.88
0.84
0.80
Kendall τ=0.89 (P<10-4)
0
10
20
30
40
50
time (x1,000 years)
Summer insolation (W/m2)
1340
1320
1300
Vegetation fraction (%)
80
60
40
20
0
e
F1
F2
N=6002
f
AR(1) coeff Residuals
0.92
0.88
0.84
Kendall τ=0.87 (P<10-4)
8000
7500
7000
6500
6000
5500
5000
4500
years before present

Figure 6.2 (previous page) Three simulated abrupt climate transitions. (**a**) transition to an icehouse Earth, (**c**) collapse of the thermo-haline circulation, (**e**) desertification of North Africa (see Appendix for details on simulations). As in the reconstructed real dynamics, the transition is preceded by slowing down as revealed by increased autocorrelation (panels **b**, **d** and **f**). The gray bands identify the transition phases. The arrows mark the width of the sliding window used to compute slowness. The smooth gray line through the time-series is the Gaussian kernel function used to filter out slow trends. All models pass a fold bifurcation *F* as a control parameter is slowly changing (relative radiation, freshwater forcing and insolation respectively). In the case of the ocean circulation and desertification model (panels **c** and **e**), there are also alternative attractors present implying hysteresis (dashed line), if the change in the control variable would be reversed upon the shift. Points F_1 and F_2 are saddle-node bifurcation points.

Comparison to model results

Approaching the problem from a different angle, to check whether the theoretically predicted critical slowing down may indeed be expected to be visible from autoregressive coefficients in climate data, we also used our methods to analyze simulation results from climate models that were slowly driven across a known threshold (Figure 6.2). The models deal with three quite different systems: the North-African paleo-monsoon system, the thermo-haline circulation, and the earth temperature as affected by the ice-albedo feedback. Model details and references are given in the Methods section and in the appendix. In all cases our indicator picked up an increase in slowness, comparable to that found in the geological records. Also, the results of bootstrap analyses and sensitivity analyses applied to model results are comparable to those from our climate data sets (Appendix, Figure A6.3 and A6.4 and Table A6.4). This lends further support to the idea that the patterns detected in the data do indeed correspond to critical slowing down as predicted by the theory.

Perspectives

It may seem rather surprising that all cases of sharp climate shifts we analyzed were announced well before they happened by changes in the pattern of fluctuations. Indeed, our bootstrap analysis shows that roughly half of the positive trends in autocorrelation may well have arisen by chance (the desertification of North Africa, the Bølling-Alleröd transition and the end of glaciations II and III). Nonetheless, our analyses also show that the combined probability of finding these trends is extremely low. Furthermore, the close similarity to what can be shown in climate models suggests that the patterns in the data may indeed represent the slowing down of a system approaching a tipping point.

Our results have profound implications for climate science. So far, support for the idea that tipping points can be the explanation for dramatic climatic shifts in the past has been based on models of specific mechanisms. Although compelling cases have been built, there is always considerable uncertainty as it is simply very difficult to prove what has been the mechanism behind such events in the far past. The slowing down that our analysis suggests does not point to any specific mechanism. Rather, it is a universal

property of systems approaching a tipping point. Therefore it represents an independent line of evidence, complementing model-based approaches suggesting that tipping points exist in the climate system. Clearly, this is an important insight as it implies that in principle internal feedbacks can propel the climate system through an episode of rapid change once a critical threshold is reached.

Obviously, detection of critical slowing down has two faces. In the hindsight it may help to tease out whether past dynamics may be explained by the existence of critical thresholds. With respect to predicting future climate change it may give us an indication of whether we are entering a situation in which the parts of the earth system may amplify rather than buffer human induced climate change. Clearly, there are challenges and limitations. Long time-series of sufficient quality are needed, and resolution needs to be sufficient to capture the characteristic timescale of the internal dynamics of the system. Similarly, good detrending is challenging but critically important, as unfiltered trends may lead to patterns in autocorrelation that are not related to the systems dynamical response to perturbations we wish to probe. An important fundamental limitation we should keep in mind, is that slowing down will only occur if the system is moving gradually towards a threshold. Therefore, transitions caused by a sudden large disturbance without a preceding gradual loss of resilience will not be announced by slowing down. Certainly, current trends in atmospheric carbon are rather fast compared to the dynamics of ice-caps and ocean heat contents, and fluctuations of such variables may therefore not show detectable slowing down on century scales. By contrast, slowing down could possibly be detected in faster subsystems that might have tipping points such as regional atmospheric circulation patterns.

In view of our current inability to predict potential abrupt climate shifts (Alley et al. 2003), having slowing-down as a clue for detecting whether such parts of the climate system may be approaching a threshold is a marked step forward in projecting future climatic changes.

Putting our results in an even wider perspective, it is important that slowing down is a universal property of systems approaching a tipping point. This implies that our techniques might in principle be used to construct operational early-warning systems for critical transitions in a wider range of complex systems where tipping points are suspected to exist, ranging from disease dynamics and physiology to social and ecological systems.

Appendix

Derivation of model simulated data

Our simulated data presented in Figure 6.2 of the main text, come from 3 climate models of different complexity.

a) We used a simple 1 dimensional climate model (Fraedrich 1978; Fraedrich 1979) to simulate a transition from a greenhouse to an icehouse earth (Figure 6.2a). The model has temperature, *T*, as the only state variable which represents the average temperature of an ocean on a spherical planet subjected to radiative heating (Fraedrich 1978) according to the equation:

$$\frac{dT}{dt} = \frac{1}{c}\{-\varepsilon\sigma T^4 + \frac{1}{4}\mu I_0 bT + \frac{1}{4}\mu I_0(1-a)\} \qquad \text{with } a_p = a - bT \qquad \text{(eqA6.1)}$$

where ε is effective emissivity, μ is relative intensity of solar radiation, I_o is solar irrandiance, c is a constant thermal inertia and a_p is the planetary albedo. Parameters a and b define a linear feedback between ice and albedo variability and temperature. In this simple climate system, there is one internal equilibrium of nonglacial conditions, which, when I_o drops below a certain threshold, there is a runaway effect to ice climate through a fold bifurcation.

We extended the deterministic skeleton of the model by including a stochastic term following the general form of a stochastic differential equation:

$$dx = f(x,\theta)dt + \sigma(x)dW\ , \qquad \text{(eqA6.2)}$$

where x is the state variable, f is the deterministic part of the model which depends on the control parameter ϑ, and σ scales the amount of noise that is introduced in the model with dW a Wiener process. In this climate model, we used as control parameter the relative radiation μ. We produced time-series by decreasing the control parameter μ linearly with time from 1 to 0.9524, allowing a transition from a warm to a cold climate. We used σ equal to 0.003 (applied multiplicatively on the state variable) and all the rest of the parameter values as they appear in Fraedrich (1978). We changed the original timescale of the model (=1 sec) by rescaling time with a factor of δ=20x10^6 (new timescale=0.6342 years). Simulations were performed in MATLAB v.7.1.0246 using an Euler-Murayama method to solve the stochastic equation with Ito calculus.

b) The thermo-haline circulation model simulation presented here is produced from the CLIMBER-2 model (Ganopolski et al. 2001; Petoukhov et al. 2000) which is a coupled climate model of intermediate complexity. The ocean component originates from the module by Stocker et al. (1992). A freshwater forcing at 44° northern latitude is applied; the average forcing is superimposed with a Gaussian white noise time-series. The 50,000 yrs transient run sees a linear increase in atmospheric CO_2 from 280 ppm to 800 ppm, implying an increased average freshwater forcing.

c) The deterministic climate model of the desertification of North Africa (Figure 6.2c) (Brovkin et al. 2003) was extended by accounting for the synoptic component w_{syn} of vertical velocity w at the top of the planetary boundary layer (see eq. A6.4 (Brovkin et al. 2003)):

$$w = w_m + w_h + w_{syn}$$
$$w_{syn} = \frac{K_T}{H_0}\left(k_{ts}^w \frac{\max(0, T_L - T_{cr})}{T_L^0 - T_{cr}} + k_{sl}^w \frac{T_L - T_B}{T_L^0 - T_B^0}\right)(1 + \xi(0, \sigma_w)) \qquad \text{(eqA6.3)}$$

and the synoptic component U_{syn} of the Hadley circulation potential U:

$$U = U_0 + U_{syn}$$
$$U_{syn} = k_{syn}^U U_0 \left(1 + \frac{T_L - T_B}{T_L^0 - T_B^0}\xi(0, \sigma_U)\right) \qquad \text{(eqA6.4)}$$

which allows for the contribution from the synoptic-scale baroclinic and barotropic atmospheric eddies with characteristic timescales from 2 to 10 days. W_m is the vertical velocity in the mean monsoon circulation and w_h is the vertical velocity associated with the mean Hadley circulation, U_0 is the mean Hadley circulation potential, T_B and T_L are surface air temperature at the southern box boundary and over land, respectively, T_B^0 and T_L^0 are their reference values, K_T is a vertical macro-eddy diffusion coefficient in the free troposphere, H_0 is a scale height for the atmospheric density, $\xi(0,\sigma_w)$ and $\xi(0,\sigma_U)$ are normally-distributed stochastic variables with a zero mean and variances σ_w and σ_U, respectively, and k_{ts}^w, k_{sl}^w and k_{syn}^U are model parameters which reflect partial contributions from the corresponding physical processes.

The terms $\frac{K_T}{H_0} k_{ts}^w \frac{\max(0, T_L - T_{cr})}{T_L^0 - T_{cr}}(1 + \xi(0, \sigma_w))$ and $\frac{K_T}{H_0} k_{sl}^w \frac{T_L - T_B}{T_L^0 - T_B^0}(1 + \xi(0, \sigma_w))$ in equation A6.3 describe the components of the synoptic-scale vertical velocity perturbation attributed to tropical storms and squall lines, respectively. These parameterizations assume that tropical storms form, when the temperature exceeds a critical threshold T_{cr} (assumed to be 26°C (Gray 1968)), while the squall lines are mainly generated due to the lower troposphere wind shear in the African Easterly Jet associated with a temperature gradient $T_L - T_B$ between Sahara and the Gulf of Guinea (Cook 1999). Parameters k_{ts}^w and k_{sl}^w were assigned 0.2 and 0.8 respectively, which reflects partial contributions to the synoptic-scale variability from the tropical storms and squall lines based on the empirical data (Grist and Nicholson 2001; Joseph 2003). The value of the variance σ_w was assigned 0.1 (Petoukhov et al. 2008).

The synoptic term of the Hadley circulation potential (eq A6.4) includes a contribution from the synoptic variability, $k_{syn}^{U} U_0$, due to the synoptic-scale perturbations of the zonally averaged wind, and from the term associated with the local fluctuations of the Hadley circulation, which is assumed to be proportional to the local horizontal temperature gradient, $k_{syn}^{U} U_0 \frac{T_L - T_B}{T_L^0 - T_B^0} \xi(0, \sigma_U)$. Parameters k_{syn}^{U} and σ_U were set equal to 0.05 and 0.1, respectively, based on empirical data (Petoukhov et al. 2008).

Derivation of paleoclimate proxy data

As we were interested in measuring slowing down before the transition, we restricted our analysis to the period just prior to the transition in both simulated and proxy records. The exact parts of the original time-series that we selected for our analysis, together with the size of the original record and data sources are presented in Table A6.1. Since the exact selection of the part of the record is critical for the outcome of our analysis, we were careful to avoid points that were part of the transition. Due to increased serial correlation as the transition trend begins, including such points would bias the estimate of the AR(1) coefficient.

Data analyses: interpolation, detrending and estimation of autocorrelation at lag 1

We applied the same analyses both to the simulated data and the real paleoclimate proxy records. Since the available paleoclimate data were of unequal density, we used linear interpolation to make our records equidistant (Table A6.2). However, as indicated in the main text, interpolation can create spurious trends in autocorrelation. A positive trend in autocorrelation could occur as an artefact of interpolation, if the density of points would decrease towards the shift (and hence the role of interpolation would increase). Therefore, we checked the evolution of the time intervals in the original records and compared them to the equidistant time intervals of the interpolated records (Figure 6.1). In general, the time intervals of the interpolated data sets was of similar magnitude as the time intervals in the original time-series close to the transition. Only in Figure A6.1a (the end of the greenhouse Earth), did the time between subsequent data points decrease towards the shift. However this happened at the very end, and can therefore not be responsible for the long term increasing autocorrelation trend detected. In any case, as shown in the next section, we analyzed the sensitivity of our results to interpolation systematically for all time-series.

We removed slow trends in the original records by applying a Gaussian kernel smoothing function (based on the Nadaraya-Watson kernel regression estimate (Hastie and Tibshirani 1990)) over the interpolated record prior to the transition and subtracted it from the interpolated record to obtain the residual time-series (Figure A6.2). The choice of the size of the bandwidth is important in this process. We picked bandwidths such that we do not overfit our data but yet filter out the slower trends in the records.

Table A6.1 Paleoclimate proxy data with details over the interpolation applied, the number of interpolated points before the transition used in the analyses and the respective approximate timescale after interpolation.

paleo record	Origin	climate proxy (units)	time range (kyrs BP)	time of transition	N	dataset
end of greenhouse Earth	ODP tropical Pacific core 1218	$CaCO_3$ (%)	(39-32) $x10^3$	34 $x10^6$	482	a
Bølling-Alleröd transition	GISP2 ice core	Temperature (^oC)	21-14.6	15000	147	b
end of Younger Dryas	Cariaco basin core PL07-58PC	Grayscale (0-255)	12.5-11.2	11600	2652	c
desertification of N. Africa	ODP Hole 658C	Terrigenous dust (%)	8.3-4.8	7500	40	d
end of glaciation I	Vostok ice core	d2H (%)	58.8-12	17000	591	e
end of glaciation II	Vostok ice core	d2H (%)	151-128	135000	258	e
end of glaciation III	Vostok ice core	d2H (%)	270-238	242000	149	e
end of glaciation IV	Vostok ice core	d2H (%)	385.3-324.6	334100	126	e

[a]Tripati, A., et al. 2005. Eocene Greenhouse-Icehouse Transition Carbon Cycle Data. IGBP PAGES/World Data Center for Paleoclimatology Data Contribution Series # 2005-056. NOAA/NGDC Paleoclimatology Program, Boulder CO, USA.

[b]Alley, R.B.. 2004. GISP2 Ice Core Temperature and Accumulation Data. IGBP PAGES/World Data Center for Paleoclimatology Data Contribution Series #2004-013. NOAA/NGDC Paleoclimatology Program, Boulder CO, USA.

[c]Hughen, K., et al. 2000. Cariaco Basin 2000 Deglacial 14C and Gray Scale Data, IGBP PAGES/World Data Center A for Paleoclimatology Data Contribution Series #2000-069.NOAA/NGDC Paleoclimatology Program, Boulder CO, USA.

[d]deMenocal, P.B., et al. 2001. Holocene Variations in Subtropical Atlantic SST. IGBP PAGES/World Data Center A for Paleoclimatology Data Contribution Series #2001-054. NOAA/NGDC Paleoclimatology Program, Boulder CO, USA.

ODP Site 658 terrigenous (%) is found at the personal webpage of deMenocal http://www.ldeo.columbia.edu/~peter/Resources/data.html

[e]Petit, J.R., et al. 2001. Vostok Ice Core Data for 420,000 Years, IGBP PAGES/World Data Center for Paleoclimatology Data Contribution Series #2001-076. NOAA/NGDC Paleoclimatology Program, Boulder CO, USA.

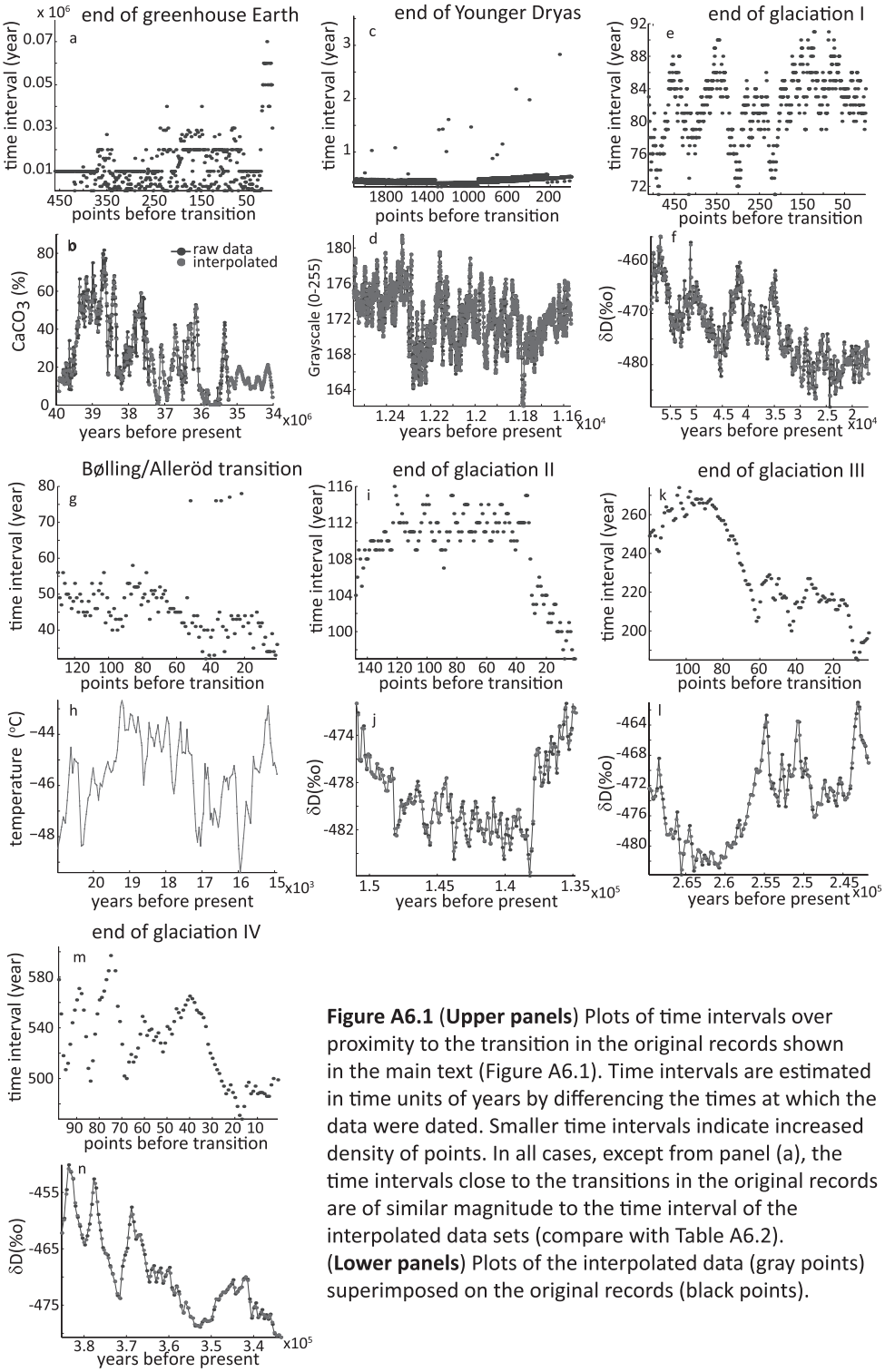

Figure A6.1 (**Upper panels**) Plots of time intervals over proximity to the transition in the original records shown in the main text (Figure A6.1). Time intervals are estimated in time units of years by differencing the times at which the data were dated. Smaller time intervals indicate increased density of points. In all cases, except from panel (a), the time intervals close to the transitions in the original records are of similar magnitude to the time interval of the interpolated data sets (compare with Table A6.2). (**Lower panels**) Plots of the interpolated data (gray points) superimposed on the original records (black points).

Table A6.2 Paleoclimate proxy data with details over the interpolation applied, the number of interpolated points before the transition used in the analyses and the respective approximate timescale after interpolation.

paleo record	interpolation	N points after interpolation	time interval after interpolation (years)
end of greenhouse Earth	Linear	462	0.01×10^6
Bølling-Alleröd transition	Linear	132	46
end of Younger Dryas	Linear	2111	0.5
desertification of North Africa*	None	30	88
end of glaciation I	Linear	513	82
end of glaciation II	Linear	150	108
end of glaciation III	Linear	122	230
end of glaciation IV	Linear	100	522

*original record is already interpolated

In Kleinen et al. (2003) the changes in power spectra were used as an indicator for the proximity to thresholds, tested in a 1D model of the thermohaline circulation of the north Atlantic. The spectrum is equivalent to the full autocorrelation function. Here, according to Held and Kleinen (2004), the spatial dynamics become degenerate at the transition, leading to the observation of the critical mode in arbitrary generic 1D time-series. By assuming time-scale separation at the bifurcation, we can use only the first entry of the autocorrelation function, i.e. the lag-1 information; in that sense the current method is more parsimonious. To calculate the autocorrelation at lag 1, which is an estimator of the slowing down of the system (van Nes and Scheffer 2007), we fitted an autoregressive model of order 1 (AR1) on data that are included within a sliding window of half the size of the record prior to the transition. The AR1 *ansatz* (Held and Kleinen 2004) is of the form $x_{t+1}=\alpha_1 x_t+\varepsilon_t$, fitted by an ordinary least squares method (OLS) with Gaussian random error ε_t. Note that we calculated no intercept, because we are fitting the AR1 model on the detrended residuals with mean zero. Although there have been modifications to the AR1 *ansatz* (Livina and Lenton 2007), where the authors utilized detrended fluctuation analysis (DFA), we used the degenerate fingerprinting approach (Held and Kleinen 2004), because of its most direct relation to generic bifurcations and straightforward applicability.

Finally, to determine the evolution of the AR1 estimates before the transition we used the nonparametric Kendall τ rank correlation coefficient to check against the null hypothesis of randomness for a sequence of measurements against time (Mann 1945).

All analyses were implemented in MATLAB v7.1.0246 (Mathworks Inc) and in R v2.4.1 (R project for Statistical Computing). Specifically, we used for a) the linear interpolation, the function *interp1* (MATLAB), b) the detrending of the records, the function *ksmooth* (R), c) the estimates of the autoregressive coefficients, the function *ar.ols* (R), d) the calculation of the trend statistic, the function *cor.test* (R) for the Kendall τ correlation statistics together with the *P* values (two-tailed with α=0.05).

The effect of interpolating on the results

We also explored the estimates of our trend statistic on the original records without interpolating missing values. Obviously, working with non equidistant data violates the basic assumptions behind time-series analysis. However, we pursue it only as an extra check on the robustness of our results. Thus, we treated the original time-series as equidistant, we removed the slow trends (using the same bandwidth for the Gaussian filter as we did in their interpolated counterparts) and estimated the autoregressive coefficients at lag 1 within a sliding window of half the size of the time-series. In all eight cases, our positive trend from the interpolated records are similar to those from the original time-series (Table A6.3). In all cases the trend statistic was of the same order of magnitude, and while there were 3 cases where interpolated records yielded a stronger increase in the AR(1) coefficient than the non-interpolated ones (end of greenhouse Earth, end of Younger Dryas, end of glaciation II), there were 3 other cases where the opposite was observed (end of glaciation I, III, end of Bølling-Alleröd) and one in which there was no real difference (glaciation IV).

Table A6.3 Summary of trend statistic for the original (non interpolated) and interpolated paleo records, and their probabilities (*P*). In the case of the desertification of North Africa the original data were already interpolated.

record	N points original/ interpolated	bandwidth size	original K τ (*P*)	interpolated K τ (*P*)
end of greenhouse Earth	461/ 462	25	0.5 ($<10^{-4}$)	0.83 ($<10^{-4}$)
end of Younger Dryas	2110/ 2111	100	0.34 ($<10^{-4}$)	0.69 ($<10^{-4}$)
end of glaciation I	512/ 513	25	0.85 ($<10^{-4}$)	0.8 ($<10^{-4}$)
Bølling-Alleröd transition	131/ 132	25	0.37 ($<10^{-4}$)	0.27 (0.001)
end of glaciation II	149/ 150	25	0.08 (0.31)	0.17 (0.27)
end of glaciation III	121/ 122	10	0.67 ($<10^{-4}$)	0.43 ($<10^{-4}$)
end of glaciation IV	99/ 100	50	0.51 ($<10^{-4}$)	0.52 ($<10^{-4}$)
desertification of North Africa	88/ 88	10	0.58 (0.001)	0.58 (0.001)

Analysis of surrogate time-series

To test for the likelihood of obtaining estimates of trend statistics by randomness, we created surrogate time-series by 3 different ways.

a) We bootstrapped our data sets by reshuffling the order of the detrended original time-series and by picking data with replacement to generate surrogate records of similar probability distribution (mean and variance) (Efron and Tibshirani 1986) (H_0 *1*).

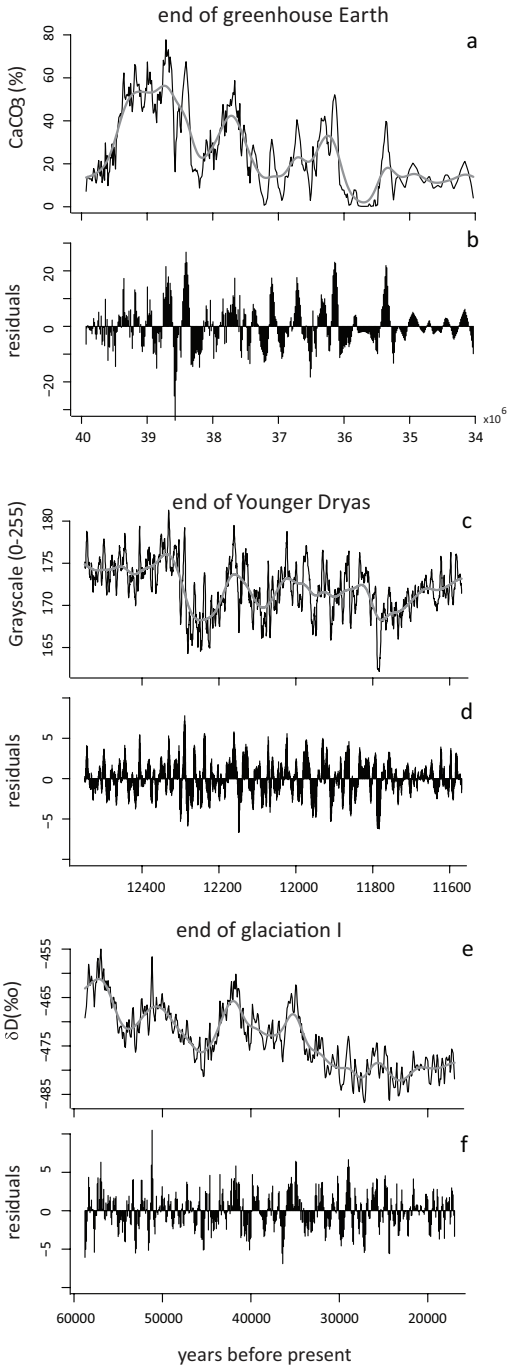

Figure A6.2 Effects of filtering on the records shown in Figure A6.1 in the main text. (**Upper panels)** Data points prior to the transition and the Gaussian kernel filter used for detrending. (**Lower panels)** The residual time-series after subtracting the trend (gray line). Records shown correspond to the panels of Figure A6.1 in the main text.

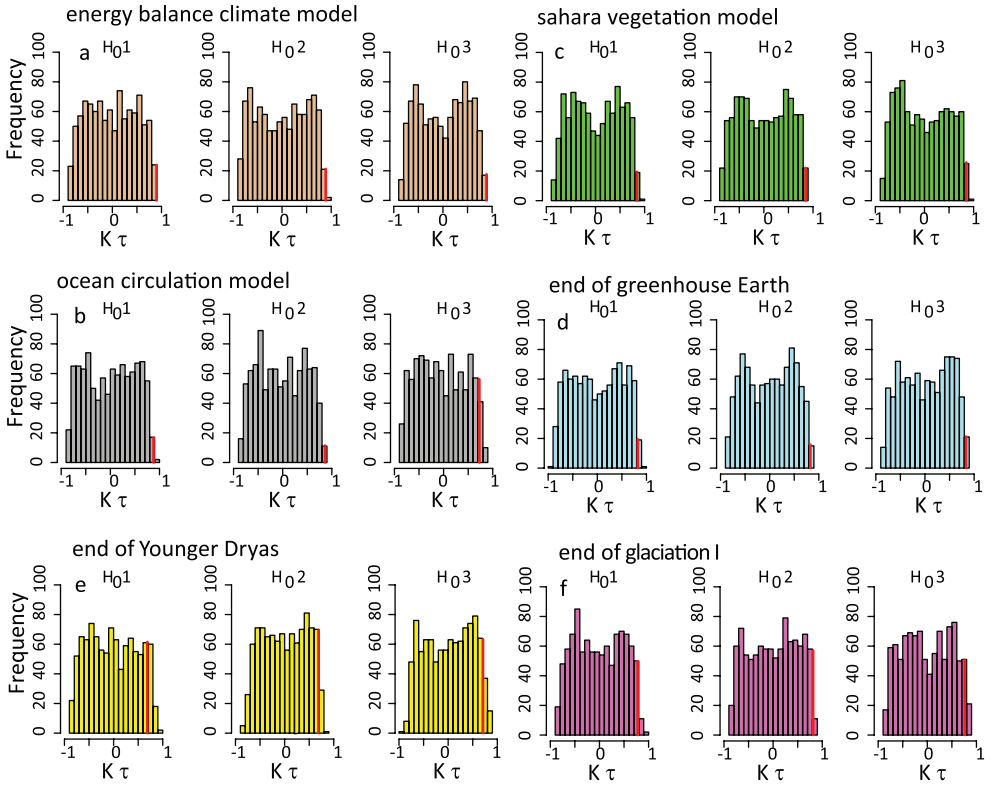

Figure A6.3 Probability distributions of the estimated trend statistic (Kendall's τ) of the ranked order test, under three alternative H_0 hypotheses for a set of 1,000 surrogate time-series. Under $H_0 1$, data sets are generated after bootstrapping the residual time-series records, under $H_0 2$ new data sets are produced with similar distribution and Fourier spectra as the residual time-series and under $H_0 3$ the surrogate time-series have been produced from a autoregressive model with similar autocorrelation at lag 1, mean and variance as in the residual records. Red lines indicate the limit over which the surrogate trend statistics are higher than the trend statistics of the original residual records. From this subset, only values of significance *P* equal or higher to the original record are used to estimate the likelihood of acquiring trend statistic estimates of similar magnitude.

b) We produced surrogate time-series with same autocorrelations and same probability distribution as the data, to test against the H_0 hypothesis that our data sets are a realisation of a Gaussian linear stochastic process (Schreiber and Schmitz 1996; Schreiber and Schmitz 2000) (H_0 *2*). We did this by replicating data of the same Fourier spectrum and amplitudes as of the original set using the MATLAB function *generate_iAAFT* (Gautama et al. 2004).

c) To test against the H_0 hypothesis that the data are produced by a colored noise process with similar variance, mean and autocorrelation at lag 1 with the original detrended time-

series (Theiler et al. 1992) (H_0 *3*), we generated surrogate sets by an AR1 model $x_{t+1}=\alpha_1 x_t+\alpha_0+\sigma\varepsilon_t$, where $\alpha_1=A(1)$, $\sigma^2=v(1-\alpha_1^2)$, $\alpha_0=\mu(1-\alpha_1)$, with v the variance, μ the mean, *A(1)* the autocorrelation at lag 1 from the original residual time-series (estimated by using function *acf* as implemented in R), and σ a scaling factor for the Gaussian random error ε_t. We estimated the probability that our estimates of the trend statistic would be observed by chance as the fraction of the 1,000 surrogate series scoring the same value or a higher one. Specifically for the Kendall τ, we estimated this probability as the number of cases in which the statistic was equal or higher than the estimate of the original record, $P(\tau \geq \tau^*)$. We also estimated the combined probability for observing the trend statistic estimate in each the H_0 hypotheses test by chance. For this, we used the Fisher's combined probability test (Sokal and Rohlf 1995) to estimate the X^2 statistic, given by:

$$X_{2k}^2 = -2\sum_{i=1}^{k}\ln(P_i) \qquad \text{(eqA6.5)}$$

where k is the amount of tests (here k=8) and P the probabilities estimated for each H_0 hypotheses test (Table A6.4). The combined probability for the X^2 statistic was given by a chi-square distribution with 2k degrees of freedom.

The probability estimates for the model and data trend statistic under the three different H_0 hypotheses are shown in Table A6.4. The probability of by chance acquiring a similar trend estimate as in the original record differs from case to case. In the case of the models, the probabilities were consistently very low (P<0.05). Similarly low probabilities were estimated in the records of the transitions of the greenhouse Earth, the Younger Dryas and the glaciation I (Figure A6.3). In the shorter time-series the probabilities of finding the observed trends by chance is much higher. Nonetheless the combined probability of finding positive trends in all eight data-series is obviously very low (Table A6.4).

Robustness against choice of window size and filtering resolution

The results of our analyses are obviously influenced by the standard deviation (defined by bandwidth size) used in the kernel function for filtering and the size of the sliding window used to compute autocorrelation. In the latter there is a trade-off between time-resolution and reliability of the estimate. Smaller windows allow one to track short-term changes in autocorrelation. However, the small number of data points in the window makes the estimate of autocorrelation less reliable. The filtering poses another trade-off. A too wide filter does not remove slow trends that may lead to spurious autocorrelation.

Especially, at the ends of the time-series the deviation becomes obvious if a too wide kernel size is used. A too narrow filter removes the short-term fluctuations that we intend to study for signs of slowing down. A systematic sensitivity analysis for our three longest time-series and the model results indicates that the results are quite robust, and that

actually we could have obtained more significant trends by tuning the parameters for the specific series (Figure A6.4).

Table A6.4 Probability of acquiring the estimated values for the trend statistic (Kendall's τ) of the original and simulated residual time-series under three alternative H_0 hypotheses for a set of 1,000 surrogate time-series. Under H_0 1, data sets are generated after bootstrapping, under H_0 2 new data sets are produced with similar distribution and Fourier spectra as the residual time-series and under H_0 3 the surrogate time-series have been produced from a autoregressive model with similar autocorrelation at lag 1, mean and variance as in the residual records. Values marked with one asterisk refer to a probability less or equal to 0.1, values with two asterisks refer to a probability of less or equal to 0.05. In italics, the combined probability for obtaining the estimated probabilities for each hypothesis is provided.

(N=1000 surrogate sets)	**H_0 1**	**H_0 2**	**H_0 3**
original record (residuals)	**Kendall τ**	**Kendall τ**	**Kendall τ**
end of greenhouse Earth	0.014**	0.004**	0.011**
end of Younger Dryas	0.086*	0.03**	0.055*
end of glaciation I	0.013**	0.011**	0.021**
Bølling-Alleröd transition	0.367	0.340	0.332
end of glaciation II	0.402	0.397	0.386
end of glaciation III	0.247	0.235	0.234
end of glaciation IV	0.186	0.043**	0.125
desertification of North Africa	0.140	0.165	0.091*
Fisher's combined probability	*0.002847*	*0.000206*	*0.001278*
simulated record (residuals)			
energy balance climate model	$<10^{-4}$**	0.002**	$<10^{-4}$**
Saharan vegetation model	0.002**	0.001**	0.006**
ocean circulation model	0.003**	$<10^{-4}$**	$<10^{-4}$**

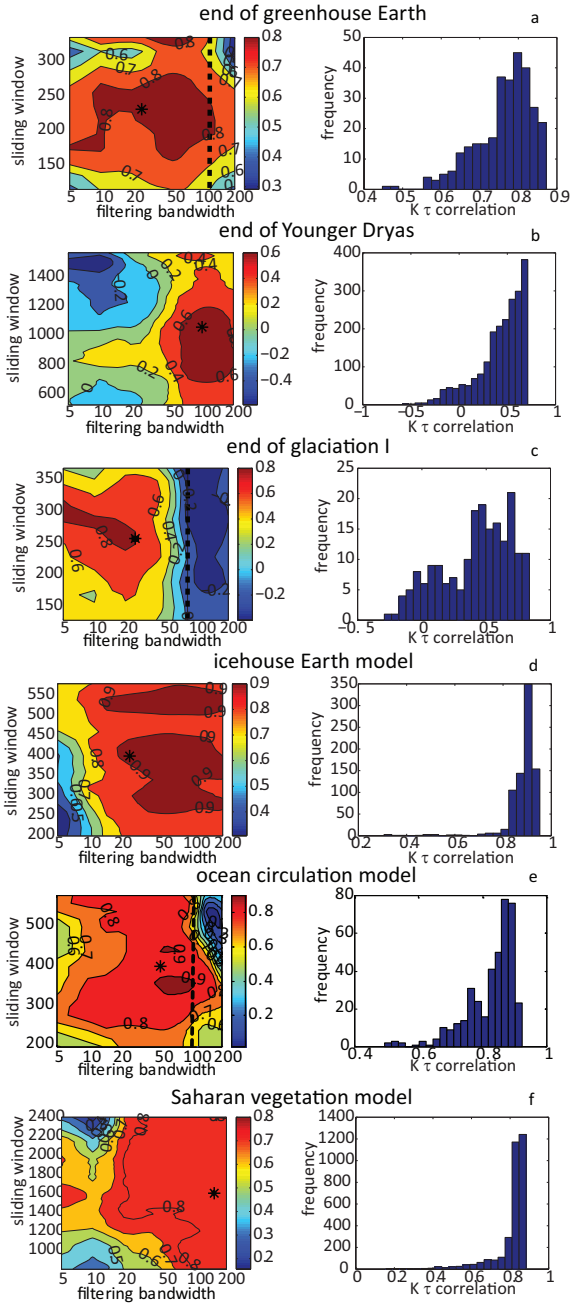

Figure A6.4 Contour plots of the effect of sliding window size and kernel filter size on observed trends in autocorrelation for the original and simulated data measured by Kendall's τ. Stars indicate the parameter choice used in the analyses. We visually inspected the fit of the kernel filter line, and demarcated where the kernel width becomes too large to follow the trend in the data (dashed vertical lines in contour plots). Histograms give the frequency distribution of the trend statistic for the scanned parameter area to the left hand side of the dashed line.

Chapter 7

Afterthoughts

The history of ecology is marked by a constant effort to find general rules that can explain patterns in nature (May 2004; Solé and Bascompte 2006). While the high complexity of ecological systems makes this search difficult, the "mirror world of math" (May 2001; Scheffer 1999) sometimes enables us to gain insight in mechanisms that would have otherwise remained elusive. In this thesis, I translate reflections from this mirror world of math into features that may serve as early-warnings for critical transitions in ecological systems. In these afterthoughts, I ponder the limitations of this approach but also its potential extensions.

Can we foresee the Unexpected?

Indicators that may signal the proximity to points at which catastrophic shifts between alternative stable states occur can be classified roughly in two categories (Table 7.1) (**Chapter 2**):

A. Generic indicators related to critical slowing down

This class includes indicators that are a direct consequence of *critical slowing down*. Mathematically, critical slowing down is linked to the fact that the dominant eigenvalue of the system becomes zero at a bifurcation point (Wissel 1984). In practice, it implies that a system becomes slow in returning to equilibrium upon a perturbation. Critical slowing down is a generic phenomenon that is associated with loss of stability prior to non-catastrophic bifurcations (known in physics as *second-order transitions*, see Glossary) (Horsthemke 2006; Solé et al. 1996; Strogatz 1994) as well as catastrophic bifurcations (or *first-order transitions*) (**Chapter 2**). Critical slowing down translates into the three flagships of leading indicators for critical transitions: increasing recovery time upon disturbance (van Nes and Scheffer 2007), rising variance (Carpenter and Brock 2006), and growing autocorrelation or power spectral reddening (Held and Kleinen 2004; Ives 1995; Kleinen et al. 2003) in the pattern of fluctuations of a system.

Critical slowing down in combination with interactions in space can also give rise to *spatial indicators* that are in a way the equivalents of the above *temporal indicators*. For example, spatial interactions may cause an increase in spatial correlation between neighboring sites in a patchy or modular environment, because diffusion processes dominate as critical slowing down makes individual sites 'lethargic' prior to transition (**Chapter 3**). Other suggested spatial indicators that can arise from critical slowing down are an increase in spatial variance (Donangelo et al. 2010; Guttal and Jayaprakash 2009) and changes in the spatial spectrum frequencies as detected by Discrete Fourier Transform (Carpenter and Brock 2010).

B. System-specific indicators

The second class includes leading indicators that are not directly related to the universal phenomenon of critical slowing down, and therefore tend to be more system-specific (**Chapter 2**). For instance, as the boundary of the stability basin is approaching the equilibrium from one side, the resulting asymmetry in the basin of attraction around the equilibrium may lead to a skewed frequency distribution of states, derived from dataseries collected in time (Guttal and Jayaprakash 2008) or space (Guttal and Jayaprakash 2009). Other more system-specific signals include changes in self-organized regular spatial patterns (Rietkerk et al. 2004) or in the frequency distribution of patch sizes (Kéfi et al. 2007a) (**Chapter 2**). Also 'flickering' - the frequent flipping between alternative states (Berglund and Gentz 2006) - can in a sense be seen as a precursor of a permanent transition to an alternative state. Flickering causes an increase in variance (Carpenter and Brock 2006) and is reflected in bimodality of the frequency distribution of states prior to a critical transition. In a similar way, flickering in space (random local shifts between alternative states) may give rise to bimodality in the frequency distribution of local states sampled over a larger area.

Table 7.1 Early-warning signals for critical transitions

indicator	temporal	spatial	mechanism
increase in recovery time	+[1,2,3]	+[4]	critical slowing down
increase in correlation	+[5,6]	+[7,8]	critical slowing down
increase in variance	+[9]	+[10,11,12]	critical slowing down
reddening of power-spectrum	+[13]	as Discrete Fourier Transform[14]	critical slowing down
peak in skewness	+[15]	+[11]	asymmetry in potential field
flickering	+[9]	as stagnation[18]	stochastic forcing triggering shifts between alternative attractors
changes in pattern formation	-	+[16]	scale dependent feedbacks
deviations in power law of patch size distributions	-	+[17]	robust criticality with local interactions

[1]Wissel 1984
[2]Gandhi et al 1998
[3]van Nes and Scheffer 2007
[4]Dakos et al 2011
[5]Ives 1995
[6]Held and Kleinen 2004
[7]Dakos et al 2010
[8]Bascompte 2001
[9]Carpenter and Brock 2006
[10]Oborny et al 2005
[11]Guttal and Jayaprakash 2009
[12]Donangelo et al 2010
[13]Kleinen and Held 2003
[14]Carpenter and Brock 2010
[15]Guttal and Jayaprakash 2008
[16]Rietkerk et al 2004
[17]Kéfi et al 2007
[18]van Nes and Scheffer submitted

While these classes of indicators provide a potentially rich toolbox for estimating the risk of an approaching critical transition, we still lack a coherent understanding of when and where different early-warnings may be expected to signal an upcoming transition. Changes in recovery time, correlation and variance (all in time and space) are expected to be universal phenomena close to bifurcation points (**Chapter 2**). However, recent modeling studies have pointed to examples where early-warning signals could not be detected before a transition (Carpenter et al. 2009; Ditlevsen and Johnsen 2010; Hastings and Wysham 2010). Do these observations imply that there are specific conditions under which the leading indicators would fail? Are some generic indicators less generic than expected? **Chapters 4** and **5** are a first attempt towards addressing such concerns.

For increases in variance as an indicator of critical slowing down, we identified at least three cases where it may not occur in systems approaching a bifurcation (**Chapter 4**): a) when environmental factors fluctuate stochastically and the system becomes less sensitive to these factors near the transition, b) when critical slowing down reduces the system's capacity to follow high frequency fluctuations in the environment, and c) when data limitations lead to spurious trends due to the prevalence of low frequencies close to a transition. In these cases, observed variance may decrease instead of increase. While variance may thus be a less generic indicator than expected, we found autocorrelation to increase towards a transition in all these cases, suggesting that it is a robust indicator of slowing down (**Chapter 4**). Our comparative analysis of all proposed temporal and spatial indicators using spatial semi-arid ecosystem models (**Chapter 5**) also illustrates that the detection of indicators of critical slowing down may be problematic in particular systems. Although we identified critical slowing down before all types of transitions, the only indicator that could capture critical slowing down was recovery time upon perturbation. A limitation of this indicator is that it requires perturbation experiments, which may be risky, as they can push the system permanently to the alternative attractor (van Nes and Scheffer 2007), or are simply impossible to conduct when the scale of the system is too large (**Chapter 2**). In short, our findings point to the conclusion that there is no silver bullet indicator. Therefore, the best way forward is probably to expand our toolbox of indicators and develop a good understanding of when each of them might be most useful.

Despite the first promising evidence for early-warnings from real systems (Drake and Griffen 2010; **Chapter 6**), there is still a long list of conditions that probably need to be satisfied in order to allow the detection of approaching thresholds. Almost all theoretical studies on leading indicators (including this thesis) assume:

- weak stochastic disturbances following a distribution that remains constant (**Chapter 2-6**);
- a homogenous spatial environment (Guttal and Jayaprakash 2009) (**Chapter 4**);
- little observation error (Carpenter and Brock 2010);
- constant parameter values (**Chapters 2-6**);
- a slowly changing driving variable that we can monitor (**Chapters 2-6**);
- a threshold that corresponds to a catastrophic bifurcation (**Chapters 2-6**);
- a single threshold rather than multiple thresholds (Brock and Carpenter 2010);
- abundant data of high resolution without gaps (**Chapters 2-6**).

Clearly, such conditions are rarely met in nature. Therefore, while the prospect of foreseeing the risk of critical transitions in ecosystems using generic early-warning signals seems exciting, we still need a better understanding of the conditions under which early-warnings can be applied in reality.

The Limits to Early-warnings and the Challenge ahead

A Measure of Resilience?

In the afterthoughts of his famous book on '*Stability and Complexity in Model Ecosystems*' (May 2001), Bob May questioned whether we would ever be able to quantify "the volume of state space into which the system may be perturbed without catastrophic collapse" (aka resilience *sensu* Holling (1973)). May identified there that a fundamental problem of measuring resilience *sensu* Holling (see Glossary) lies in its multidimensional nature (May 2001). How can we quantify the magnitude of disturbance that a system is capable to absorb both in state space (e.g. an instant extinction event) and in parameter space (e.g. a sudden change in nutrient recycling rate)? Could early-warning indicators measure the *ecological resilience* (Holling 1996) of a system?

Put simply, ecological resilience is determined by the size and height of the system's basin of attraction (Box 7.1) (Holling 1973). The chance of a given disturbance to push the state of the system over the border of its basin of attraction depends not only on how wide the basin is, but also on the steepness of the basin's slope. The slope of the basin of attraction defines the rate with which the system recovers from a disturbance. *Recovery rate* is a measure of stability for a system (Pimm 1984), and is also viewed as an alternative notion of resilience termed *engineering resilience* (see Glossary) (Holling 1996). Critical slowing down related leading indicators are directly related to engineering resilience, and they cannot be regarded as direct measures of ecological resilience. However, based on the observation that the relationship between ecological resilience and engineering resilience is almost linear in most simple models, as well as in a few complex model examples (van Nes and Scheffer 2007), critical slowing down related leading indicators may serve as indirect indicators of ecological resilience. Although, this family of indicators can provide the seeds for developing novel ways to answer May's unanswered question and tackle Holling's biggest challenge, we still have to deal with the problem that a real system is characterized in many dimensions, and that these dimensions are often quite incomparable in terms of their units and characteristic time scales.

Signaling Bistability?

Although most of the discussion on early-warning signals revolves around their potential as indicators of catastrophic shifts between alternative states, the same signals can also be identified in cases where there is no switch to an alternative state. Whether the system is approaching a catastrophic or non-catastrophic bifurcation, or even a non-catastrophic transition with no bifurcation (Figure 7.1a-c), a drop in recovery rate may take place as expressed by a decreasing eigenvalue (Figure 7.1a1, b1, c1). The reason behind the drop in

eigenvalue in all these cases is the same: a nonlinearity in the rates of change of the system close to the threshold causes small deviations around equilibrium to be absorbed more slowly (Figure 7.1a2, b2, c2). Thus, slowing down and its derived indicators will occur in a broad class of situations where no catastrophic threshold exists (**Chapter 2**).

BOX 7. 1 | The relationship between ecological resilience, recovery rate and stability

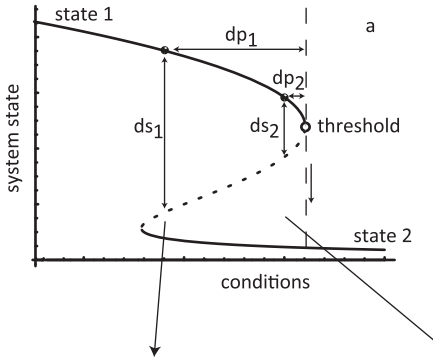

Ecological resilence (*ecR*) depends on the distance to the border of the unstable manifold in state space (*ds*) and on the distance to the critical threshold (*dp*) in parameter space [*ecR = f(ds,dp)*] (panel a). We can approximate ds as the distance to the border of the attraction basin and dp as the height h of the attraction basin to the alternative state (panels b, c). Recovery rate (*recR*) (or engineering resilience) depends on the slope of the basin of attraction, which is defined by ds and dp [*recR =dp/ds*]. This slope can be approximated by the eigenvalue |λ| which determines the stability of the current equilibrium of the system [*recR*≡|λ|]. As the system approaches the threshold, dp becomes smaller, recovery rate decreases, the current state loses stability, and ecological resilience declines. However, resilience is not approximated by |λ|, because *ds* is not exactly known. Recovery rate is only an indirect measure of resilience.

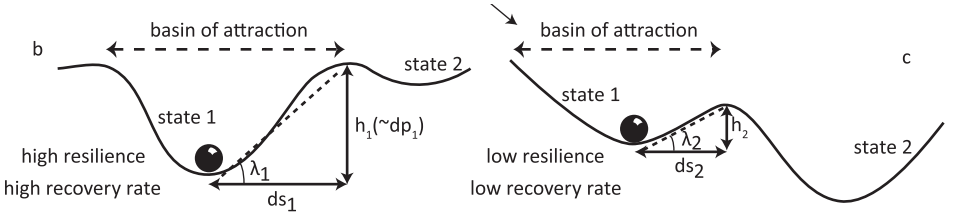

This brings us to the broader question of how we may know that the system is bistable and therefore that an approaching threshold signaled by slowing down may be catastrophic? For bistability a strong positive feedback is required (see **Introduction**). Scheffer and Carpenter (2003) proposed some methods to judge from data whether a system has alternative stable states. The only reliable indicators of bistability, however, are essentially based on visiting the alternative attractor. Therefore, the proposed early-warnings cannot be used to signal bistability. This is true not only for the critical slowing down related indicators (van Nes and Scheffer 2007; **Chapter 2**), but also for the range of indicators derived from spatial patterns (Kéfi et al. 2010; Kéfi et al. 2007a; Kéfi et al. 2011; van de Koppel and Crain 2006). Perhaps, perturbation experiments towards different directions in state space can in theory help to map asymmetries in recovery rates that could signal directions of proximate boundaries to alternative basins of attraction. Novel potential analysis techniques may contribute to this (Livina et al. 2010). However, since visiting the alternative states is required to know that they are there, only patterns such as hysteresis in the response to a control variable, or the emergence of bimodality in the

frequency distribution of states in time or space (e.g. due to 'flickering') can be interpreted as signals of bistability. Thus, a direct link between the occurrence of leading indicators and bistability simply cannot be expected.

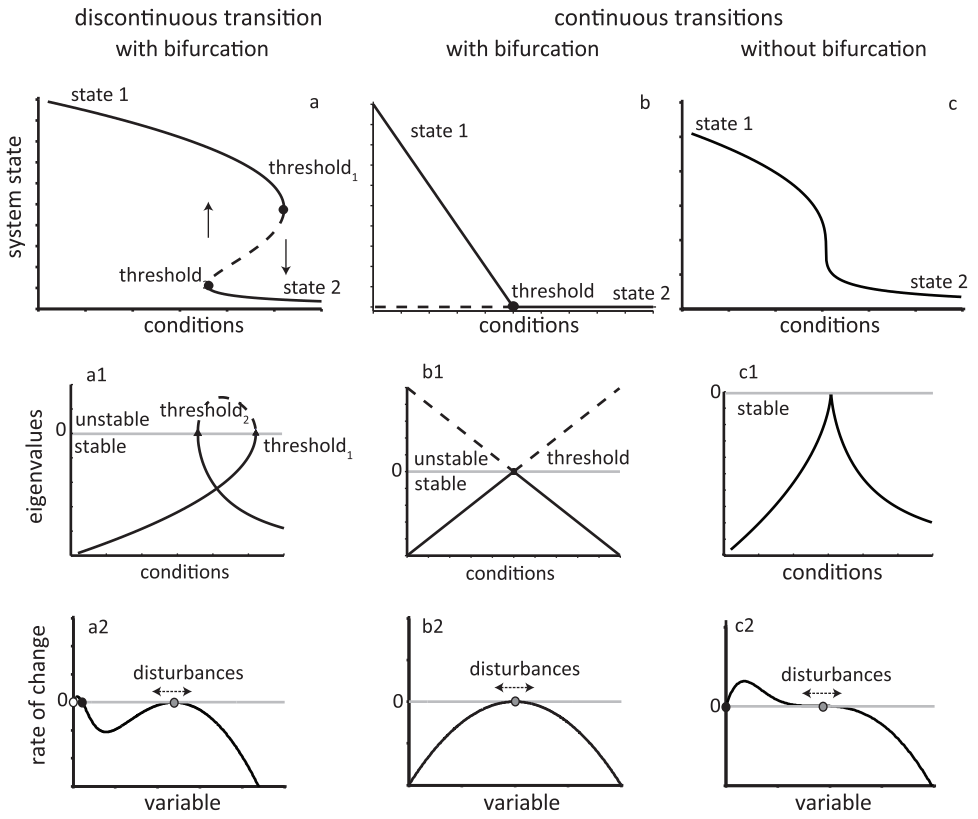

Figure 7.1 Critical slowing down prior to catastrophic and non-catastrophic transitions. (**a**) *Catastrophic* bifurcation. (**b**) *Non-catastrophic* bifurcation. (**c**) *Non-catastrophic* transition with no bifurcation. (**a1**-**c1**) The eigenvalues tend to zero as the conditions bring the system to the critical threshold. (**a2**-**c2**) Rates of change for all models at threshold. Note that small disturbances around equilibrium are absorbed with a rate almost equal to zero. The system at this point shows the maximum degree of slowing down. (Black dots stable equilibria; white dots unstable equilibria; gray dots equilibria at transition point)

Different Transitions, same Warnings?

The above discussion implies that we do not have leading indicators that are specific to critical transitions. Slowing down appears to be a generic phenomenon prior to a very broad class of transitions. Transitions due to bifurcation points (catastrophic or non-catastrophic) are associated by eigenvalues that approach zero (Strogatz 1994; Thompson 2002). This means that we should in principle be able to find indicators of slowing down

before this broad class of zero-eigenvalue local bifurcations. Transitions due to very high levels of noise (noise-induced transitions) are also expected to be preceded by critical slowing down (Horsthemke 2006; Leung 1988). However, whether critical slowing down will translate into the proposed leading indicators prior to this type of transitions remains unclear (**Chapter 4**). Transitions also occur around more complex classes of bifurcations, such as the ones involving shifts between cyclic and chaotic regimes, phase-locking, or collisions of trajectories with basin boundaries (global bifurcations) (Leung 1998; **Chapter 2**). For these transitions we still need to identify whether critical slowing down occurs, and - if it does - whether it can be translated into a usable indicator (Box 7.2).

There are also marked transitions that may not be associated with bifurcation points. For instance, gradually increasing magnitude of disturbances can eventually push a system to cross the basin boundary and switch to an alternative attractor. Such a transition will often be announced by rising skewness (Guttal and Jayaprakash 2008; **Chapter 2**). Another example occurs in 'slow-fast' limit cycles. Consider for instance the case of a fast growing resource under the control of a slowly changing consumer, as in the classic case of spruce budworm dynamics (Ludwig et al. 1978) (Box 7.2 panel b). Although the system is not formally crossing a bifurcation point, the trajectory of the resource undergoes repeated abrupt shifts. These shifts can be considered as catastrophic transitions for the fast changing variable. Indeed, at the transitions the eigenvalue of the fast changing variable goes to zero (Box 7.2 panel b). This illustrates that even transitions in the *transient* dynamics of a system may be preceded by the proposed leading indicators.

In conclusion, while a truly generic family of indicators seems to exist for a very broad class of transitions, there is a flip side to this genericity. Although the leading indicators tell us that something important may be about to happen, they do not tell us what precisely that 'something' may be. Thus, next to the indicators, knowledge of the underlying mechanisms is important to put the signals in the right context.

The Distance to Transition?

In theory, as the dominant eigenvalue of the system tends to zero at a critical transition, autocorrelation reaches unity (**Chapter 2, 4**). Therefore, the difference between the current autocorrelation and one, should quantify the distance to the transition. This would be true, if the transition occurred exactly at the bifurcation point. In a stochastic environment, however, this never happens, as the system shifts always before the actual bifurcation. Moreover, recovery rates are system specific in the sense that even in the absence of any bifurcation slow systems have a slow recovery rate than fast systems. Therefore, early-warnings can only be relative measures of proximity to a critical transition. In other words, they are not predictive tools, but can be used within particular systems to rank situations according to the risk of an upcoming shift. For instance, different reefs could be ranked in terms of their apparent resilience, or a long time-series can be used to see if resilience of a system may be increasing or decreasing. Although specific thresholds in indicators have been proposed to signal an increased likelihood of a transition (e.g. a spectral density ratio of low to high frequencies that passes 1 (Biggs et al.

2009b)), such critical indicator levels seem unlikely to be transferrable across different systems.

Although absolute values of indicators may remain difficult to interpret, combining different indicators can often help to obtain further information. For instance, in some systems an increase in variance combined with a peak in skewness may be an unequivocal signal of an approaching catastrophic shift (Guttal and Jayaprakash 2009). Also, combining spatial and temporal indicators (**Chapter 5**), or comparing indicators to estimates from null models (Kéfi et al. 2011) may help to estimate the risk of a nearby transition.

Towards an applied science of Early-warnings

Clearly, we are only starting to see where and how early-warning signals can be best picked up. It is obvious that the detection of early-warnings will always be easier in some systems than in others. In general, the feasibility of detecting early-warning signals will greatly depend on the controllability and the scale of the system. For instance, critical slowing down has been quantified successfully in a series of experiments in various fields ranging from chemistry (Kramer and Ross 1985) and lasers (Tredicce et al. 2004) to human movement control (Kelso et al. 1986; Scholz et al. 1987). Environmental systems are of course much more challenging to control for this kind of experiments, but also there we have small 'closed' systems with defined boundaries (e.g. lakes) that may be better candidates to study early-warning signals than 'open' systems (e.g. oceans).

Time scales are another important aspect. Systems with fast time scales simply offer better possibilities to collect data, and tend to be more suitable for manipulation and experimentation. For instance, measuring recovery time in perturbation experiments for transitions in fast components of human physiology (e.g. migraine) may yield better results than conducting the same experiments in coral reefs, or than performing experiments on relevant scales in the climate system; a task that is simply impossible. In addition to the feasibility of experimentation due to scale, also the singularity of such large-scale systems makes the estimation of leading indicators more difficult compared to systems for which we have many instances (e.g. lakes), where this modularity allows the provision of multiple sources of information.

Obviously, certain indicators will also be more reliable than others in estimating the risk of an upcoming transition. Probably, when the system permits experimentation, recovery time from perturbations is the most straightforward and easily measured indicator of critical slowing down (**Chapter 5**). On the other hand, a growing number of studies offer promising results for other indicators as well. Increasing autocorrelation has been found in ancient climate transitions (Livina and Lenton 2007; **Chapter 6**), correlation and skewness rose in extinction experiments (Drake and Griffen 2010), deviations in power laws were identified in overgrazed semi-arid ecosystems (Kéfi et al. 2007b), and increased variance has been shown in overexploited fish populations (Hsieh et al. 2006) as well as in other marine regime shifts (Beaugrand et al. 2008). In addition to these mainly ecological examples, there is also work in epileptic seizures (McSharry et al. 2003), the onset of Self-

Organized Criticality (SOC) in earthquakes (Ramos 2010), meltdowns in financial systems (Gorban et al. 2010), pattern formation in asthma attacks (Venegas et al. 2005), and the 'death' of buzzwords in the Web (Neuman et al. 2010).

In addition to an expanded collection of empirical studies, we definitively need further development in the theory of the existing leading indicators, as well as search for others (Gonzalez et al. 2011; Lim and Epureanu 2011; Mayer et al. 2006) (Box 7.2). So far, we have analyzed early-warnings in a range of ecological models that describe eutrophication (Carpenter and Brock 2006), predator-prey cycles (Chisholm and Filotas 2009), competition (Chisholm and Filotas 2009), desertification (**Chapter 5**), trophic cascades (Carpenter et al. 2008), resource-competition (Carpenter et al. 2009), Allee effects (Takimoto 2009), and overexploitation (Guttal and Jayaprakash 2008; van Nes and Scheffer 2007; **Chapter 3, 4**). Most of these studies are based on simple models and have neglected more complex behaviors or more complicated topologies, such as the ones encountered in most ecological networks (Box 7.2). It will be important to expand the range of models we are studying to include more complex situations, if we want to bridge the gap between the overly simple minimal models and reality. In addition to such models, experimental data and retrospective studies should be conducted in order to test and improve our existing protocols (**Chapter 6**) for analyzing data in search of early-warning signals.

Can we avoid the Unexpected?

No doubt 'forewarned is forearmed'. However, knowing the risk of an approaching transition may be a necessary but not sufficient condition for avoiding it. This implies that early-warnings can at best be only part of the solution to the sustainable management of ecosystems as well as other systems at the brink of collapse.

The reason why it is difficult to avoid an unexpected transition is not only that early-warnings are not predictive tools or that they may be detected too late (Biggs et al. 2009b; Contamin and Ellison 2009), but also that we face a deep uncertainty when it comes to managing ecological systems. This uncertainty results from a combination of stochastic factors, imprecise model forecasts, insufficient data, hidden nonlinearities (Carpenter 2003; Clark et al. 2001), and the constantly evolving interactions of the socio-ecological aspects of a system (Chapin et al. 2009; Margalef 1997).

One approach for avoiding the Unexpected in face of this uncertainty is the development of policies based on a precautionary principle (Rockström et al. 2009; Scheffer 2009). Also we may try to match biophysical and sociopolitical windows of opportunity (Biggs et al. 2010) in order to minimize delays in decision-making (Scheffer et al. 2003). A quite different approach known as *resilience thinking* (Walker and Salt 2006) accepts that surprises will always happen and focuses at building resilience to maintain essential aspects of the functioning of a system in the face of change (Gunderson and Holling 2001), and stresses the importance of developing adaptive capacity to changing conditions (Berkes et al. 2003).

BOX 7. 2 | Early-warning signals for Complex behaviors

a. complex dynamics

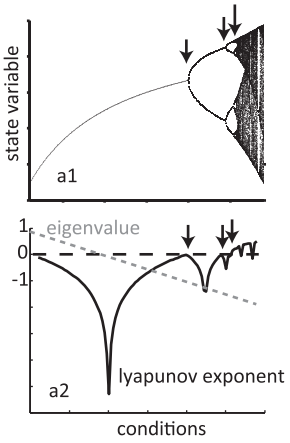

a. **En route to chaos** eigenvalues are not valuable anymore for critical slowing down indicators. Instead, indicators of stability of trajectories (like lyapunov exponents) are more informative.

b. In **transient transitions**, the fast variable switches back and forth between the attractors. Prior to the transitions the eigenvalues of the trajectories reach zero. In this case, leading indicators can be measured.

c. **Global bifurcations** occur when a trajectory hits the unstable manifold to switch to an alternative attractor. As the trajectories approach the manifold, they slow down. Such slowing down can be seen as a delay in part of the cycle.

d. Transitions due to outcompetition in an **ecological network**. Indicators for individual nodes of the network may not all signal the transition. Instead, some nodes are more informative than others, or multivariate indices can be more valuable. Important elements in these cases can be cross-correlations between nodes and their degree of interaction.

b. transitions in slow-fast cycles

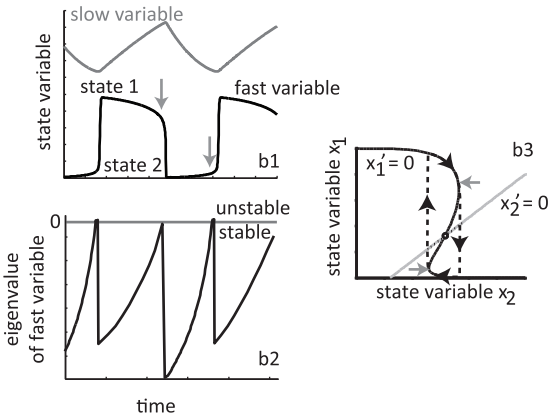

c. global bifurcations

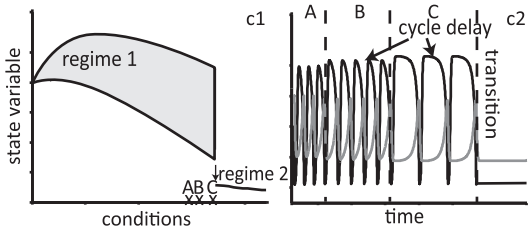

d. complex topologies

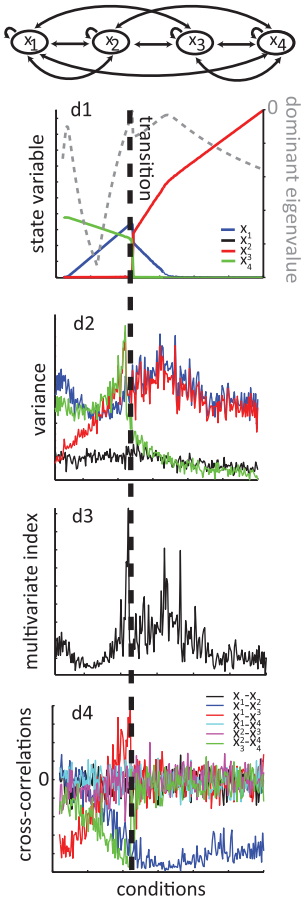

Acknowledging that early-warning signals may be at best a modest addition to the toolbox for sustainability, the finding that we may be able to probe resilience in even the largest and most complex systems is exciting. Despite the fact that we are still in the early stages of their development, the perspectives of these new tools may well increase with the potential of integrating multiple sources of information (experimental, field studies, historical data, remote sensing, modeling) (Biggs et al. 2009a; Carpenter 2003), with improved use of statistics of extreme events (Albeverio et al. 2006; Ellison and Agrawal 2005), and innovative ways of using information technology (SRC 2010; Galaz et al. 2010).

In this thesis, I looked into the mirror world of math to find that simple patterns tend to mark the behavior of systems prior to an unexpected transition. In the worst case such patterns are an illusion in the real world, an inevitable consequence of our human tendency to see patterns even where they do not exist (Clark et al. 2001). In the best case, the results from the mirror world of math can put us on the track of a widely applicable theory of early-warnings for critical transitions. Finding out which of the two is true is surely worth the effort.

References

Aguiar, M. R., and O. E. Sala. 1999. Patch structure, dynamics and implications for the functioning of arid ecosystems. Trends in Ecology & Evolution 14:273-277.

Albeverio, S., V. Jentsch, and H. Kantz. 2006. Extreme Events in Nature and Society. Berlin, Springer.

Alley, R. B., J. Marotzke, W. D. Nordhaus, J. T. Overpeck, D. M. Peteet, R. A. Pielke, R. T. Pierrehumbert, P. B. Rhines, T. F. Stocker, L. D. Talley, and J. M. Wallace. 2003. Abrupt climate change. Science 299:2005-2010.

Anderson, C. N. K., C. H. Hsieh, S. A. Sandin, R. Hewitt, A. Hollowed, J. Beddington, R. M. May, and G. Sugihara. 2008. Why fishing magnifies fluctuations in fish abundance. Nature 452:835-839.

Arvelund, E. Calm before the storm? Low volatility often precedes market downturn. (accessed on January 28, 2002)

Bagowski, C. P., and J. E. Ferrell. 2001. Bistabillity in the JNK cascade. Current Biology 11:1176-1182.

Bailey, R. M. 2011. Spatial and temporal signatures of fragility and threshold proximity in modelled semi-arid vegetation. Proceedings of the Royal Society B: Biological Sciences 278:1064-1071.

Bakke, J., O. Lie, E. Heegaard, T. Dokken, G. H. Haug, H. H. Birks, P. Dulski, and T. Nilsen. 2009. Rapid oceanic and atmospheric changes during the Younger Dryas cold period. Nature Geoscience 2:202-205.

Bascompte, J. 2001. Aggregate statistical measures and metapopulation dynamics. Journal of Theoretical Biology 209:373-379.

Bascompte, J., and R. V. Solé. 1996. Habitat fragmentation and extinction thresholds in spatially explicit models. Journal of Animal Ecology 65:465-473.

Bates, D. S. 1991. The crash of 87 - Was it expected - The evidence from options markets. Journal of Finance 46:1009-1044.

Bates, D. S. 1996. Jumps and stochastic volatility: Exchange rate processes implicit in deutsche mark options. Review of Financial Studies 9:69-107.

Beaugrand, G., M. Edwards, K. Brander, C. Luczak, and F. Ibanez. 2008. Causes and projections of abrupt climate-driven ecosystem shifts in the North Atlantic. Ecology Letters 11:1157-1168.

Beisner, B. E., D. T. Haydon, and K. Cuddington. 2003. Alternative stable states in ecology. Frontiers in Ecology and the Environment 1:376-382.

Bellwood, D. R., T. P. Hughes, C. Folke, and M. Nystrom. 2004. Confronting the coral reef crisis. Nature 429:827-833.

Bence, J. R. 1995. Analysis of short time-series - Correcting for autocorrelation. Ecology 76:628-639.

Berglund, N., and B. Gentz. 2006. Noise-Induced Phenomena in Slow-Fast Dynamical Systems- A sample-paths approach, Springer.

Berkes, F., J. Colding, and C. Folke. 2003. Navigating Social-Ecological Systems: Building Resilience for Complexity and Change. Cambridge, UK, CambridgeUniversityPress.

Biggs, R., S. R. Carpenter, and W. A. Brock. 2009a. Spurious certainty: How ignoring measurement error and environmental heterogeneity may contribute to environmental controversies. Bioscience 59:65-76.

Biggs, R., S. R. Carpenter, and W. A. Brock. 2009b. Turning back from the brink: Detecting an impending regime shift in time to avert it. Proceedings of the National Academy of Sciences 106:826-831.

Biggs, R., F. R. Westley, and R. A. Carpenter. 2010. Navigating the back loop: fostering social innovation and transformation in ecosystem management. Ecology and Society 15:9.

Box, G. E. P., Jenkins G.M., and G.C. Geinsel. 2008. Time-series Analysis Forecasting and Control. New Jersey, Wiley.

Brock, W. A., and S. R. Carpenter. 2006. Variance as a leading indicator of regime shift in ecosystem services. Ecology and Society 11.

Brock, W. A., and S. R. Carpenter. 2010. Interacting regime shifts in ecosystems: implication for early warnings. Ecological Monographs 80:353-367.

Brock, W. A., S. R. Carpenter, and M. Scheffer. 2006. Regime shifts, environmental signals, uncertainty and policy choice. *In* J. Norberg, and G. Cumming, eds. A Theoretical Framework for Analysing Social-Ecological Systems. New York, Columbia University Press.

Brockner, J. 1992. The escalation of commitment to a failing course of action - Toward theoretical progress. Academy Of Management Review 17:39-61.

Brovkin, V., M. Claussen, V. Petoukhov, and A. Ganopolski. 1998. On the stability of the atmosphere-vegetation system in the Sahara/Sahel region. Journal of Geophysical Research Atmospheres 103:31613-31624.

Brovkin, V., S. Levis, M. F. Loutre, M. Crucifix, M. Claussen, A. Ganopolski, C. Kubatzki, and V. Petoukhov. 2003. Stability analysis of the climate-vegetation system in the northern high latitudes. Climatic Change 57:119-138.

Carpenter, S., W. Brock, J. Cole, and M. Pace. 2009. Leading indicators of phytoplankton transitions caused by resource competition. Theoretical Ecology 2:139-148.

Carpenter, S. R. 2003, Regime shifts in lake ecosystems: pattern and variation: Excellence in Ecology Series, v. 15, International Ecology Institute.

Carpenter, S. R. 2005. Eutrophication of aquatic ecosystems: Bistability and soil phosphorus. Proceedings of the National Academy of Sciences of the United States of America 102:10002-10005.

Carpenter, S. R., and W. A. Brock. 2006. Rising variance: a leading indicator of ecological transition. Ecology Letters 9:311-318.

Carpenter, S. R., and W. A. Brock. 2010. Early warnings of regime shifts in spatial dynamics using the discrete Fourier transform. Ecosphere 1:art10.

Carpenter, S. R., W. A. Brock, J. J. Cole, J. F. Kitchell, and M. L. Pace. 2008. Leading indicators of trophic cascades. Ecology Letters 11:128-138.

Carpenter, S. R., D. Ludwig, and W. A. Brock. 1999. Management of eutrophication for lakes subject to potentially irreversible change. Ecological Applications 9:751-771.

Chapin, F. S., G. P. Kofinas, C. Folke, S. R. Carpenter, P. Olsson, N. Abel, R. Biggs, R. L. Naylor, E. Pinkerton, D. M. Stafford, W. Steffen, B. Walker, O. R.Young. 2009. Resilience-Based Stewardship: Strategies for Navigating Sustainable Pathways in

a Changing World. *In* C. Folke, G. P. Kofinas, and I. I. I. F. S. Chapin, eds. Principles of Ecosystem Stewardship, Springer New York.

Chisholm, R. A., and E. Filotas. 2009. Critical slowing down as an indicator of transitions in two-species models. Journal of Theoretical Biology 257:142-149.

Chow, S. N., J. MalletParet, and E. S. VanVleck. 1996. Dynamics of lattice differential equations. International Journal of Bifurcation and Chaos 6:1605-1621.

Clark, J. S., S. R. Carpenter, M. Barber, S. Collins, A. Dobson, J. A. Foley, D. M. Lodge M. Pascual, R. Pielke, W. Pizer, C. Pringle, W. V. Reid, K. A. Rose, O. Sala, W. H. Schlesinger, D. H. Wall,D. Wear.2001. Ecological forecasts: An emerging imperative. Science 293:657-660.

Clark, P. U., N. G. Pisias, T. F. Stocker, and A. J. Weaver. 2002. The role of the thermohaline circulation in abrupt climate change. Nature 415:863-869.

Contamin, R., and A. M. Ellison. 2009. Indicators of regime shifts in ecological systems: What do we need to know and when do we need to know it? Ecological Applications 19:799-816.

Cook, K. H. 1999. Generation of the African easterly jet and its role in determining West African precipitation. Journal of Climate 12:1165-1184.

Crowley, T. J., and W. T. Hyde. 2008. Transient nature of late Pleistocene climate variability. Nature 456:226-230.

Dakos, V., M. Scheffer, E. H. van Nes, V. Brovkin, V. Petoukhov, and H. Held. 2008. Slowing down as an early warning signal for abrupt climate change. Proceedings of the National Academy of Sciences 105:14308-14312.

Dakos, V., E. van Nes, R. Donangelo, H. Fort, and M. Scheffer. 2010. Spatial correlation as leading indicator of catastrophic shifts. Theoretical Ecology 3:163-174.

Daskalov, G. M., A. N. Grishin, S. Rodionov, and V. Mihneva. 2007. Trophic cascades triggered by overfishing reveal possible mechanisms of ecosystem regime shifts. Proceedings of the National Academy of Sciences 104:10518-10523.

Davis, S., P. Trapman, H. Leirs, M. Begon, and J. A. P. Heesterbeek. 2008. The abundance threshold for plague as a critical percolation phenomenon. Nature 454:634-637.

deMenocal, P., J. Ortiz, T. Guilderson, and M. Sarnthein. 2000. Coherent high- and low-latitude climate variability during the holocene warm period. Science 288:2198-2202.

Ditlevsen, P. D., and S. J. Johnsen. 2010. Tipping points: Early warning and wishful thinking. Geophysical Research Letters 37.

Donangelo, R., H. Fort, V. Dakos, M. Scheffer, and E. H. Van Nes. 2010. Early warnings for catastrophic shifts in ecosystems: Comparison between spatial and temporal indicators. International Journal of Bifurcation and Chaos 20:315-321.

Drake, J. M., and B. D. Griffen. 2010. Early warning signals of extinction in deteriorating environments. Nature 467:456-459.

Economist, The. CSI: credit crunch. (October 18, 2007).

Efron, B., and R. Tibshirani. 1986. Bootstrap methods for standard errors, confidence intervals, and other measures of statistical accuracy. Statistical Science 1:54-77.

Elger, C. E., and K. Lehnertz. 1998. Seizure prediction by non-linear time-series analysis of brain electrical activity. European Journal of Neuroscience 10:786-789.

Ellison, A. M., and A. A. Agrawal. 2005. The statistics of rarity. Ecology 86:1079-1080.

Eppinga, M. B., P. C. de Ruiter, M. J. Wassen, and M. Rietkerk. 2009. Nutrients and hydrology indicate the driving mechanisms of peatland surface patterning. American Naturalist 173:803-818.

Fisher, M. E. 1974. Renormalization group in theory of critical behavior. Reviews of Modern Physics 46:597-616.

Fraedrich, K. 1978. Structural and Stochastic Analysis of a zero-dimensional climate system. Quarterly Journal of the Royal Meteorological Society 104:461-474.

Fraedrich, K. 1979. Catastrophes and resilience of a zero-dimensional climate system with ice-albedo and greenhouse feedback. Quarterly Journal of the Royal Meteorological Society 105:147-167.

Galaz, V., B. Crona, T. Daw, O. Bodin, M. Nyström, and P. Olsson. 2010. Can web crawlers revolutionize ecological monitoring? Frontiers in Ecology and the Environment 8:99-104.

Gandhi, A., S. Levin, and S. Orszag. 1998. "Critical slowing down" in time-to-extinction: an example of critical phenomena in ecology. Journal of Theoretical Biology 192:363-376.

Ganopolski, A., V. Petoukhov, S. Rahmstorf, V. Brovkin, M. Claussen, A. Eliseev, and C. Kubatzki. 2001. CLIMBER-2: a climate system model of intermediate complexity. Part II: model sensitivity. Climate Dynamics 17:735-751.

Gardiner, C. W. 2003. Handbook of Stochastic Methods for Physics, Chemistry and the Natural Sciences: Spronger Series in Synergatics, Springer.

Gautama, T., D. P. Mandic, and M. M. Van Hulle. 2004. A novel method for determining the nature of time-series. IEEE Transactions on Biomedical Engineering 51:728-736.

Gilmore, R. 1981. Catastrophe theory for scientists and engineers, John Wiley & Sons.

Gonzalez, J. L., E. L. De Faria, and M. P. Albuquerque. 2011. Nonadditive Tsallis entropy applied to the Earth's climate. Physica A: Statistical Mechanics and its Applications 390:587-594.

Gorban, A. N., E. V. Smirnova, and T. A. Tyukina. 2010. Correlations, risk and crisis: From physiology to finance. Physica A: Statistical Mechanics and its Applications 389:3193-3217.

Grasman, J., and O.A. van Herwaarden. 1999. Asymptotic methods for the Fokker-Planck equation and the exit problem in applications: Synergetics Series, Springer-Verlag.

Gray, W. M. 1968. Global view of origin of tropical disturbances and storms. Monthly Weather Review 96:669-700.

Grist, J. P., and S. E. Nicholson. 2001. A study of the dynamic factors influencing the rainfall variability in the West African Sahel. Journal of Climate 14:1337-1359.

Gunderson, L., and C. S. Holling. 2001. Panarchy: understanding transformations in human and natural systems. Washington, Island Press.

Guttal, V., and C. Jayaprakash. 2007. Impact of noise on bistable ecological systems. Ecological Modelling 201:420-428.

Guttal, V., and C. Jayaprakash. 2008. Changing skewness: an early warning signal of regime shifts in ecosystems. Ecology Letters 11:450-460.

Guttal, V., and C. Jayaprakash. 2009. Spatial variance and spatial skewness: leading indicators of regime shifts in spatial ecological systems. Theoretical Ecology 2:3-12.

Handa, I. T., R. Harmsen, and R. L. Jefferies. 2002. Patterns of vegetation change and the recovery potential of degraded areas in a coastal marsh system of the Hudson Bay lowlands. Journal of Ecology 90:86-99.

Hanski, I. 1998. Metapopulation dynamics. Nature 396:41-49.

Hare, S. R., and N. J. Mantua. 2000. Empirical evidence for North Pacific regime shifts in 1977 and 1989. Progress in Oceanography 47:103-145.

Hastie, T. J. A., and R. J. Tibshirani. 1990, Generalized additive models: Monographs on statistics and applied probability, v. 43. London, Chapman and Hall.

Hastings, A., and D. B. Wysham. 2010. Regime shifts in ecological systems can occur with no warning. Ecology Letters 13:464-472.

Held, H., and T. Kleinen. 2004. Detection of climate system bifurcations by degenerate fingerprinting. Geophysical Research Letters 31.

Hens, T., and K. R. Schenk-Hoppe. 2009. Handbook of financial markets: Dynamics and Evolution. North Holland.

HilleRisLambers, R., M. Rietkerk, F. Van den Bosch, H. T. Prins, and H. De Kroon. 2001. Vegetation pattern formation in semi-arid grazing systems. Ecology 82:50-61.

Holling, C. S. 1973. Resilience and stability of ecological systems. Annual Review of Ecology and Systematics 4:1-23.

Holling, C. S. 1996. Engineering resilience vs. ecological resilience. *In* P. C. Schulze, ed. Engineering within Ecological Constraints. Washington DC, National Academy Press.

Holyst, J. A., K. Kacperski, and F. Schweitzer. 2002. Social impact models of opinion dynamics. Annual Reviews of Computational Physics 9:253-273.

Hong, H., and J. C. Stein. 2003. Differences of opinion, short-sales constraints, and market crashes. Review of Financial Studies 16:487-525.

Horsthemke, W. 2006. Noise-Induced Transitions : Theory and Applications in Physics, Chemistry, and Biology.

Hsieh, C. H., C. S. Reiss, J. R. Hunter, J. R. Beddington, R. M. May, and G. Sugihara. 2006. Fishing elevates variability in the abundance of exploited species. Nature 443:859-862.

Hughes, T. P. 1994. Catastrophes, phase shifts, and large-scale degradation of a Caribbean coral reef. Science 265:1547-1551.

Ives, A. R. 1995. Measuring resilience in stochastic systems. Ecological Monographs 65:217-233.

Ives, A. R., B. Dennis, K. L. Cottingham, and S. R. Carpenter. 2003. Estimating community stability and ecological interactions from time-series data. Ecological Monographs 73:301-330.

Janssen, R. H. H., M. B. J. Meinders, E. H. van Nes, and M. Scheffer. 2008. Microscale vegetation-soil feedback boosts hysteresis in a regional vegetation-climate system. Global Change Biology 14:1104-1112.

Joseph, E., Jenkins, G., Fuentes, J., Kucera, P., Gaye, A., Gerlach, J., and M. Garstang. 2003. New Opportunities for GV Measurement Program in West Africa. The 1st International GPM GV Requirements Workshop.

Judd, S. L., and M. Silber. 2000. Simple and superlattice Turing patterns in reaction-diffusion systems: bifurcation, bistability, and parameter collapse. Physica D 136:45-65.

Kambhu, J., S. Weidman, and N. Krishnan. 2007. New Directions for Understanding Systemic Risk: A Report on a Conference Cosponsored by the Federal Reserve Bank of New York and the National Academy of Sciences The National Academies Press.

Kéfi, S., M. Eppinga, P. de Ruiter, and M. Rietkerk. 2010. Bistability and regular spatial patterns in arid ecosystems. Theoretical Ecology 3:257-269.

Kéfi, S., M. Rietkerk, C. L. Alados, Y. Pueyo, V. P. Papanastasis, A. ElAich, and P. C. de Ruiter. 2007a. Spatial vegetation patterns and imminent desertification in Mediterranean arid ecosystems. Nature 449:213-217.

Kéfi, S., M. Rietkerk, M. Roy, A. Franc, P. C. de Ruiter, and M. Pascual. 2011. Robust scaling in ecosystems and the meltdown of patch size distributions before extinction. Ecology Letters 14:29-35.

Kéfi, S., M. Rietkerk, M. van Baalen, and M. Loreau. 2007b. Local facilitation, bistability and transitions in arid ecosystems. Theoretical Population Biology 71:367-379.

Keitt, T. H., M. A. Lewis, and R. D. Holt. 2001. Allee effects, invasion pinning, and species' borders. American Naturalist 157:203-216.

Kelso, J. A. S., J. P. Scholz, and G. Schöner. 1986. Nonequilibrium phase transitions in coordinated biological motion: critical fluctuations. Physics Letters A 118:279-284.

Kleinen, T., H. Held, and G. Petschel-Held. 2003. The potential role of spectral properties in detecting thresholds in the Earth system: application to the thermohaline circulation. Ocean Dynamics 53:53-63.

Knowlton, N. 2004. Multiple "stable" states and the conservation of marine ecosystems. Progress in Oceanography 60:387-396.

Kramer, J., and J. Ross. 1985. Stabilization of unstable states, relaxation, and critical slowing down in a bistable system. The Journal of Chemical Physics 83:6234-6241.

Krugman, P. Revenge of the Glut. The New York Times. (March 2, 2009).

Kump, L. R. 2005. Palaeoclimate - Foreshadowing the glacial era. Nature 436:333-334.

Kuznetsov, Y. A. 1995. Elements of Applied Bifurcation Theory. New York, Springer-Verlag.

Lawton, J. 2001. Earth system science. Science 292:1965-1965.

LeBaron, B. 1992. Some relations between volatility and serial correlations in stock-market returns. Journal of Business 65:199-219.

LeBaron, B. 2000. The stability of moving average technical trading rules on the Dow Jones Index. Derivatives Use, Trading & Regulation 5:324-338.

Legendre, P., and M. J. Fortin. 1989. Spatial pattern and ecological analysis. Plant Ecology 80:107-138.

Lehnertz, K., and C. E. Elger. 1998. Can epileptic seizures be predicted? Evidence from nonlinear time-series analysis of brain electrical activity. Physical Review Letters 80:5019-5022.

Lenton, T. M., H. Held, E. Kriegler, J. W. Hall, W. Lucht, S. Rahmstorf, and H. J. Schellnhuber. 2008. Tipping elements in the Earth's climate system. Proceedings

of the National Academy of Sciences of the United States of America 105:1786-1793.

Lenton, T. M., R. J. Myerscough, R. Marsh, V. N. Livina, A. R. Price, S. J. Cox, and G. Team. 2009. Using GENIE to study a tipping point in the climate system. Philosophical Transactions of the Royal Society A- Mathematical Physical and Engineering Sciences 367:871-884.

Lessios, H. A., D. R. Robertson, and J. D. Cubit. 1984. Spread of Diadema mass mortality through the Caribbean. Science 226:335-337.

Leung, H. K. 1988. Critical slowing down near a noise-induced transition point. Physical Review A 37:1341-1344.

Leung, H. K. 1998. Critical slowing down in synchronizing nonlinear oscillators. Physical Review E - Statistical Physics, Plasmas, Fluids, and Related Interdisciplinary Topics 58:5704-5709.

Leung, H. K. 2000. Bifurcation of synchronization as a nonequilibrium phase transition. Physica A: Statistical Mechanics and its Applications 281:311-317.

Lim, J., and B. I. Epureanu. 2011. Forecasting a class of bifurcations: Theory and experiment. Physical Review E - Statistical, Nonlinear, and Soft Matter Physics 83.

Litt, B., R. Esteller, J. Echauz, M. D'Alessandro, R. Shor, T. Henry, P. Pennell et al. 2001. Epileptic seizures may begin hours in advance of clinical onset: A report of five patients. Neuron 30:51-64.

Liu, Z. H., M. Pagani, D. Zinniker, R. DeConto, M. Huber, H. Brinkhuis, S. R. Shah et al. 2009. Global Cooling During the Eocene-Oligocene Climate Transition. Science 323:1187-1190.

Livina, V. N., F. Kwasniok, and T. M. Lenton. 2010. Potential analysis reveals changing number of climate states during the last 60 kyr. Climate of the Past 6:77-82.

Livina, V. N., and T. M. Lenton. 2007. A modified method for detecting incipient bifurcations in a dynamical system. Geophysical Research Letters 34.

Lo, A. W., H. Mamaysky, and J. Wang. 2000. Foundations of technical analysis: Computational algorithms, statistical inference, and empirical implementation. Journal of Finance 55:1705-1765.

Ludwig, D., D. D. Jones, and C. S. Holling. 1978. Qualitative analysis of insect outbreak systems the spruce budworm and forest. Journal of Animal Ecology 47:315-332.

Luthi, D., M. Le Floch, B. Bereiter, T. Blunier, J.-M. Barnola, U. Siegenthaler, D. Raynaud et al. 2008. High-resolution carbon dioxide concentration record 650,000-800,000[thinsp]years before present. Nature 453:379-382.

MA, Millenium Ecosystem Assessment 2005. Ecosystems and human well-being. Our human planet: summary for decision makers. Washington, D.C., USA, Island Press.

Mann, H. B. 1945. Nonparametric tests against trend. Econometrica 13:245-259.

Margalef, R. 1997. Our Biosphere: Excellence in Ecology, International Ecology Institute.

Matsumoto, G., and T. Kunisawa. 1978. Critical slowing-down near transition region from resting to time-ordered states in squid giant-axons. Journal of the Physical Society of Japan 44:1047-1048.

May, R. M. 1977. Thresholds and breakpoints in ecosystems with a multiplicity of stable states. Nature 269:471-477.

May, R. M. 2001. Stability and complexity in model ecosystems. Princeton Landmarks in Biology, Princeton University Press.

May, R. M. 2004. Uses and Abuses of Mathematics in Biology. Science 303:790-793.

May, R. M., S. A. Levin, and G. Sugihara. 2008. Complex systems - Ecology for bankers. Nature 451:893-895.

Mayer, A. L., C. W. Pawlowski, and H. Cabezas. 2006. Fisher Information and dynamic regime changes in ecological systems. Ecological Modelling 195:72-82.

McSharry, P. E., L. A. Smith, L. Tarassenko, J. Martinerie, M. Le Van Quyen, M. Baulac, and B. Renault. 2003. Prediction of epileptic seizures: Are nonlinear methods relevant? Nature Medicine 9:241-242.

Mormann, F., R. G. Andrzejak, C. E. Elger, and K. Lehnertz. 2007. Seizure prediction: the long and winding road. Brain 130:314-333.

Narisma, G. T., J. A. Foley, R. Licker, and N. Ramankutty. 2007. Abrupt changes in rainfall during the twentieth century. Geophysical Research Letters 34.

Neumaier, A., and T. Schneider. 2001. Estimation of parameters and eigenmodes of multivariate autoregressive models. Acm Transactions on Mathematical Software 27:27-57.

Neuman, Y., O. Nave, and E. Dolev. 2010. Buzzwords on their way to a tipping-point: A view from the blogosphere. Complexity 16(4):58-68.

Noy-Meir, I. 1975. Stability of grazing systems an application of predator prey graphs. Journal of Ecology 63:459-482.

Okubo, A. 1980. Diffusion and ecological problems: mathematical models: Biomathematics, v. 10. Berlin, Springer Verlag.

Ovaskainen, O., and I. Hanski. 2002. Transient dynamics in metapopulation response to perturbation. Theoretical Population Biology 61:285-295.

Ovaskainen, O., K. Sato, J. Bascompte, and I. Hanski. 2002. Metapopulation models for extinction threshold in spatially correlated landscapes. Journal of Theoretical Biology 215:95-108.

Pascual, M., and F. Guichard. 2005. Criticality and disturbance in spatial ecological systems. Trends in Ecology & Evolution 20:88-95.

Peterson, G. D. 2002. Contagious disturbance, ecological memory, and the emergence of landscape pattern. Ecosystems 5:329-338.

Petit, J. R., J. Jouzel, D. Raynaud, N. I. Barkov, J. M. Barnola, I. Basile, M. Bender, J. Chappellaz, M. Davis, G. Delaygue, M. Delmotte, V. M. Kotlyakov, M. Legrand, V. Y. Lipenkov, C. Lorius, L. Pepin, C. Ritz, E. Saltzman, M. Stievenard. 1999. Climate and atmospheric history of the past 420,000 years from the Vostok ice core, Antarctica. Nature 399:429-436.

Petoukhov, V., A. V. Eliseev, R. Klein, and H. Oesterle. 2008. On statistics of the free-troposphere synoptic component: an evaluation of skewnesses and mixed third-order moments contribution to the synoptic-scale dynamics and fluxes of heat and humidity. Tellus Series a-Dynamic Meteorology and Oceanography 60:11-31.

Petoukhov, V., A. Ganopolski, V. Brovkin, M. Claussen, A. Eliseev, C. Kubatzki, and S. Rahmstorf. 2000. CLIMBER-2: a climate system model of intermediate complexity. Part I: model description and performance for present climate. Climate Dynamics 16:1-17.

Petraitis, P. S., and S. R. Dudgeon. 1999. Experimental evidence for the origin of alternative communities on rocky intertidal shores. Oikos 84:239-245.

Pimm, S. L. 1984. The Complexity and Stability of Ecosystems. Nature 307:321-326.

Pimm, S. L., and J. H. Lawton. 1977. Number of Trophic Levels in Ecological Communities. Nature 268:329-331.

Rahmstorf, S. 1996. Bifurcations of the Atlantic thermohaline circulation in response to changes in the hydrological cycle. Nature 379:847-847.

Rahmstorf, S. 2002. Ocean circulation and climate during the past 120,000 years. Nature 419:207-214.

Ramos, O. 2010. Criticality in earthquakes. Good or bad for prediction? Tectonophysics 485:321-326.

Reynolds, J. F., D. M. S. Smith, E. F. Lambin, B. L. Turner, M. Mortimore, S. P. J. Batterbury, T. E. Downing et al. 2007. Global desertification: Building a science for dryland development. Science 316:847-851.

Rial, J. A., R. A. Pielke, M. Beniston, M. Claussen, J. Canadell, P. Cox, H. Held et al. 2004. Nonlinearities, feedbacks and critical thresholds within the earth's climate system. Climatic Change 65:11-38.

Rietkerk, M., M. C. Boerlijst, F. van Langevelde, R. HilleRisLambers, J. van de Koppel, L. Kumar, H. H. T. Prins et al. 2002. Self-organization of vegetation in arid ecosystems. American Naturalist 160:524-530.

Rietkerk, M., S. C. Dekker, P. C. de Ruiter, and J. van de Koppel. 2004. Self-organized patchiness and catastrophic shifts in ecosystems. Science 305:1926-1929.

Rinaldi, S., and M. Scheffer. 2000. Geometric analysis of ecological models with slow and fast processes. Ecosystems 3:507-521.

Ripa, J., and M. Heino. 1999. Linear analysis solves two puzzles in population dynamics: the route to extinction and extinction in coloured environments. Ecology Letters 2:219-222.

Rockström, J., W. Steffen, K. Noone, Ö. Persson, F. S. Chapin, E. F. Lambin, T. M. Lenton et al. 2009. A safe operating space for humanity. Nature 461:472-475.

Scheffer, M. 1998. Ecology of Shallow Lakes: Population and Community Biology. London, Chapman and Hall.

Scheffer, M. 1999. Searching explanations of nature in the mirror world of math. Conservation Ecology 3.

Scheffer, M. 2009. Critical Transitions in Nature and Society: Princeton Studies in Complexity. Princeton, New Jersey, Princeton University Press.

Scheffer, M., J. Bascompte, W. A. Brock, V. Brovkin, S. R. Carpenter, V. Dakos, H. Held E. H. van Nes, M. Rietkerk, G. Sugihara. 2009. Early-warning signals for critical transitions. Nature 461:53-59.

Scheffer, M., S. Carpenter, J. A. Foley, C. Folke, and B. Walker. 2001. Catastrophic shifts in ecosystems. Nature 413:591-596.

Scheffer, M., and S. R. Carpenter. 2003. Catastrophic regime shifts in ecosystems: linking theory to observation. Trends in Ecology & Evolution 18:648-656.

Scheffer, M., S. H. Hosper, M. L. Meijer, B. Moss, and E. Jeppesen. 1993. Alternative equilibria in shallow lakes. Trends in Ecology and Evolution 8:275-279.

Scheffer, M., and E. H. van Nes. 2007. Shallow lakes theory revisited: various alternative regimes driven by climate, nutrients, depth and lake size. Hydrobiologia 584:455-466.

Scheffer, M., F. Westley, and W. Brock. 2003. Slow response of societies to new problems: Causes and costs. Ecosystems 6:493-502.

Schmitz, O. J., E. L. Kalies, and M. G. Booth. 2006. Alternative dynamic regimes and trophic control of plant succession. Ecosystems 9:659-672.

Schneider, T., and A. Neumaier. 2001. Algorithm 808: ARfit - A matlab package for the estimation of parameters and eigenmodes of multivariate autoregressive models. Acm Transactions on Mathematical Software 27:58-65.

Scholz, J. P., J. A. S. Kelso, and G. Schöner. 1987. Nonequilibrium phase transitions in coordinated biological motion: Critical slowing down and switching time. Physics Letters A 123:390-394.

Schreiber, T., and A. Schmitz. 1996. Improved surrogate data for nonlinearity tests. Physical Review Letters 77:635.

Schreiber, T., and A. Schmitz. 2000. Surrogate time-series. Physica D: Nonlinear Phenomena 142:346-382.

Schroder, A., L. Persson, and A. M. De Roos. 2005. Direct experimental evidence for alternative stable states: a review. Oikos 110:3-19.

Schroeder, M. 1991. Fractals, Chaos, Power Laws: Minutes from an Infinite Paradise, Freeman.

Shnerb, N. M., P. Sarah, H. Lavee, and S. Solomon. 2003. Reactive Glass and Vegetation Patterns. Physical Review Letters 90:038101.

Sokal, R. R., and F. J. Rohlf. 1995. Biometry: the principles and practice of statistics in biological research. New York, W.H. Freeman & Co.

Solé, R. V., and J. Bascompte. 2006. Self-organization in Complex Ecosystems: Monographs in Population Biology, v. 42.

Solé, R. V., S. C. Manrubia, B. Luque, J. Delgado, and J. Bascompte. 1996. Phase transitions and complex systems. Complexity 1:13-26.

Stanley, E. 1971. Introduction to Phase Transitions and Critical Phenomena. Oxford, Clarendon Press.

Stocker, T. F., D. G. Wright, and L. A. Mysak. 1992. A zonally averaged, coupled ocean atmosphere model for paleoclimate studies. Journal of Climate 5:773-797.

SRC, Stockholm Resilience Center. Regime Shifts DataBase: Large persistent changes in ecosystem services. (www.regimeshifts.org)

Stommel, H. 1961. Thermohaline convection with two stable regimes of flow. Tellus 13:224-230.

Strogatz, S. H. 1994. Nonlinear Dynamics and Chaos with Applications to Physics, Biology, Chemistry and Engineering, Perseus Books.

Sutherland, J. P. 1974. Multiple stable points in natural communities. American Naturalist 108:859-873.

Takimoto, G. 2009. Early warning signals of demographic regime shifts in invading populations. Population Ecology 51:419-426.

Theiler, J., S. Eubank, A. Longtin, B. Galdrikian, and J. D. Farmer. 1992. Testing for Nonlinearity in Time-Series - the Method of Surrogate Data. Physica D 58:77-94.

Thom, R. 1994. Structural Stability and Morphogenesis, Perseus Books.

Thompson, J. M. T. S., H. B. Stewart. 2002. Nonlinear Dynamics and Chaos. Chichester, UK, Wiley.

Tredicce, J. R., G. L. Lippi, P. Mandel, B. Charasse, A. Chevalier, and B. Picque. 2004. Critical slowing down at a bifurcation. American Journal of Physics 72:799-809.

Tripati, A., J. Backman, H. Elderfield, and P. Ferretti. 2005. Eocene bipolar glaciation associated with global carbon cycle changes. Nature 436:341-346.

Tsonis, A. A., K. Swanson, and S. Kravtsov. 2007. A new dynamical mechanism for major climate shifts. Geophysical Research Letters 34.

Turing, A. M. 1952. The chemical basis of morphogenesis. Philosophical Transactions of the Royal Society of London Series B-Biological Sciences 237:37-72.

van Baalen, M. 2000. Pair approximation for different spatial geometries *In* U. Diekmann, Law, R., and Metz, J. A. J. T., ed. The Geometry of Ecological Interactions. Simplifying Spatial Complexity. Cambridge, Cambridge University Press.

van de Koppel, J., and C. M. Crain. 2006. Scale-dependent inhibition drives regular tussock spacing in a freshwater marsh. American Naturalist 168:E136-147.

van de Koppel, J., M. Rietkerk, N. Dankers, and P. M. Herman. 2005. Scale-dependent feedback and regular spatial patterns in young mussel beds. American Naturalist 165:E66-E77.

van Nes, E. H., and M. Scheffer. 2003. Alternative attractors may boost uncertainty and sensitivity in ecological models. Ecological Modelling 159:117-124.

van Nes, E. H., and M. Scheffer. 2005. Implications of spatial heterogeneity for regime shifts in ecosystems. Ecology 86:1797–1807.

van Nes, E. H., and M. Scheffer. 2007. Slow recovery from perturbations as a generic indicator of a nearby catastrophic shift. American Naturalist 169:738-747.

Vandermeer, J., L. Stone, and B. Blasius. 2001. Categories of chaos and fractal basin boundaries in forced predator-prey models. Chaos Solitons & Fractals 12:265-276.

Vandermeer, J., and P. Yodzis. 1999. Basin boundary collision as a model of discontinuous change in ecosystems. Ecology 80:1817-1827.

Venegas, J. G., T. Winkler, G. Musch, M. F. V. Melo, D. Layfield, N. Tgavalekos, A. J. Fischman et al. 2005. Self-organized patchiness in asthma as a prelude to catastrophic shifts. Nature 434:777-782.

von Hardenberg, J., E. Meron, M. Shachak, and Y. Zarmi. 2001. Diversity of vegetation patterns and desertification. Physical Review Letters 8719:Art. No. 198101.

Walker, B., and D. Salt. 2006. Resilience Thinking: Sustaining Ecosystems and People in a Changing World, Island Press.

Whaley, R. E. 1993. Derivatives on market volatility: hedging tools long overdue. Journal of Derivatives 1:71-84.

Wissel, C. 1984. A universal law of the characteristic return time near thresholds. Oecologia 65:101-107.

Woodwell, J. C. 1998. A simulation model to illustrate feedbacks among resource consumption, production, and factors of production in ecological-economic systems. Ecological Modelling 112:227-247.

Zahler, R. S., and H. J. Sussmann. 1977. Claims and accomplishments of applied catastrophe theory. Nature 269:759-763

Glossary

Alternative stable states	Different (multiple) states (equilibria) of a system under the same external conditions. The state to which a system converges is path-dependent.
Attractor	The dynamic regime to which a system converges after some time. Examples of attractors: point, cyclic (periodic), quasiperiodic, chaotic
Basin of attraction	Set of initial conditions that lead to a particular state (equilibrium).
Bifurcation	A critical threshold in conditions at which the qualitative behavior of a system changes.
Bistability	The case where two alternative stable states exist.
Catastrophic bifurcation	Bifurcation where the current state of a system disappears and the system is forced to move to an alternative state.
Catastrophic shift	An abrupt shift in the state of a system induced by a small perturbation that pushes the system across the border of the basin of attraction.
Critical transition	Abrupt shift in the behavior of a system when certain parameters reach a threshold. Most pronounced example is a catastrophic bifurcation.
Critical slowing down	The phenomenon that the return time of a disturbance back to equilibrium increases close to a bifurcation.
Eigenvalue (dominant)	Maximum factor that expresses how much linearized deviations from equilibrium diverge in time. It approximates the recovery rate back to equilibrium after a perturbation.
Equilibrium	The condition at which competing processes are balanced. At a stable equilibrium, a system returns to it upon a small perturbation. At an unstable equilibrium, a system moves away from it upon a small perturbation.

Fold bifurcation	The threshold (in a parameter) at which a stable and an unstable equilibrium collide. It marks the disappearance of both equilibria.
Hysteresis	As conditions are changing in a bistable system, the system remains on the same state until a catastrophic bifurcation is reached at which it shifts to the alternative state. If conditions are changed in the opposite direction, the system jumps back to the original state only until it meets another catastrophic bifurcation. The distance (in parameter space) between the two catastrophic bifurcations defines the size of the hysteresis. The bigger the size, the more difficult for a catastrophic shift to be reversed.
Leading indicators (for critical transitions)	Divergence of the statistical properties in the pattern of fluctuations of a system close to a critical transition.
Positive feedback	A process through which something has a positive effect on itself.
Regime shift	A sharp change from one regime (state) to a contrasting one. A regime is a dynamic 'state' of a system: it can be a stable point or a cycle.
Resilience (ecological)	The magnitude of disturbance a system can tolerate before it shifts into a different state.
Self-organized patterns	Patterns in space that emerge from the interaction between many units.
Transition	*Discontinuous (first-order)*: Abrupt change in the qualitative behavior of a system. *Continuous (second-order)*: Smooth change in the qualitative behavior of a system. *Noise-induced*: Change in the qualitative behavior of a system in the presence of high noise intensity.
Threshold	A point where the system is very sensitive to changing conditions.
Tipping point	A point where the system may flip to another state.

Summary

Complex systems ranging from ecosystems to financial markets and the climate may have tipping points where a sudden shift to a contrasting regime can occur. As such critical transitions can have dire consequences, being able to predict them is very important. However, predicting critical points is extremely difficult. This thesis explores the idea that generic early-warning signals may allow us to estimate the risk of an approaching critical transition for a wide class of systems even if we lack mechanistic understanding of their functioning.

Work in different disciplines suggests that there are indicators that can be used to signal the risk of an upcoming catastrophic shift (**Chapter 2**). Most of these indicators are considered generic because they are related to critical slowing down: the universal phenomenon of decreasing return rate to equilibrium in the vicinity of critical (bifurcation) points. Due to critical slowing down, recovery time, autocorrelation, variance, and low frequencies, may all increase as a system moves slowly towards a critical transition. Additionally, other more system-specific indicators exist. Skewness can increase due to the asymmetry of the system's basin of attraction; self-organized spatial patterns can change in characteristic ways; and the size distribution of spatial patches can change, if a system approaches a transition. Examples of all of these leading indicators have been found in cases ranging from ecosystems and the climate to the human physiology.

A common handicap in the identification of leading indicators in time-series is that lag times for detection are typically long. The consequence is that reaction time can be insufficient to prevent a shift. In **Chapter 3** we show that increased spatial correlation may serve as a powerful early-warning signal in systems consisting of many coupled units. We demonstrate that the interaction of critical slowing down with diffusion causes spatial correlation to increase as the system approaches a systemic transition. We further explored the idea of using spatial correlation as an early-warning indicator in three spatially-explicit ecosystem models with alternative attractors. The analysis revealed that as a control parameter slowly pushes the system towards the threshold, spatial correlation between neighboring units in a modular system tends to increase well before the transition. We also showed that such an increase in spatial correlation represents a better early-warning signal than indicators derived from time-series provided that there is sufficient spatial heterogeneity and connectivity in the system.

In **Chapter 4** we explore the robustness of the two most studied early-warning indicators for time-series: autocorrelation and variance. We found both analytically and in simulations that variance may sometimes decrease rather than increase close to a transition. This can happen when the system becomes less sensitive to environmental fluctuations near the threshold, or when critical slowing down reduces the system's capacity to follow high frequency fluctuations in the environment. In addition, variance can become systematically underestimated close to a transition due to the prevalence of

low frequencies that cannot be picked up correctly in the limited length of the time-series that tend to be available for such analyses. By contrast, we found autocorrelation to be a robust indicator, in the sense that it always increased towards critical transitions. Our analytical approach reveals how this difference in robustness between variance and autocorrelation can be understood.

While autocorrelation appears to be a robust indicator for critical transitions, there are still transitions and systems where the supposedly generic leading indicators have not yet been tested. **Chapter 5** is the first study that brings together all generic and system-specific indicators both in time and space in order to test their feasibility in announcing upcoming transitions. We explored this idea in arid ecosystem models, where vegetation may collapse to desert due to increasing water limitation. In particular, we used three models that describe desertification, but differ in the spatial vegetation patterns they produce. Strikingly, we found that in all models post-perturbation recovery time increased before vegetation collapsed. However, in one of the models slowing down failed to translate into rising variance and correlation. This occurred in the model where regular self-organized vegetation patterns were present. This finding implies an important limitation to the use of variance and correlation as indicators for critical transitions. However, changes in such self-organized patterns themselves are a reliable indicator of an upcoming transition. Our results illustrate that while slowing down may be a universal phenomenon at critical transitions, its detection through indirect indicators may be problematic in particular systems.

Chapter 6 puts theory into practice for the case of ancient abrupt climate shifts. In the Earth's history, periods of relatively stable climate have often been interrupted by sharp transitions to a contrasting state. These abrupt climate shifts may correspond to critical transitions at tipping points. However, this is hard to prove for events in the remote past. We analyzed eight ancient climate shifts and showed that they were all preceded by an increase in autocorrelation indicating slowing down starting well before the actual shift. These results constitute the first independent empirical evidence for the idea that past abrupt shifts were associated to the passing of critical thresholds.

In the **Afterthoughts** I conclude that since critical slowing down is a fundamental feature of a broad class of bifurcations, various indicators of slowing down can potentially be used as generic early-warning signals for upcoming catastrophic shifts. In addition, other more system-specific signals exist. None of these signals can predict when a transition is going to occur, or whether the upcoming transition will be catastrophic. Rather, the indicators should be seen as tools for probing the resilience of a system. As loss of resilience can pave the way for surprising transitions, the indicators discussed in this thesis offer a new perspective to foresee when we should expect the Unexpected.

Samenvatting

Complexe systemen zoals ecosystemen, de financiële markt en het klimaat, kunnen kantelpunten hebben, waarbij er plotseling een overgang naar een contrasterende toestand kan optreden. Omdat zulke bifurcatiepunten mogelijk ernstige gevolgen kunnen hebben, is het wenselijk om ze te kunnen voorspellen. Een dergelijke voorspelling is echter buitengewoon moeilijk. Dit proefschrift onderzoekt of er generieke waarschuwingssignalen bestaan, die ons in staat kunnen stellen om het risico van naderende bifurcatie te voorspellen, zelfs als we het precieze mechanisme niet kennen.

Onderzoek in verschillende disciplines suggereert, dat er indicators bestaan die kunnen worden gebruikt om het risico op een catastrofische bifurcatie in te schatten (**Hoofdstuk 2**). De meeste van deze signalen worden als generiek beschouwd, omdat ze zijn gerelateerd aan ”critical slowing down”. Dit is een universeel fenomeen, dat optreedt in de buurt van bifurcatiepunten, waarbij de systemen na verstoring vertraagd terugkeren naar hun evenwicht. Normaliter zal, naarmate een systeem langzaam naar een bifurcatie beweegt, de hersteltijd na een verstoring, de autocorrelatie, de variantie en de lage frequenties in het signaal toenemen door critical slowing down. Bovendien bestaan er ook andere, meer systeemspecifieke indicatoren. Bijvoorbeeld wanneer een systeem een bifurcatiepunt nadert, kan een asymmetrische verdeling van de toestandsvariabele ontstaan, die veroorzaakt wordt door een toenemend asymmetrisch aantrekkingsgebied, (“basin of attraction”), In andere systemen met ruimtelijke zelfgeorganiseerde patronen. kunnen die patronen op een karakteristieke wijze veranderen. Voorbeelden van zulke indicatoren zijn aangetroffen in systemen variërend van ecosystemen, het klimaat tot menselijke fysiologie.

Een algemeen probleem met het bepalen van indicatoren voor bifurcaties met behulp van tijdreeksen, is dat er relatief veel data nodig is om de indicatoren met voldoende nauwkeurigheid te bepalen. Als gevolg hiervan kan de tijd om de omslag te voorkomen onvoldoende zijn. In **Hoofdstuk 3** laten we zien dat toenemende ruimtelijke correlatie kan dienen als krachtig en vroegtijdig waarschuwingssignaal voor bifurcaties in systemen die ruimtelijk gekoppeld zijn door uitwisseling. We laten theoretisch zien, dat de ruimtelijke correlatie toeneemt, als het systeem een bifurcatie benadert. Dit gebeurt door de interactie tussen critical slowing down en diffusie. Vervolgens hebben we in drie ruimtelijk expliciete ecologische modellen (met alternatieve evenwichten) onderzocht of ruimtelijke correlatie ook in de praktijk als waarschuwingssignaal bruikbaar zou kunnen zijn. De analyse toont aan, dat wanneer de verandering van een parameter het systeem langzaam naar een bifurcatie brengt, de ruimtelijke correlatie tussen naburige punten reeds ver vóór het omslagpunt de neiging heeft toe te nemen. Ook laen we zien, dat een dergelijke toename in ruimtelijke correlatie beter werkt dan indicatoren die van tijdreeksen afgeleid zijn (maar alleen als voldoende ruimtelijke heterogeniteit en connectiviteit is).

In **Hoofdstuk 4** onderzoeken we de robuustheid van de twee meest bestudeerde waarschuwingsindicatoren voor tijdreeksen: autocorrelatie en variantie. We tonen zowel analytisch als door simulaties aan, dat variantie soms kan afnemen in plaats van toenemen dichtbij een bifurcatie. Dit kan gebeuren al het systeem dichtbij de bifurcatie minder gevoelig wordt voor beïnvloeding in de omgeving, of wanneer critical slowing down de capaciteit van het systeem om te reageren op snelle (i.e. hoogfrequente) verstoringen vermindert. Daarnaast kan de variantie dichtbij een omslagpunt systematisch worden onderschat, door de lage frequenties die daar veel voorkomen. Deze lage frequenties kunnen dan niet goed worden opgepikt in de beperkte lengte van de tijdreeksen die over het algemeen beschikbaar zijn voor dergelijke analyses. Daarentegen bleek autocorrelatie een robuuste indicator, omdat die altijd toenam in de richting van een omslagpunt. We laten in een analytische benadering zien hoe dit verschil in robuustheid tussen variantie en autocorrelatie kan worden verklaard.

Alhoewel autocorrelatie een robuuste indicator voor bifurcatiepunten lijkt te zijn, zijn de waarschuwingsindicatoren nog niet getest voor alle overgangen en systemen. **Hoofdstuk 5** is de eerste studie die alle universele en systeemspecifieke indicatoren voor zowel ruimtelijke als temporele systemen bij elkaar brengt, en hun bruikbaarheid voor het voorspellen van kritische overgangen test. Hiervoor hebben we drie modellen van aride ecosystemen gebruikt, waarin bij toenemend watertekort vegetatie wordt verdrongen door woestijn. De modellen beschrijven alle drie woestijnvorming, maar verschillen in de ruimtelijke vegetatiepatronen die ze produceren. Opvallend was dat bij alle modellen de hersteltijd van de vegetatie na een verstoring langer werd bij toenemende watertekorten en dreigende instorting van de vegetatie. Echter, in één model werd deze vertraging niet vertaald in toenemende variantie en correlatie, namelijk in het model met regelmatige vegetatiepatronen. Dit is een belangrijke beperking voor de toepasbaarheid van variantie en correlatie als indicatoren voor een omslag. Gelukkig zijn veranderingen in de patronen zelf al een goede indicator voor een op handen zijnde omslag. Onze resultaten illustreren dat hoewel critical slowing down een universeel fenomeen is bij bifurcaties, de detectie ervan door middel van indirecte indicatoren in sommige systemen problematisch kan zijn.

Hoofdstuk 6 brengt de theorie in praktijk voor de casus van abrupte omslagen in het paleoklimaat. In de geologische geschiedenis van de aarde worden perioden met een relatief stabiel klimaat onderbroken door scherpe overgangen. Deze abrupte overgangen kunnen door bifurcaties veroorzaakt zijn. Echter, dit is natuurlijk moeilijk te bewijzen voor gebeurtenissen in het verre verleden. We hebben acht historische klimaatveranderingen geanalyseerd, en aangetoond dat ze alle werden voorafgegaan door toename autocorrelatie in het signaal. Dit wijst op het optreden van kritische vertraging, ver vóór het optreden van de daadwerkelijke omslag. Deze resultaten vormen de eerste onafhankelijke empirische aanwijzijng voor de stelling dat abrupte veranderingen van het paleoklimaat verband houden met het passeren van bifurcatiepunten.

In de **Nabeschouwingen** (**Afterthoughts**) concludeer ik dat diverse indicatoren van vertraging in het herstel van verstoringen potentieel kunnen worden gebruikt als generieke waarschuwingssignalen voor op handen zijnde catastrofische omslagen. Dit is te verwachten omdat critical slowing down een fundamenteel kenmerk is bij verschillende

soorten bifurcaties. Bovendien bestaan er ook andere, meer systeemspecifieke signalen. Echter, geen van de signalen kan voorspellen wanneer een overgang daadwerkelijk zal plaatsvinden, of dat de komende bifurcatie een kritisch omslagpunt zal zijn. De indicatoren zouden veeleer als gereedschap voor het onderzoeken van de veerkracht van een systeem moeten worden gezien. Een afname van de veerkracht van een systeem kan de kans op verrassende kantelpunten vergroten. De indicatoren die in dit proefschrift worden besproken, bieden een nieuw perspectief om te voorzien wanneer we het onverwachte zouden kunnen verwachten.

Περίληψη

Πολύπλοκα συστήματα, όπως οικοσυστήματα, χρηματοπιστωτικές αγορές, ή ακόμη και το ίδιο το κλίμα, μερικές φορές πλησιάζουν σε κάποιο κρίσιμο όριο στο οποίο μπορεί να συμβεί μια ξαφνική μετάπτωση από την τρέχουσα κατάσταση προς ένα διαμετρικά αντίθετο καθεστώς. Καθώς τέτοιες μεταπτώσεις μπορεί να έχουν ολέθριες συνέπειες, είναι πολύ σημαντική η δυνατότητα να τις προβλέψουμε. Ωστόσο, η πρόβλεψη τέτοιων μεταπτώσεων είναι εξαιρετικά δύσκολη. Η παρούσα διατριβή εξετάζει το κατά πόσο θα μπορούσαμε να αναπτύξουμε γενικά σήματα έγκαιρης προειδοποίησης, τα οποία θα μας επέτρεπαν να υπολογίσουμε το ενδεχόμενο μιας επερχόμενης "κρίσιμης" μετάπτωσης για μια ευρεία κατηγορία συστημάτων, ακόμη και όταν οι λεπτομέρειες της λειτουργίας τους δε μας είναι πλήρως κατανοητές.

Μελέτες από διάφορους επιστημονικούς κλάδους υποστηρίζουν την ύπαρξη δεικτών έγκαιρης προειδοποίησης (early-warning signals) που μπορούν να χρησιμοποιηθούν για να επισημάνουν το ενδεχόμενο μιας επερχόμενης καταστροφικής "κρίσιμης" μετάπτωσης (critical transition) (**Κεφάλαιο 2**). Οι περισσότεροι από αυτούς τους δείκτες θεωρούνται *γενικοί*, επειδή σχετίζονται με την επονομαζόμενη "κρίσιμη επιβράδυνση" (critical slowing down), δηλαδή το καθολικό φαινόμενο της μείωσης του ρυθμού αποκατάστασης ισορροπίας πριν από μία μαθηματική διακλάδωση (bifurcation point). Εξαιτίας της κρίσιμης επιβράδυνσης, ο χρόνος αποκατάστασης (return time), η αυτοσυσχέτιση (autocorrelation), η διακύμανση (variance), και οι χαμηλές συχνότητες (low spectral density), συνήθως αυξάνονται, καθώς το σύστημα πλησιάζει σταδιακά προς το κρίσιμο σημείο μίας απροσδόκητης καταστροφικής μετάπτωσης. Εκτός από τους γενικούς δείκτες, υπάρχουν άλλοι, περισσότερο *ειδικοί* δείκτες. Επειδή η συμμετρία της λεκάνης ισορροπίας στην οποία βρίσκεται ένα σύστημα μεταβάλλεται, καθώς ένα σύστημα πλησιάζει μία επικείμενη κρίσιμη μετάπτωση, η κατανομή της μεταβλητής που περιγράφει την τρέχουσα κατάσταση του συστήματος μπορεί να γίνει ασύμμετρη. Για ένα σύστημα που κατανέμεται στο χώρο με συγκεριμένο είδος μοτίβων, το σχήμα των μοτίβων μπορεί να αλλάξει με συγκεκριμένο τρόπο, εφόσον το σύστημα πλησιάζει προς μια επικείμενη κρίσιμη μετάπτωση. Κατά ανάλογο τρόπο, και η κατανομή του μεγέθους των μοτίβων μπορεί να μεταβληθεί. Παραδείγματα όλων αυτών των δεικτών έγκαιρης προειδοποίησης έχουν παρατηρηθεί σε οικολογικά συστήματα και το κλίμα, καθώς και στην ανθρώπινη φυσιολογία.

Ένα κοινό μειονέκτημα του προσδιορισμού των δεικτών έγκαιρης προειδοποίησης σε χρονοσειρές είναι η μεγάλη διάρκεια που απαιτείται για την ανίχνευσή τους. Ως αποτέλεσμα, ο διαθέσιμος χρόνος αντίδρασης για την αποτροπή μιας κρίσιμης μετάβασης μπορεί να είναι ανεπαρκής. Στο **Κεφάλαιο 3** δείξαμε πως η αύξηση της συσχέτισης μεταξύ γειτονικών μονάδων στο χώρο μπορεί να χρησιμεύσει ως ένα ισχυρό σήμα έγκαιρης προειδοποίησης σε συστήματα που αποτελούνται από πολλές συζευγμένες μονάδες στο χώρο. Αποδείξαμε ότι η αλληλεπίδραση μεταξύ της "κρίσιμης επιβράδυνσης" και του φαινομένου της διάχυσης έχει ως αποτέλεσμα την αύξηση της

συσχέτισης στο χώρο, καθώς το όλο σύστημα προσεγγίζει μια κρίσιμη μετάπτωση. Περαιτέρω, διερευνήσαμε τη χρήση της χωρικής συσχέτισης ως δείκτη έγκαιρης προειδοποίησης σε τρία μοντέλα οικοσυστημάτων με εναλλακτικά σημεία ισορροπίας. Η ανάλυση έδειξε ότι, καθώς μία παράμετρος "σπρώχνει" σιγά σιγά το σύστημα προς το κρίσιμο σημείο μετάπτωσης, η συσχέτιση μεταξύ γειτονικών μονάδων στο χώρο αυξάνεται πολύ πριν από τη μετάπτωση. Δείξαμε επίσης ότι μια τέτοια αύξηση της συσχέτισης στο χώρο αποτελεί καλύτερο σήμα έγκαιρης προειδοποίησης σε σχέση με άλλους δείκτες που προέρχονται απευθείας από την χρονοσειρά, με την προϋπόθεση ότι η χωρική ετερογένεια και σύζευξη στο σύστημα είναι επαρκής.

Στο **Κεφάλαιο 4** μελετήσαμε την αξιοπιστία των δύο πιο διαδεδομένων δεικτών έγκαιρης προειδοποίησης για χρονοσειρές: την αυτοσυσχέτιση και τη διακύμανση. Βρήκαμε, τόσο με αναλυτικές μεθόδους όσο και με προσομοιώσεις, ότι η διακύμανση μπορεί μερικές φορές να μειωθεί αντί να αυξηθεί πριν από μία κρίσιμη μετάπτωση. Αυτό μπορεί να συμβεί όταν το σύστημα γίνεται λιγότερο ευαίσθητο στις διακυμάνσεις του περιβάλλοντος κοντά στο κρίσιμο σημείο μετάπτωσης, ή όταν, λόγω της κρίσιμης επιβράδυνσης, μειώνεται η ικανότητα του συστήματος να ακολουθήσει διαταραχές υψηλής συχνότητας στο περιβάλλον. Επιπλέον, η διακύμανση μπορεί να υποτιμηθεί συστηματικά πριν από μία κρίσιμη μετάπτωση λόγω της επικράτησης χαμηλών συχνοτήτων που δεν μπορούν να εντοπιστούν σωστά στο περιορισμένο μήκος χρονοσειρών που συνήθως είναι διαθέσιμες για τέτοιου είδους αναλύσεις. Αντιθέτως, βρήκαμε πως η αυτοσυσχέτιση είναι αξιόπιστος δείκτης έγκαιρης προειδοποίησης, με την έννοια ότι πάντοτε αυξάνει πριν από μία κρίσιμη μετάπτωση. Η αναλυτική μας προσέγγιση επιτρέπει να κατανοήσουμε τις συνθήκες υπό τις οποίες προκύπτει αυτή η διαφορά στην αξιοπιστία μεταξύ διακύμανσης και αυτοσυσχέτισης.

Παρόλο που η αυτοσυσχέτιση φαίνεται να είναι αξιόπιστος δείκτης έγκαιρης προειδοποίησης για κρίσιμες μεταπτώσεις, εξακολουθούν να υπάρχουν μεταπτώσεις στις οποίες δεν έχουν δοκιμαστεί ακόμη οι *γενικοί* δείκτες έγκαιρης προειδοποίησης. Το **Κεφάλαιο 5** είναι η πρώτη μελέτη που συγκεντρώνει όλους τους *γενικούς* και *ειδικούς* δείκτες τόσο σε χώρο- όσο και χρόνο- σειρές, προκειμένου να αξιολογηθεί η αποτελεσματικότητα τους ως προάγγελλοι επερχόμενων μεταπτώσεων. Διερευνήσαμε αυτήν την ιδέα σε μοντέλα χερσαίων άνυδρων οικοσυστημάτων, όπου η βλάστηση μπορεί να καταρρεύσει λόγω περιορισμένων υδατικών πόρων. Πιο συγκεκριμένα, χρησιμοποιήσαμε τρία μοντέλα ερημοποίησης, τα οποία διέφεραν ως προς το είδος των χωρικών προτύπων βλάστησης που παράγουν. Βρήκαμε ότι, σε όλα τα μοντέλα, ο χρόνος αποκατάστασης ισορροπίας μετά από μία διαταραχή αυξήθηκε, πριν καταρρεύσει η βλάστηση. Ωστόσο, σε ένα από τα μοντέλα η κρίσιμη επιβράδυνση απέτυχε να μεταφραστεί σε αύξηση της διακύμανσης και της αυτοσυσχέτισης. Αυτό συνέβη στο μοντέλο όπου η βλάστηση αυτο-οργανώνεται σε συμμετρικά πρότυπα στο χώρο. Το εύρημα αυτό υποδηλώνει ένα σημαντικό περιορισμό στη χρήση της διακύμανσης και της αυτοσυσχέτισης ως δείκτες για κρίσιμες μεταπτώσεις. Ωστόσο, αλλαγές στο σχήμα των προτύπων στο χώρο αποτελούν από μόνα τους αξιόπιστο δείκτη για μια επερχόμενη μετάπτωση. Τα αποτελέσματά μας δείχνουν ότι ενώ η κρίσιμη επιβράδυνση μπορεί να είναι καθολικό φαινόμενο πριν από κρίσιμες μεταπτώσεις, ο εντοπισμός της μέσω έμμεσων δεικτών μπορεί να είναι προβληματικός σε ορισμένα συστήματα.

Το **Κεφάλαιο 6** επιχειρεί να εφαρμόσει τη θεωρία στην πράξη στην περίπτωση κάποιων απότομων παλαιοκλιματικών αλλαγών. Στην ιστορία της Γης, διάφορες περίοδοι με σχετικά σταθερό κλίμα συχνά διακόπτονταν από απότομες μεταβάσεις σε αντίθετες συνθήκες. Αυτές οι απότομες αλλαγές του κλίματος ίσως αντιστοιχούν σε κρίσιμες μεταπτώσεις σε κρίσιμα σημεία μαθηματικών διακλαδώσεων. Ωστόσο, αυτό είναι δύσκολο να αποδειχθεί για γεγονότα που έλαβαν χώρα στο μακρινό παρελθόν. Στο κεφάλαιο αυτό, αναλύσαμε οκτώ απότομες παλαιοκλιματικές αλλαγές και βρήκαμε αύξηση αυτοσυσχέτισης σε όλες, γεγονός που υποδηλώνει πως σε όλες τις περιπτώσεις υπήρξε κρίσιμη επιβράδυνση πολύ πριν την μετάπτωση. Τα αποτελέσματα αυτά συνιστούν την πρώτη ανεξάρτητη μελέτη βασισμένη σε εμπειρικά στοιχεία που υποστηρίζει την ιδέα ότι προηγούμενες απότομες κλιματικές αλλαγές ήταν συνδεδεμένες με κρίσιμες μεταπτώσεις.

Στον **Επίλογο** καταλήγω στο συμπέρασμα ότι, δεδομένου ότι η κρίσιμη επιβράδυνση είναι θεμελιώδες χαρακτηριστικό μιας ευρείας κατηγορίας μαθηματικών διακλαδώσεων, οι έμμεσοι δείκτες της επιβράδυνσης μπορούν δυνητικά να χρησιμοποιηθούν ως γενικά σήματα έγκαιρης προειδοποίησης για επερχόμενες καταστροφικές μεταπτώσεις. Υπάρχουν, επίσης, άλλα, περισσότερο ειδικά σήματα. Παρόλα αυτά, κανένα από αυτά τα σήματα δεν μπορεί να προβλέψει το πότε πρόκειται να συμβεί μία μετάπτωση ή το κατά πόσο η επικείμενη μετάπτωση θα είναι καταστροφική. Αντίθετα, οι δείκτες αυτοί είναι απλώς εργαλεία διάγνωσης της ανθεκτικότητας ενός συστήματος. Καθώς η απώλεια ανθεκτικότητας ενός συστήματος μπορεί να οδηγήσει σε απροσδόκητες μεταπτώσεις, οι δείκτες που εξετάζονται στην παρούσα διατριβή προσφέρουν μια νέα προοπτική διάγνωσης του πότε μπορούμε να προσμένουμε το απροσδόκητο.

Acknowledgements

Proposition #8: Flat lands, broad horizons [this country].

September 2004 - June 2011, The Netherlands: 7 years, 3 cities, 7 houses, 5 bikes, 3 languages, 23 housemates, 2 diplomas, lots of bread-and-cheese, plenty of coffee, many good friends, countless memories. Wouldn't you call that a "second" home?

This journey started when I followed a course on the Ecology of Shallow Lakes during the first year of my master's program. It took few weeks for Marten Scheffer to undermine my determination to become a field aquatic ecologist, and for Egbert van Nes to push me out of my basin of attraction. No surprise, I tipped into dynamical systems theory. Fortunately, I had two great people to catch me.

I can't be more grateful to Marten Scheffer for being where I am now and what I am as a scientist. His broad horizons, thinking out-of-the-box, and scientific intuition opened a completely different world for me. Marten taught me how to see the general patterns, how to be rigorous but interesting at the same time, how to work with other people, and how fascinating it is to switch between different fields. Above all Marten, you have been a source of creativity and inspiration. My deepest gratitude for the trust and freedom you have given me all these years.

Egbert van Nes has always been my precious daily supervisor; resourceful, interested and helpful every time I had a problem. I want to thank you, Egbert, for teaching me all I know about how to answer difficult questions using simple approaches. I have learnt a lot from your genuine curiosity and your rigorous approach for finding the answers.

Marten and Egbert, thank you for having me on board on such an interesting and challenging topic, for treating me as a colleague, and above all for your friendship. I truly believe you will never stop being an integral part of my scientific and personal life.

I would also like to acknowledge the Bodossakis Foundation for awarding me a scholarship that enabled me to come for my masters in the Netherlands in the first place.

Luckily, this thesis has been shaped by the input of many people. I had the unique opportunity to work and interact with great scientists who all had an impact on what I did. First of all, Steve Carpenter has been a reference point when it comes to the core of this thesis, but also to the way of approaching science. I am grateful for the time you had for me Steve, when I visited you in the Center of Limnology in Wisconsin. At the same time Buz Brock and Tony Ives introduced me to tricky issues of time-series analyses and shared their skepticism on various issues of my work always in a constructive manner. Jordie Bascompte offered advice for the tough questions and was always willing to help. George

Sugihara broadened my vision on nonlinear techniques and showed me how to read between the lines, when I spent a few months in his lab. Max Rietkerk asked the difficult questions and helped to find the answers. Victor Brovkin, Herman Held, Vladimir Pethoukhov, Raul Donangelo, Hugo Fort, and Paolo D'Odorico all shared their knowledge with me in various papers of this thesis. Sonia Kéfi has been a great friend and colleague with whom I am sure we will keep on working together for a long time.

People usually believe that when working with theory, life can be lonely. Fortunately, this was not the case for me. I had the pleasure to be part of a very lively community in Wageningen. My fellows, Andrea, Andreu, Annelies, Bastiaan, Betania, Carol, Darya, Dirk v. A., Els, Gissell, Ingrid, Jaqui, Jelle, Jeroen, Jochem, Jordie, Kristina, Marina, Mazhar, Mihalis, Nika, Raquel, Remi and Rosalie, all made sure that life among grad students was fun and creative. PhD meetings, theoretical group discussions, scientific events, trips, sharing ideas and having beers were all part of it. Of course, this feeling was nurtured in the friendly atmosphere created by all the colleagues in the Aquatic Ecology Group who I would like to warmly thank for integrating me in their "AEW familie".

This adventure has benefited greatly by lots of interactions with many amazing people. People who, as Buz Holling puts it, are "good on islands". I want to express my gratitude to Brian Walker that revived the Resilience Alliance Young Scholars group, and made it possible for me to become part of a fantastic crowd with whom we share a great deal of ideas. Duan, Terry, Jacopo, Chanda, Mike, Allyson, Tim, Martin, Luisa, Maja, Ciara, thank you all! Thanks to the YSSPers Lise, Goran, Sinisa, and Connie who made the stay in Vienna the summer of 2009 a wonderful experience, together with the help of Arkadii Kryazhimskii, Brian Fath and John Casti who hosted me in the Dynamical Systems group in the International Institute for Applied System Analysis. Also big thanks to the people from the Stockholm Resilience Center, especially to Oonsie, Bea, Victor, Lisen, Orjan, Per, Garry, Thorsten, Ellin, and Albert, for making my visits to the center so productive and pleasant. Likewise, my gratitude to Jef Huisman and his group in the University of Amsterdam- Dedmer, Jolanda, Maaike, Pedro, Verena, and above all my good friend and colleague Elisa- for hosting me for a few months in 2007, and to Sergio Rinaldi for the eye-opening discussions on dynamical system's theory in his house in Nice amidst good food and wine.

The blessing of working in a dynamic international environment is also a curse as people come and go. I definitely do miss my paranymphs: Mascha and Dirk. Not only because you helped me in preparing for this moment- creating, translating, questioning-, but mainly because you have been always there. No need to tell you how important you are for me. I was lucky enough to find good friends in Utrecht, who have made it feel like home all these years. Birka and Joseph, Erik and Anja, Yukina and Willem, Janis and Lena, Vera and Edwin, Juliette and Erik, Sara and Wing, Jos and Lih King, thank you very much for being around. Andries, there is always time for a drink and a spare racket for squash, whenever Oslo feels too cold. Θωμά, I hope we make it once more to sail με τον παππού. Franklin, thanks for the wonderful groovy moments. Milena and Marten, thank you for making me feel part of your family. Sarian and Meri, I will never forget that you caught me when I was falling. Tanja, Stefan, Lea and Janosch, thank you for being my little family in Berlin. Krassi and Luisa, thank you for thinking about me so generously all these years. Γιώργο and

Χριστίνα, my visits to BCN were more than therapy. Γιώργο Α., thank you for being such an honest observer of my life. Κουμπαράκο and family, ευχαριστώ για την εκτίμηση και την αγάπη όλα αυτά τα χρόνια. My friends in Thessaloniki, Mihalis and Pavlina, who have always been there to remind me where I come from. Thumbs up to Skype for helping me keep contact with all my friends who are far away. Αλέξανδρε, stay online! Σταύρο, δε νομίζω πως η απόσταση χωρίζει, καθώς μοιράστηκαμε αυτά τα χρόνια πολύ περισσότερα απ' όσα φανταζόμασταν. Όλγα, Δήμητρα, σας ευχαριστώ για την αγάπη και την συμπαράστασή σας, όποτε σας χρειάστηκα.

Ilka, thank you for making me smile again.

Μαμά, Μπαμπά, δε νομίζω πως χρειάζεται να αναφέρω πως όλα αυτά που κατάφερα δε θα ήταν δυνατά χωρίς τη δική σας υποστήριξη και αγάπη. Αυτό που χρειάζεται μόνο να πω και να ξαναπώ είναι πως σας αγαπώ πολύ και πως μου λείψατε.

This thesis is about expecting the unexpected. Now that I look back at all the tipping points that came across my life all these years, I feel happy that I was never really able to expect the unexpected.

A few words about the author

Vasilis Dakos was born in 1977 in Thessaloniki in Greece. He started studying Physics at Aristotle University of Thessaloniki in 1995, and graduated with a degree in Biology in 2001. For his diploma thesis, he worked on the application of biotic and habitat indices of ecological quality of rivers and streams in Northern Greece under the supervision of Maria Lazaridou. After working for a year on a research project on toxin producing cyanobacteria in the Federal Environmental Agency in Berlin, together with Ingrid Chorus and Jutta Fastner, he moved to the Netherlands to pursue a Master's degree as a fellow of Bodossakis Foundation. In 2006 he received a degree in Hydrology and Water Quality Management with honors from Wageningen University. During his Master's thesis, Vasilis explored the theoretical consequences of seasonality on the dynamics of multispecies communities working together with Egbert H. van Nes. A year later, in 2007, he started his PhD in Theoretical Ecology under the supervision of Marten Scheffer and Egbert van Nes in the Department of Aquatic Ecology in Wageningen University.

Vasilis' research focuses on the emerging topic of early-warning signals for critical transitions in ecological, but not only, systems, as presented in this thesis. He has been collaborating among others with Steve Carpenter, Buz Brock, Tony Ives, Jordi Bascompte, Jef Huisman, George Sugihara, John Casti, Tim Lenton, Terry Hughes, and Max Rietkerk. He has been regularly invited to present his work in various labs, workshops and conferences. Since 2008 he is active member of the Resilience Alliance Young Scholars (RAYS). In 2010, he was a recipient of the Dutch Science Academy grant for participating in IIASA's Young Scientist Summer Program in Vienna. Vasilis' interests lie on coupling resilience science with ecological theory using theoretical approaches and working in an interdisciplinary context.

List of publications

Dakos V., van Nes E. H., D'Odorico P., and Scheffer M. (submitted). How robust are early-warning signals for critical transitions?

Benincà E., **Dakos V.**, van Nes E. H., Huisman J., and Scheffer M. (in revision). Resonance of plankton communities with temperature fluctuations. *American Naturalist*

Biggs D., Biggs R., **Dakos V.**, Schoon M., and Scholes B. (in press). Are we entering an era of concatenated global crises? *Ecology & Society*.

Dakos V., Kéfi S., Rietkerk M., van Nes E. H., and Scheffer M. (in press). Slowing down in spatially patterned systems at the brink of collapse. *American Naturalist*.

Lenton T. M., Livina V. N., **Dakos V.**, van Nes E. H., and Scheffer M. (in press). Early-warning of climate tipping points: comparing methods to limit false alarms. *Philosophical Transactions of the Royal Society A*.

van de Leemput I., Veraart A. J., **Dakos V.**, de Klein J. J. M., Strous M., and Scheffer M. (2011). Predicting microbial nitrogen pathways from basic principles. *Environmental Microbiology and Environmental Microbiology Reports*, doi:10.1111/j.1462-2920.02450.x.

Dakos V., van Nes E. H., Donangelo R., Fort H., and Scheffer M. (2010). Spatial correlation as leading indicator of catastrophic shifts. *Theoretical Ecology*, 3: 163-174.

Donangelo R., Fort H., **Dakos V.**, Scheffer M., and van Nes E. H. (2010). Early warnings of catastrophic shifts in ecosystems: Comparison between spatial and temporal indicators. *International Journal of Bifurcation and Chaos*, 20(2): 315–321.

Scheffer M., Bascompte J., Brock W.A., Brovkin V., Carpenter S.R., **Dakos V.**, Held H., van Nes E.H., Rietkerk M., and Sugihara G. (2009). Early-warning signals for critical transitions. *Nature*, 461: 53-59.

Dakos V., Benincà E., van Nes E.H., Philippart C.J.M., Scheffer M., and Huisman J. (2009). Interannual variability in species composition explained as seasonally entrained chaos. *Proceedings of the Royal Society B: Biological Sciences*, 276: 2871-2880.

Dakos V., Scheffer M., van Nes E. H., Brovkin V., Petoukhov V., and Held H. (2008). Slowing down as an early warning signal for abrupt climate change. *Proceedings of the National Academy of Science USA*, 105(38): 14308-14312.

Chatzinikolaou Y., **Dakos V.**, and Lazaridou-Dimitriadou M. (2008). Assessing the ecological integrity of a transboundary large Mediterranean river. *International Review Hydrology*, 93(1): 73-87.

Chatzinikolaou Y., **Dakos V.**, and Lazaridou-Dimitriadou M. (2006). Longitudinal impacts of anthropogenic pressures on benthic macroinvertebrate assemblages in a large transboundary Mediterranean river during the low flow period. *Acta hydrochimica hydrobiologica*, 34: 453–463.

Lekka E., Kagalou I., Lazaridou-Dimitriadou M., Albanis T., **Dakos V.**, Lambropoulou D., and Sakkas V. (2004). The Assessment of the Water and Habitat Quality of a Mediterranean River (Kalamas, Epirus, Hellas), in Accordance with the EU Water Framework Directive. *Acta hydrochimica hydrobiologica,* 32 (3): 175-188.

Netherlands Research School for the
Socio-Economic and Natural Sciences of the Environment

C E R T I F I C A T E

The Netherlands Research School for the
Socio-Economic and Natural Sciences of the Environment (SENSE),
declares that

Vasileios Dakos

born on 25 May 1977 in Thessaloniki, Greece

has successfully fulfilled all requirements of the
Educational Programme of SENSE.

Wageningen, 1 June 2011

the Chairman of the SENSE board	the SENSE Director of Education
Prof. dr. Rik Leemans	Dr. Ad van Dommelen

The SENSE Research School has been accredited by the Royal Netherlands Academy of Arts and Sciences (KNAW)

KONINKLIJKE NEDERLANDSE
AKADEMIE VAN WETENSCHAPPEN

The SENSE Research School declares that **Mr. Vasileios Dakos** has successfully fulfilled all requirements of the Educational PhD Programme of SENSE with a work load of 56 ECTS, including the following activities:

SENSE PhD courses

- Environmental Research in Context
- Research Context Activity: Organizing special workshop, connecting research and performance: Expect the Unexpected (1 June 2011, Wageningen).

Other PhD and MSc courses

- Techniques for Writing and Presenting Scientific Papers
- A primer in ecological networks: Data and Theory
- Advanced Statistics
- Nonlinear Dynamical Systems

Management Skills

- Communication team Aquatic Ecology Department, Resilience Alliance Young Scholar facilitation committee
- Co-organisation of panel discussion in Resilience2011 conference
- Co-organisation of session in NERN meeting 2011, Co-organisation of panel discussion in Resilience 2011 conference

Didactic Skills

- Master student supervision

Oral Presentations

- Expecting unexpected transitions: how early can we anticipate change? Resilience Conference, 14 – 17 April 2008, Stockholm Sweden
- Expecting the unexpected: From lake ecology to climate change, SENSE symposium Cutting edge of freshwater ecology",10 October 2008, Wageningen, The Netherlands
- Interannual variability in species composition explained as seasonally entrained chaos Shallow Lakes Conference, 23 – 28 November 2008, Punta del Este, Uruguay
- Spatial correlation as an early warning signal for transitions in ecosystems Ecological Society of America, 2-7 August 2009, Albuquerque, USA
- Spatial correlation as an early warning signal for transitions in ecosystems NERN 2009, 9 – 10 February 2010, Lunteren, The Netherlands

SENSE Coordinator PhD Education and Research

Mr. Johan Feenstra

The research described in this thesis was financially supported by the Netherlands Organization for Scientific Research through an Open Programma project (NWO 5120301) awarded to E.H. van Nes and M. Scheffer.

Financial support for printing this thesis, from the Aquatic Ecology and Water Quality Management Group (WUR) and the Center for the Analysis of Critical Transitions (CAST) through a Spinoza award to Marten Scheffer, is gratefully acknowledged.